

A 65-METER  
TELESCOPE  
FOR  
MILLIMETER  
WAVELENGTHS

J. W. FINDLAY  
S. von HOERNER

NATIONAL RADIO  
ASTRONOMY  
OBSERVATORY

CHARLOTTESVILLE  
VIRGINIA

A 65-METER TELESCOPE FOR MILLIMETER WAVELENGTHS

J. W. Findlay

S. von Hoerner

The report of a design study made by the  
National Radio Astronomy Observatory.

April 1972

Library of Congress Catalog Card Number 72-90554

National Radio Astronomy Observatory  
Edgemont Road  
Charlottesville, Virginia 22901



THE 65-METER TELESCOPE FOR MILLIMETER WAVELENGTHS

## C O N T E N T S

		<u>Page No.</u>
CHAPTER I.	A SURVEY AND SUMMARY	
	1. Introduction.....	1
	2. The Scientific Objectives of the Telescope.....	3
	3. Special Features of the Design.....	8
	4. The Estimated Cost.....	11
CHAPTER II.	THE TELESCOPE DESIGN	
	1. General Description.....	14
	2. Rotation in Azimuth.....	14
	3. The Tower Structure and Elevation Bearings.....	19
	4. The Reflector Structure, The Spherical Joints and the Panels.....	20
	5. The Surface Plates, Their Fabrication and Setting.....	29
	6. The Cassegrain System, The Feed Support and The Observing Rooms.....	49
	7. The Position Reference System.....	55
	8. The Drive and Control System.....	64
	9. The Telescope Computer.....	72
CHAPTER III.	THE TELESCOPE PERFORMANCE	
	1. Introduction.....	77
	2. The Dynamic Behavior of the Telescope Structure.....	77
	3. The Accuracy of the Homologous Per- formance.....	79
	4. The Effects of Wind and Temperature....	84
	5. The Surface and Tracking Accuracy Budgets.....	91
	6. The Estimated Performance Under Various Climatic Conditions.....	98
	7. Performance of Other Radio Telescopes...	100
CHAPTER IV.	TELESCOPE SITES	
	1. Criteria for Site Selection.....	106
	2. Sources of Information on the Primary Criteria.....	111

	<u>Page No.</u>
3. Specific Sites.....	118
4. Summary and Conclusions.....	127
CHAPTER V.	
ESTIMATES OF COST	
1. Fabrication and Erection Costs.....	129
2. Site Development Costs.....	132
3. Operating Manpower and Costs.....	132
4. The Final Design Phase.....	133
5. Cost Escalation.....	135
APPENDICES	
I. NRAO Reports and Memoranda.....	139
II. Systems Development Laboratory Report H-10.....	140
III. Engineering Drawings.....	141
IV. Reports from Contractors and Others...	142

L I S T O F F I G U R E S

	<u>Page No.</u>
Plate 1 - Frontispiece - Artist's conception of the telescope	
Figure 1 - Natural limits for steerable radio telescopes.....	2
Figure 2 - Outline drawing of the telescope-- horizon position.....	14
Figure 3 - Outline drawing of the telescope-- zenith position.....	15
Figure 4 - The azimuth track and rails.....	17
Figure 5 - The side view of an azimuth truck....	18
Figure 6 - The elevation bearings.....	21
Figure 7 - The homologous joints which support the panel structures.....	23
Figure 8 - An example of a spherical joint (No. 45) in the reflector.....	25
Figure 9 - The geometry of the B-panels.....	28
Figure 10 - The NRAO surface plate.....	32
Plates 2 and 3 - Photographs of the NRAO surface plate.	33 & 34
Figure 11 - The machined contour surface plate....	38
Figure 12 - Measurement of the antenna surface....	39
Figure 13 - The targets used for measuring the surface of the 140-foot telescope...	42
Figure 14 - The use of a pentaprism to measure the antenna surface.....	43
Figure 15 - The modulated light beam technique for distance measuring.....	47
Figure 16 - The NRAO modulated light beam system..	48
Figure 17 - The geometrical optics of the Cassegrain system.....	50
Figure 18 - The feed-support structure.....	53
Figure 19 - The principle of the stable reference platform.....	58
Figure 20 - A typical record of the angular fluctuations of the optical path used in the reference platform tests.....	59
Figure 21 - Power spectrum of the angular fluctuations of the optical path used in the reference platform tests.....	60
Figure 22 - A general view of the stable reference platform.....	62

Page No.

Figure 23	- Block diagram of the reference platform control system.....	65
Figure 24	- A block diagram of the servo drive for one axis of the telescope.....	71
Figure 25	- Block diagram for one unit of the drive and control system.....	73
Figure 26	- The main modes of oscillation of the telescope.....	80
Figure 27	- One-way zenith absorption of radio waves in the atmosphere.....	99
Figure 28	- Nationwide pattern of clear days.....	112
Figure 29	- Precipitable water over VLA sites Y15 (New Mexico) and Y23 (Arizona).....	120
Figure 30	- Work and cost schedule.....	133

## PREFACE

The work which is described in this report has been done by a group of scientists and engineers at the National Radio Astronomy Observatory\*. The names of two members of that group have been used as authors in order that the report may be easily referenced. As the report shows, a considerable amount of the work has been carried out by engineering companies working with the design group. We wish to acknowledge all contributors to the design, and so we list them below.

### The NRAO Design Group

B. G. Clark  
J. W. Findlay  
D. S. Heeschen  
V. Herrero  
O. Heine<sup>†</sup>  
W. G. Horne  
H. Hvatum  
K. I. Kellermann  
L. J. King  
J. Payne  
S. von Hoerner  
C. M. Wade  
W-Y. Wong  
C. Yang

### Engineering Companies

Systems Development Laboratories<sup>†</sup>  
Los Angeles, California  
Simpson, Gumpertz & Heger  
Cambridge, Massachusetts  
Western Development Laboratories  
Division, Philco-Ford  
Palo Alto, California  
The Rohr Corporation  
Chula Vista, California  
LTV Electrosystems  
Dallas, Texas  
Radiation Systems Inc.  
McLean, Virginia  
Micro-T Incorporated  
Pittsburgh, Pennsylvania

---

\* The National Radio Astronomy Observatory is operated by Associated Universities, Inc., under contract with the National Science Foundation.

<sup>†</sup> Mr. O. Heine of the Systems Development Laboratory has worked throughout the design as a member of the design group. He has had Dr. W. Blythe and Mr. J. Muradliyan associated with him in his design work.



In the course of this work we have learned much from discussions with many others experienced in antenna design. One example has been with the staff at the Max-Planck-Institut für Radioastronomie in Bonn. A parallel design study has been carried out by that group; we have exchanged many design details with them and with their associated engineers from Krupp, MAN and Siemens. Similarly, we have benefited from meetings with the members of the antenna group at the Jet Propulsion Laboratory. In recognizing this assistance, for which we are most grateful, we must emphasize that the design presented here is our own, and we do not imply that it has the approval of those whose help we acknowledge.

May we conclude with two expressions of hope? First, that the work reported here may prove to be acceptable to all those who practice the art of using the tools of radio astronomy and, second, that sometime such a radio telescope will be built for them to use.

*J. W. Findlay  
S. von Hoerner*

# CHAPTER I

## A SURVEY AND SUMMARY

### 1. Introduction

This report gives the results of a design effort which establishes the feasibility of building a 65-meter diameter, fully-steerable radio telescope and provides an estimate of the cost of such an instrument, including the development of a suitable, typical site which, at 1972 prices, is 9.42 million dollars.

The present design is the outcome of work of many years; it incorporates the homology principle as stated and worked out in 1965 by S. von Hoerner. When this principle is correctly applied, a 65-meter telescope used under good observing conditions can be expected to work to wavelengths as short as 3.5 mm (86 GHz). The design was planned to meet the specifications given in Table 1.

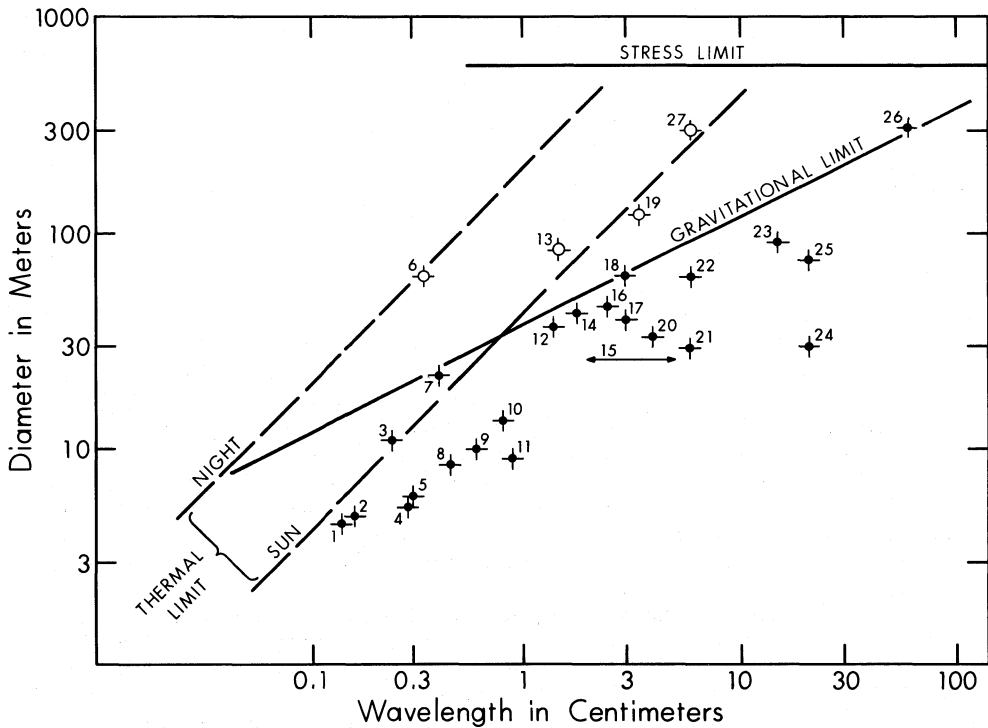
Table 1. 65-meter Telescope Design Specification

---

Dish diameter	:	65 meters (213 feet)
Mounting	:	Altitude-Azimuth
Elevation range	:	From horizon to 35° beyond the zenith
Sky cover	:	Complete--but no tracking inside a small zone near zenith of about 1 degree in radius
*RMS surface accuracy	:	0.222 mm (0.009 inches)
*Short wavelength limit	:	3.5 mm (86 GHz)
*Tracking accuracy	:	3 arc seconds RMS
Slew rates (both axes)	:	20° per minute
Optics	:	Prime focus $f/D = 0.42$ . Cassegrain--subreflector diameter 3.7 m (12 feet)
Instrument cabins	:	Behind prime focus; behind Cassegrain focus
Equipment room	:	Rotates in azimuth

---

\* This performance is only possible under benign environmental conditions.



KEY

- |                            |                                |
|----------------------------|--------------------------------|
| 1. AEROSPACE CORPORATION   | 15. VARIOUS 85-FOOT TELESCOPES |
| 2. UNIVERSITY OF TEXAS     | 16. ALGONQUIN, CANADA          |
| 3. KITT PEAK, NRAO         | 17. OWENS VALLEY               |
| 4. JPL, GOLDSTONE          | 18. GOLDSTONE                  |
| 5. HAT CREEK               | 19. NEROC DESIGN               |
| 6. 65-M TELESCOPE DESIGN   | 20. WERTHOVEN, GERMANY         |
| 7. RT-22, CRIMEA, RUSSIA   | 21. MARK II, JODRELL BANK      |
| 8. MIT, LINCOLN LABORATORY | 22. PARKES, AUSTRALIA          |
| 9. BONN, GERMANY           | 23. 300-FOOT, NRAO             |
| 10. ITAPETINGA, BRAZIL     | 24. MARK III, JODRELL BANK     |
| 11. NRC, CANADA            | 25. MARK I, JODRELL BANK       |
| 12. HAYSTACK, NEROC        | 26. ARECIBO                    |
| 13. BONN, GERMANY, 100 M   | 27. ARECIBO WHEN RESURFACED    |
| 14. 140-FOOT, NRAO         |                                |

Figure 1. Natural limits for steerable radio telescopes. Telescopes plotted with open circles are either not yet completed or have not yet demonstrated the performance indicated.

It is realized that such specifications surpass those of other large radio telescopes so far built. As von Hoerner (1967a) has shown in general terms, there are natural limits set by the effects of gravity, temperature, wind and material strength to the size of any reflector telescope. The size limit is related to the telescope's precision, measured in turn by its short wavelength limit. Figure 1 is a later version of Figure 2 in von Hoerner's paper. A wide variety of telescopes, one of which is only in the design stage, and the present design, are shown. None pass the gravitational limit except those which have taken care to do so (Bonn 100 meter, NERO design, and the present design) and Arecibo, where the reflector surface is fixed to the ground.

The design work has shown that the performance stated in Table 1 can be achieved under good climatic conditions. The actual conditions are discussed in detail in Chapter III; in general they require a situation typical of a clear night where the wind is below 18 miles per hour. When such conditions do not exist, during a calm, sunny day, for example, the telescope performance will deteriorate and accurate measurements only at wavelengths longer than 10 mm (30 GHz) will be possible. Thus, the best use of the instrument will be achieved by careful planning of the experimental work to be performed. It is large enough to be an important instrument when used at centimeter wavelengths; its design allows for rapid change-over from one wavelength to another and good scheduling of the programs can thus make the best use of the telescope at all times.

## 2. The Scientific Objectives of the Telescope

(a) General objectives. The broad scientific objective of the new telescope is to extend a wide variety of radio astronomical observations of many phenomena in the universe to wavelengths shorter than a few centimeters. The best large reflecting telescopes of today work well to wavelengths of about 3 cm (10 GHz). Although the radio universe has not been deeply explored at wavelengths between 3 cm and 3.5 mm (10 GHz - 86 GHz), existing smaller radio telescopes have already made many exciting new discoveries in this wavelength range; the new telescope will have 35 times the collecting area of the NRAO 36-foot instrument, which is at present the largest in the world capable of good work at 3.5 mm. The 65-meter telescope will thus give both the ability for deeper exploration and also will allow of much more accurate measurements for a wide variety of astronomical problems.

(b) Molecular spectral lines. The array of problems currently of most interest in molecular line work, but which are presently not soluble because of limited sensitivity and spatial resolution of existing equipment, is already large and is rapidly growing. These problems are largely soluble only at millimeter wavelengths and with telescopes larger than existing ones for several reasons.

(i) We now know that interstellar molecules of typical molecular weight (20 to 50) are populated up to quite high rotational energy levels; because the transition probabilities increase rapidly toward higher levels, the brightness temperatures of the lines arising from these higher levels are correspondingly large. These higher transitions occur at millimeter wavelengths for nearly all astrophysically interesting molecules. Because of these excitation conditions, far fewer molecules are needed to produce a detectable line at millimeter wavelengths than at longer (cm) wavelengths.

(ii) Significant structural detail in molecular clouds has been established at angular sizes as small as 1 arc minute, and physical arguments indicate that smaller structure yet is to be expected. In several of these cases (e.g.,  $\text{NH}_3$ ) the brightness in the lines is low, making these objects difficult to study even with a large array at the required resolutions. Observations of other transitions, or other molecules, at millimeter wavelengths, appear necessary to solve these problems.

It is believed that many additional interstellar molecules will be discovered with an improvement over current sensitivity of perhaps no more than a factor of five at millimeter wavelengths. Among these are several molecules containing hitherto undetected atoms such as Fe, Mg, Cl, and P. Even if these are not detected with such an improvement in sensitivity, the corresponding upper limits that can be placed on their abundances will be low enough to be very significant in terms of understanding interstellar chemistry. More complicated molecules containing only H, N, C, and O may also be discovered, and the important question might be answered of how large interstellar molecules may be.

Several problems involving presently known molecules will be soluble with better spatial resolution. Better positions for several point-like molecular clouds are needed to establish how well they coincide with small infrared sources that are being discovered frequently in the molecular regions. The physical relation between different molecular species on the small-scale level is important in determining if chemical abundances or formation processes vary rapidly with location in molecular clouds. This type of detail is essential even to derive meaningful relative abundances of the various molecular species, which in turn is necessary even to begin a study of interstellar chemistry.

Perhaps the best indication of the essential advantages of the millimeter range for molecular work is shown by the number of new molecules found, and their frequencies, over the past three years. In 1968-1969, before millimeter facilities were available, three new interstellar molecules were found at centimeter wavelengths. In 1970, the first year of good millimeter line observations, seven molecules were found of which four were at millimeter wavelengths. In 1971-72, eleven molecules were found, eight of them at millimeter wavelengths. To understand

the excitation of molecules, several transitions need to be observed. In 1971-72, some 26 new transitions of previously known interstellar molecules were detected, and all but four of these lay in frequencies above 25 GHz. Only through the study of these additional lines has it been possible to deduce such fundamental parameters as the density and temperature within the interstellar clouds, quantities which have not in fact been deducible in any other direct way.

The following Table 2 lists lines already detected in the frequency range from 20 GHz - 115 GHz (1.5 cm to 2.6 mm wavelength). The frequency

Table 2. Known Molecular Lines in the Frequency Range 20-115 GHz

Molecule	Transition	Frequency GHz
H <sub>2</sub> O water	6 <sub>16</sub> →5 <sub>23</sub>	22.24
NH <sub>3</sub> ammonia	Inversion doublets	22.83
" "	" "	23.10
" "	" "	23.69
" "	" "	23.72
" "	" "	23.87
" "	" "	24.13
" "	" "	25.06
CN cyanogen	N = 1→0	113.49
CO carbon monoxide	J = 1→0	115.27
C <sup>13</sup> O <sup>16</sup> carbon monoxide	J = 1→0	110.20
C <sup>12</sup> O <sup>18</sup> " "	J = 1→0	109.78
HCN hydrogen cyanide	J = 1→0	88.63
HC <sup>13</sup> N hydrogen cyanide	J = 1→0	86.34
Unknown U.89.2	?	89.19
Unknown U.90.6	?	90.67
CS carbon monosulfide	J = 2→1	97.98
OCS carbonyl sulfide	J = 9→8	109.46
H <sub>2</sub> CO formaldehyde	3 <sub>12</sub> →3 <sub>13</sub>	28.97
H <sub>2</sub> CO "	1 <sub>01</sub> →0 <sub>00</sub>	72.84
HNCO isocyanic acid	4 <sub>04</sub> →3 <sub>03</sub>	87.02
HNCO " "	1 <sub>01</sub> →0 <sub>00</sub>	21.98
HC <sub>3</sub> N cyanoacetylene	J = 8→7	72.78
HC <sub>3</sub> N "	J = 9→8	81.88
HC <sub>3</sub> N "	J = 10→9	90.98
HC <sub>3</sub> N "	J = 11→10	100.08
CH <sub>3</sub> OH methyl alcohol	4 <sub>2</sub> →4 <sub>1</sub>	24.93
CH <sub>3</sub> OH " "	5 <sub>2</sub> →5 <sub>1</sub>	24.93

Table 2, continued

Molecule	Transition	Frequency GHz
CH <sub>3</sub> OH methyl alcohol	6 <sub>2</sub> →6 <sub>1</sub>	25.02
CH <sub>3</sub> OH " "	7 <sub>2</sub> →7 <sub>1</sub>	25.12
CH <sub>3</sub> OH " "	8 <sub>2</sub> →8 <sub>1</sub>	25.29
CH <sub>3</sub> OH " "	4 <sub>1</sub> →3 <sub>0</sub>	36.20
CH <sub>3</sub> OH " "	5 <sub>1</sub> →4 <sub>0</sub>	85.52
CH <sub>3</sub> CN methyl cyanide	6 <sub>5</sub> →5 <sub>5</sub>	110.33
CH <sub>3</sub> CN " "	6 <sub>4</sub> →5 <sub>4</sub>	110.35
CH <sub>3</sub> CN " "	6 <sub>3</sub> →5 <sub>3</sub>	110.36
CH <sub>3</sub> CN " "	6 <sub>1</sub> →5 <sub>1</sub>	110.38
CH <sub>3</sub> CN " "	6 <sub>0</sub> →5 <sub>0</sub>	110.38
H <sub>2</sub> CCO	4 <sub>04</sub> →3 <sub>03</sub>	80.83
CH <sub>3</sub> C <sub>2</sub> H methylacetylene	4 <sub>04</sub> →3 <sub>0</sub>	85.46
	4 <sub>1</sub> →3 <sub>1</sub>	85.46

range from 25 GHz - 50 GHz has not yet been explored to any large extent, and many other lines can be expected in that region. The table has not been extended below 20 GHz since some existing large telescopes can work in that frequency range. The table has also been extended somewhat above the telescope's 86 GHz design limit, since it can be expected to be very useful for line work in that range.

The molecular species already identified by their microwave lines can be expected to show many other lines arising from other transitions. A reasonable listing of these suggest that 30 or so more lines may be found with good instruments. Even this does not exhaust the future possibilities. As has already been suggested, molecules or radicals such as PN, HCP, FeO, CH<sub>3</sub>C $\dot{\text{C}}$ , HC<sub>2</sub>CHO, NH<sub>2</sub>CN and NgO may exist and in their turn could be a rich source of lines in this part of the microwave spectrum.

(c) Observations in the radio continuum. We will again emphasize those tasks where the short wavelength performance of the telescope makes it unique, and thus refer mainly to observations made above about 20 GHz (1.5 cm). We will however note in passing that the telescope will be a major instrument in its own right and will do much more valuable work in the centimetric and decimetric wavelength range.

In the field of extragalactic studies, quasars and radio-bright galaxies will be studied. New radio outbursts in quasars and in the

nuclei of galaxies often show effects first and most strongly at the short wavelength end of the spectrum. Their changes in intensity and polarization with time can be of help in explaining the mechanism of radio energy production. The radio spectra and polarization of galaxies and quasars should be extended to shorter wavelengths to add knowledge of magnetic fields and particle energies.

In our own galaxy the telescope will be used to map the fine structure in regions of ionized hydrogen and to study gas and dust concentrations where stars may be forming. Some (usually unusual) stars have already been found to be radio emitters, and some novae have also been found to show short-wavelength radio enhancements. These are fields for further study. The telescope can also have a wide field of view and thus can make surveys of the sky with good angular resolution and high sensitivity.

A large millimeter-wave telescope will have many uses in solar-system astronomy. It will observe active regions on the sun to improve our understanding of the origins of solar disturbances. Measurements of the millimeter-wave spectra of the planets will help discover the constituents of planetary atmospheres. Studies of temperature and polarization measurements of the moon and planets will tell more of the surface and subsurface properties of these bodies.

(d) Interferometric observations. It is not too early to speak of millimeter-wave interferometry; experimental work is already being undertaken by various radio astronomical groups. The 65-meter telescope will be a powerful instrument either for use with one or more smaller nearby telescopes in the phase-coherent mode or as one end of a very long baseline interferometer. Such VLBI experiments have already been made at 22 GHz, and the extension of the method to higher frequencies requires, at present, mainly improvements in technology and the availability of at least one large radio telescope.

(e) Conclusion. Any look forward in a rapidly advancing subject such as radio astronomy is always colored by the most recent discoveries. At present, these are very largely in the field of molecular spectroscopy, and the future of this field looks very bright. Only a very few years ago studies of the highly energetic quasars were more in the forefront of interest. These problems are still with us; so also are the problems of cosmology and the origins of the intense non-thermal emission of energy in the whole spectral region from radio to X-ray wavelengths.

The 65-meter telescope has the accuracy to make great advances possible at millimeter waves, yet it is large enough to continue and extend radio astronomical research at longer wavelengths. It will therefore be versatile enough to meet the future challenges which will arise as astronomy grows and changes.



### 3. Special Features of the Design

(a) Homologous deformation. The telescope design uses the principle of homologous deformation, or more shortly of "homology". Any massive structure must deflect under its own weight, and if, as is true of the reflector of a radio telescope, it must be moved with respect to the gravitational force, it will deform by different amounts as it moves. Suppose, however, that the entire reflector supported at its elevation bearings could be so designed that the reflector surface is a true paraboloid of revolution when the reflector points to the zenith and also when it points to any position between zenith and the horizon. It would then (in the absence of distortions due to wind or temperature) be a perfect radio telescope. It is known that this condition can be satisfied provided we are willing to let the focal length of the reflector surface change. We also have to allow the direction of the telescope's radio beam to move in a slightly different way from the way the elevation axis rotates. When we achieve this result that the reflector surface keeps the same geometrical shape but only changes by a scale factor, we say that the deformation has been homologous.

This principle has been the basic technique by which the whole of the present reflector structure has been designed. The method uses the well-established techniques by which stress and deflection analyses of complex structures made up of elastic material can be computed with a high accuracy. The programs developed to make these computations are novel, and include many checks to ensure that the structural design which results is both practical and accurate.

It should be emphasized that, although the homology program for designing the reflector structure is novel, the results of the design have also been checked by well-established methods of structural analysis. The initial structural geometry and the use of relatively few members were chosen to make the behavior of the actual structure conform closely to the predictions. Individual members are tubular steel pipes; these come together at joints which are specially designed, half-spherical castings welded together. The tubes in turn are welded to the spheres; sometimes where the geometry requires it, a cast tapered end is used to connect the steel tubular member to the sphere.

Simplicity in geometry and good joints are very valuable in ensuring that the structure does in fact behave under its gravity loads as the computations predict. That this will be so has been well demonstrated; for example, the agreement between calculated and measured distortions was excellent for the 300-foot telescope at NRAO, the 210-foot telescope at Goldstone and the 120-foot Haystack antenna. The Bonn 100-meter dish also relies on accurate computer predictions of deflections, but the final test of measurement has not yet been made on that telescope.

The homology program results in a structure with the required deflection pattern, and the program has been extended to obtain other practical results. It ensures that the structure can be built using for many of its members the regularly available sizes of tubes or pipes, although some members must be specially fabricated. The departures from homological perfection brought about by these choices, as well as by the manufacturing and erection tolerances of the members, have been calculated and shown to be acceptable. The survival strength of the structure in wind, snow and ice is adequately met by the design program.

(b) The pointing system. It is necessary to know very precisely (to within a few seconds of arc) where the radio beam of the telescope is pointed. Although homology neutralizes the effects of gravity on the reflector performance, the whole telescope will deform under gravity and the more conventional means of measuring its beam position--by using accurate angle measuring encoders on the azimuth and elevation axes--would show considerable differences between these axial position measures and the actual beam position. Other factors, such as wind forces, temperature differences, small movements of the telescope foundations or lack of exact leveling of the azimuth track, all result in position errors.

These gravitational, steady-wind and other position errors can be much reduced if the position of the structural axis of the parabolic reflector can be referred directly to a fixed reference system on the ground. This method has proved most useful in the Australian National Radio Astronomy Observatory's 210-foot telescope at Parkes, N.S.W., and it is also used in the NASA/JPL 210-foot telescope at Goldstone and in the Canadian NRC Algonquin Park 150-foot telescope. All these instruments have a central, independently founded tower, shielded from the sun and wind, which carries at its top the system which references the direction in which the reflector is pointing.

The same principle, but in a novel form, is used in the design of the 65-meter telescope. The reflector axis is referenced to a platform which is held in the position where the elevation and azimuth axes of the telescope intersect. This reference platform is locked to remain fixed in its azimuth and elevation angular position as the telescope moves (the platform may make small linear movements in absolute position) and highly accurate encoders measure the reflector angular position relative to this stable reference platform. Instead of mounting this reference platform on a central shielded tower, it is held locked to the ground by a servo-control system which gets its error indications from beams of light transmitted in fixed directions from several stations on the ground around the telescope and reflected from mirrors on the reference platform back to the ground.

The position reference system is intended to reduce the pointing errors of the whole telescope to the very low values required. The

repeatable pointing errors due to gravity will be measured in the calibration procedure and then allowed for by the pointing computer. The reference platform has already been the subject of considerable design and test. A test stand of one element of the optical system has been built and has been operated at Green Bank for several months. This has demonstrated that the method will not fail because of irregularities in the atmosphere causing instability in the direction of the light beam. The design of the reference platform has been carried to a fairly advanced stage, since its performance is critical to that of the whole telescope. A suitable type of autocollimator has been chosen and the servo system which will lock the platform to the light beams has been designed. Specifications for such critical components as the 22-bit angle encoders (corresponding to 0.31 arc seconds resolution) have been issued and offers to supply have been received and evaluated.

(c) The reflector surface. The requirements of a reflector surface which will work well at millimeter wavelengths are stringent. The surface plates must be fabricated and measured, then mounted on the telescope, measured and set in position; all these operations must result in a surface which maintains in reasonable regimes of wind and temperature an accuracy (RMS) of 0.22 mm (0.009 inches). Higher accuracies than this have already been achieved on other telescopes with diameters up to 72 feet but the methods of fabrication have been too expensive for adoption in the present design.

One method of fabricating the plates has been developed and tested at NRAO. This method produces an aluminum surface plate, with the required surface curvature and accuracy, of about 6 feet by 2-1/2 feet in size. The actual surface is made from originally flat 1/8-inch aluminum sheet. This is set to the required shape by 36 adjusting screws which deform it, acting against an aluminum support frame. Tests have shown that this type of construction gives a surface within the accuracy limits and one which withstands the required loads without permanent deformation or structural hysteresis. The cost of manufacturing this surface is reasonable.

The surface is so important a part of the whole telescope that other methods by which the surface plates might be made have been explored. Studies have been carried out by two companies experienced in the design and fabrication of antennas. Several alternative methods of making the surface plates have been considered; one of these which would machine the surface of a previously fabricated surface plate on its support structure is an acceptable alternative to the NRAO surface plate already described.

The reflector plates must finally be mounted and set in position to a high accuracy on the reflector support structure. Two methods for doing this setting have been evaluated. The first uses a combination of

a measure of the distance from a point at the dish center to a target on the dish surface with a measure of the elevation angle of the target, also taken from the dish center. The distance measure is made by a high-quality steel tape and the angle is measured by comparing it to the angle by which a quartz pentaprism deflects a ray of light. This is a well-tested system, and it can give the required measurement accuracy.

A second method for surveying the surface has been devised. This measures two distances from the dish center to a target on the surface. The first distance is direct to the target; the second is from the dish center to a point near the dish focus and then to the target. Both distances are measured accurately and rapidly using a modulated laser-light instrument. This method also can give the required measurement accuracy.

Accuracy and speed of measurement are both important in the task of surveying the surface, since the best time to measure will be on calm nights after the structure has reached a fairly uniform temperature. The final check of the success of the surface setting is, of course, the radio measurement of the gain or aperture efficiency of the telescope at short wavelengths.

#### 4. The Estimated Cost

(a) General. We have developed in Chapter V a complete estimate of the cost of bringing the telescope to completion on a site in the southwestern United States. This estimate includes the cost of the final engineering of the design, fabrication and erection of all parts of the telescope, acquisition and preparation of a typical site, including buildings and final test and check-out of the instrument. It includes the cost of all items, such as the control computer, to make the instrument fully operational. It does not include the cost of radiometers with their feeds, back-ends, data processing, extraction and recording equipment, since these items are provided from the Observatory's annual budget. An estimate is given, however, of how the telescope would impact the NRAO budget, both in this respect and in the additional manpower and cost which the new telescope would add to the NRAO operating budget.

(b) The telescope cost estimate. Table 3 is a summarized version of the later Table 25 in Chapter V.

In arriving at the site figure, we have assumed that the telescope was being built on one of the possible VLA sites, but we have included all work required at the site to make the 65-meter telescope fully operational. If in fact this telescope and the VLA were to share a site, the costs of site development would be shared between them, and our figure of \$634,000 is too high.

We have estimated (see Table 27) that the new telescope would require a staff at the site of 26 and that its annual operating budget would

Table 3. Summary of the Cost Estimate (in 1972 dollars)

	<u>Thousands of \$</u>
Fabrication of main structure	1,916
Erection of complete telescope	1,080
Surface plates, including installation and adjustment	1,540
Azimuth and elevation machinery	675
Foundation and track	146
Position reference system, drive and control system	1,160
Feed legs, access system, cabling, painting, start-up and test	592
Site acquisition, preparation and buildings	634
Project management and engineering	450
	<hr/> 8,193
Add 15% contingency	<hr/> 9,422 <hr/>

be \$512,000. With rather less certainty, we suggest that the new telescope would require an added \$250,000 yearly, divided between the NRAO electronics budget items for other observing equipment and test and repair equipment. This funding should start when the construction of the telescope is approved.

Finally (see Table 30), we estimate that the time for completion from the availability of funding would be 36 months.

(c) Cost escalation. In the situation at the time of writing (February 1972), it seems still prudent to assume a steady escalation of costs of labor and materials over the years. We will arbitrarily adopt a rate of 6 percent per year, to apply to all figures (which have all been in 1972 dollars).

The earliest date by which funds could be available to NRAO for this telescope is January 1, 1974. By that date our total cost, including contingency, would have grown to \$10.587 million. Projections of cost beyond that date can be left (at present) to others more skilled than ourselves.

#### References

von Hoerner, S. 1967(a). Astron. J., 72, 35-47.

## CHAPTER II

### THE TELESCOPE DESIGN

#### 1. General Description

Figures 2 and 3 show two outline drawings of the telescope. It is an altitude-azimuth instrument; one in which the whole structure rotates in azimuth on rail tracks about a central pintle bearing. The reflector can be rotated about a horizontal elevation axis between two bearings carried at the top of the support towers. The telescope is driven in azimuth by electric motors geared to the wheels on the azimuth track and in elevation by motors geared to pinions which drive a bull gear on the elevation wheel. Control by a high-speed computer system allows the telescope to slew, scan and track under servo-mechanism control at a wide range of rates.

The optics of the instrument can be either Cassegrain or prime focus. When used as a Cassegrain, the radio waves reflected from the main 65-meter parabolic reflector are reflected a second time at a much smaller diameter (12 feet or 3.7 meters) hyperboloid mirror (subreflector) which is near the focal point of the main mirror. The radio energy is then focussed to the feed horn in the main equipment cabin in the center of the parabolic reflector. For use as a prime focus instrument, the subreflector is removed and the energy is collected by a feed horn in the equipment room at the vertex of the feed support legs.

Thus duality of methods of using the telescope is of great value since for very short wavelength work the Cassegrain mode is most desirable while, if research is to be done at wavelengths longer than a few centimeters, the prime focus mode is generally more practical.

#### 2. Rotation in Azimuth (SDL Report No. H-10, Sections 4 and 5)\*

The main components which provide for the azimuth rotation are the telescope foundation, on which the azimuth rails are mounted, the

---

\* References of this kind indicate the source of the original design material; to locate it see the final section entitled Appendices.

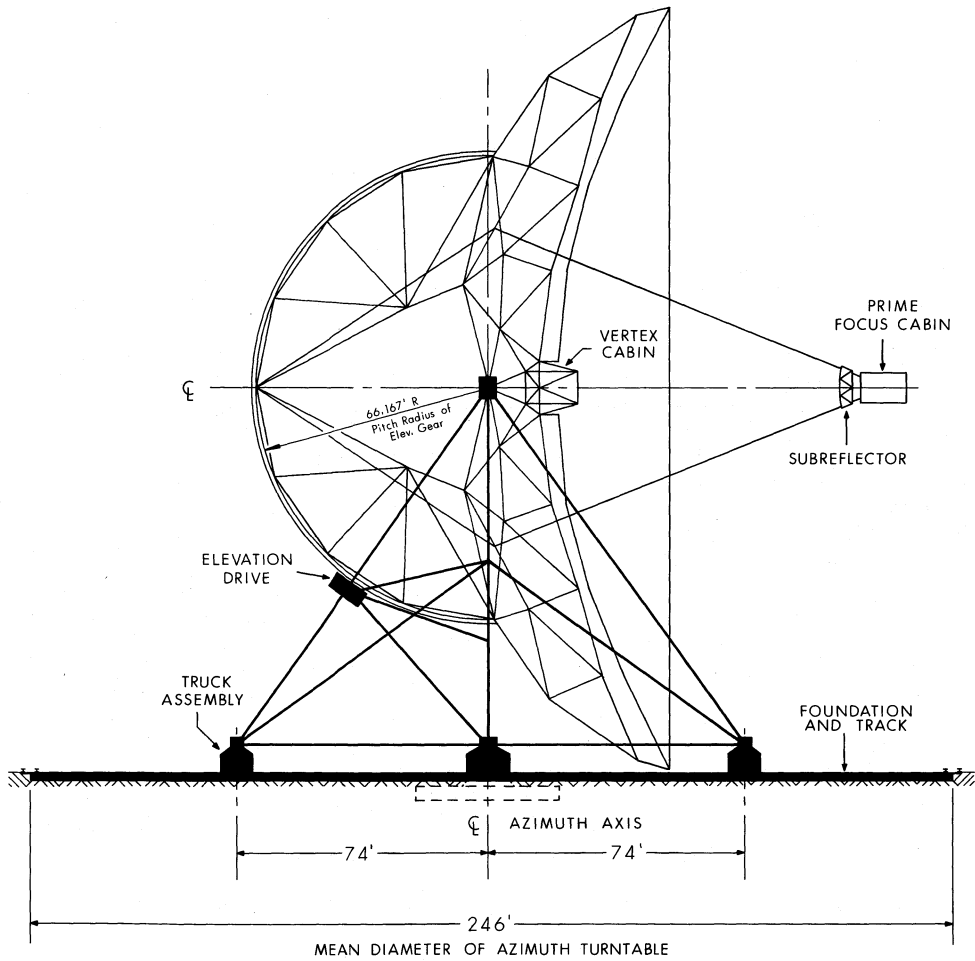


Figure 2. Outline drawing of the telescope--horizon position.

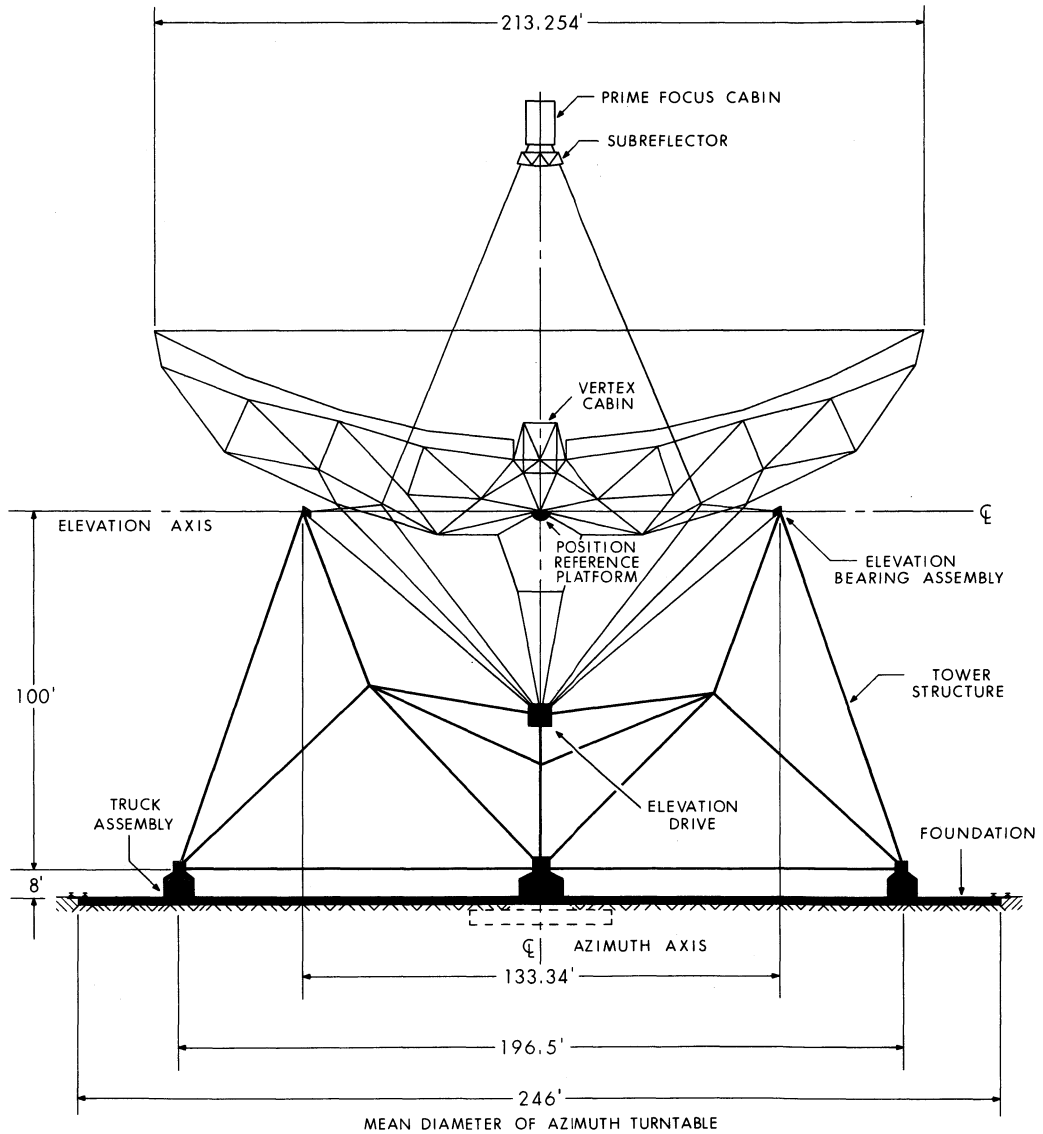


Figure 3. Outline drawing of the telescope--zenith position.



trucks with their drive motors, gear trains and brakes and the central pintle bearing. Precise knowledge of the azimuth pointing is derived from the reference platform, but pointing is also measured with lower precision by an encoder mounted at the pintle bearing.

(a) The telescope foundation and rails. The foundation is a ring of concrete with steel reinforcement 9 feet wide and 2 feet deep with a mean radius of 123 feet. This supports the rail track, which is made of two concentric circles of 175-CR crane rail giving a 5-foot width for the rail track. Figure 4 shows details of how the rail (which is crowned) is mounted on the foundation. The top surface of the rails will be set and maintained level to  $\pm 0.125$  inches (3.2 mm) by shims. This accuracy is not difficult to achieve and is desirable to give smooth rotation for the azimuth drive. There are six positions around the rail where the trucks can be tied to the foundation (for stowing the telescope in high winds).

The foundation and rail has to be adequately strong to carry the telescope loads, and it must also resist deflections (be stiff enough) so as not to contribute much to the flexibility of the structure in any dynamic modes. In fact, from both these points of view, the foundation and rail is somewhat over-designed, since it has been derived from the work done for the earlier 300-foot telescope design\*. The design will be reviewed when subsurface conditions at the selected site are known.

(b) The azimuth trucks. Four trucks, each of which has eight wheels, carry the whole moving weight and other vertical telescope loads to the tracks. These trucks also carry the azimuth drive motors, gear trains and brakes; the drive forces are provided by the friction between the driven wheels and the rails. Each truck may experience a maximum vertical load of about 500 tons; again, as in the case of the foundation, the actual design is conservative and capable of carrying greater loads. Figure 5 shows the side view of a truck; further details are on Drawing No. 111-D-008, Sheets 1-3.

Several important requirements have to be met by the trucks, and these have all been allowed for in the design. The load on any one truck must be fairly evenly divided between the eight wheels, even when the rail top surface is not exactly level and when it deflects under load. Each truck must provide for a braking force onto the rail, so that the telescope can be held still with the wheel loads reduced. The four driven wheels must be so arranged that when the telescope is being driven the drive force at a wheel must be tangential to the wheel and lie in the plane of the wheel. The frictional forces between the wheels and the rail in both the static and the rolling cases must not be too great; nor must the difference between static and rolling friction be too large.

---

\* A 300-foot High-Precision Radio Telescope, National Radio Astronomy Observatory, May 1969.

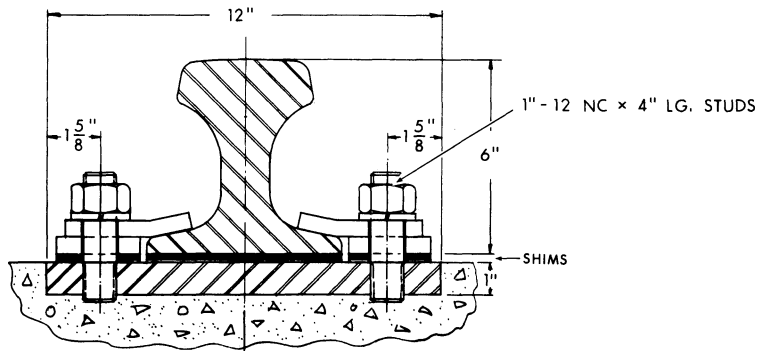
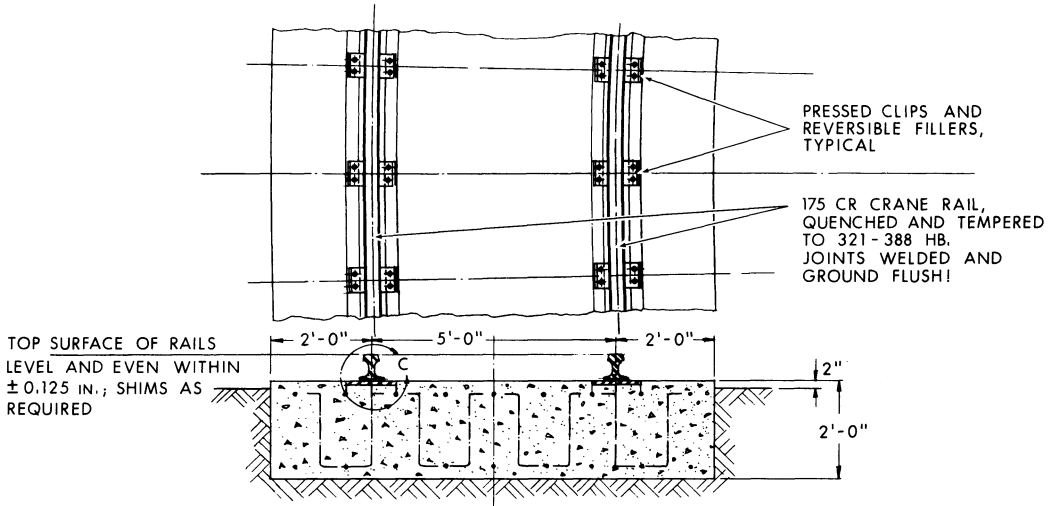


Figure 4. The azimuth track and rails.

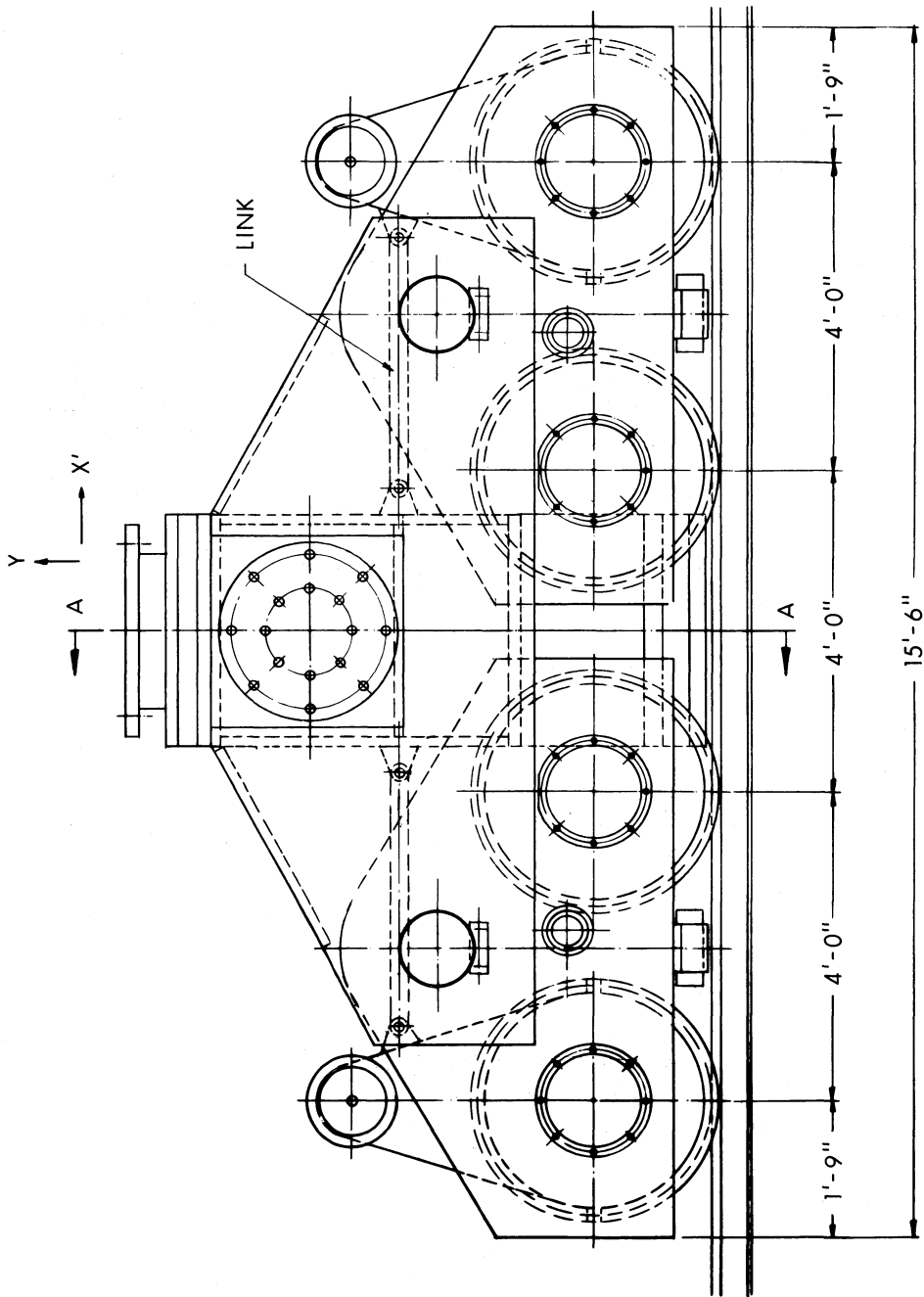


Figure 5. The side view of an azimuth truck.

The other important components in the trucks are the DC servo motors and gear trains. These are described further under the drive and control system.

(c) The pintle bearing and cable-twist. The whole structure rotates about the pintle bearing as its center, and this bearing has to withstand any lateral forces which are given to the telescope by winds. Although, in principle, the pintle bearing need carry no other loads, the present design does allow the bearing to carry some part of the vertical loads due to the weight of the tower. Also, since the azimuth track does not lie exactly in a plane, the bearing must accept loads due to small tilts of the structure as well as the lateral wind-generated loads.

Accordingly, a preloaded, self-aligning bearing has been designed which can take both up and down vertical loads, radial loads and any alignment moments generated as the structure rotates. The preload eliminates play; to meet the load requirements a combination of a self-aligning spherical roller thrust bearing preloaded by a self-aligning cylindrical thrust bearing is used. The alignment surface curvatures of the two bearings coincide. The detailed design of the bearing is given on Drawing 111-D-006.

The azimuth cabling of the telescope passes through a 24-inch diameter hole in the center of this bearing; this in turn requires that the coarse azimuth encoder be gear driven and not axially mounted, but adequate accuracy can be achieved by this method of encoder drive.

The cables from the moving parts of the telescope pass to the fixed ground through the cable-twist. In the present design, the bundle of cables 60 feet long is suspended through the central tower member, through the pintle bearing and down to a point 30 feet below ground. The  $\pm 270^\circ$  rotation of the telescope twists this bundle, rather than using a wind-up drum. This feature and the straightforward pintle-bearing foundation are shown in Drawing 111-D-004.

### 3. The Tower Structure and Elevation Bearings (SDL Report H-10, Chapters 3 and 6)

(a) The tower structure. The main function of the towers is to provide the support structure between the elevation bearings (which carry the reflector) and the azimuth trucks and pintle bearing. However, there are various further demands placed on the tower, and the design has been made to satisfy all these requirements. For example, the tower structure must:

- (i) Have reasonably small deflections due to wind forces.
- (ii) Meet the survival loads imposed on it.
- (iii) Give a satisfactory dynamic behavior for the telescope structure.

- (iv) Not impose any stresses on the reflector under normal operating conditions which could distort the reflector beyond the limits set by the shortest usable wavelength of the telescope
- (v) Block as little as possible the light beams in their paths from the ground-based autocollimators to the mirrors on the reference platform.

The tower structure which meets these requirements is an improvement on the structure designed earlier for the 300-foot antenna. The base configuration has been simplified; the lower weight permits the use of only four trucks and welded tubular members have been chosen for the structure. The details of the tower are shown in Drawings 111-D-002, Sheets 1-3. The total weight of structural steel in the tower is 366 tons. The dynamic properties of the tower are discussed later in this report.

(b) The elevation bearings. For the optimum performance of the homologous reflector, it is necessary that applied or reacted forces and moments imposed at the elevation bearings be kept at the lowest possible levels in order to minimize secondary, unpredictable surface deformations.

For these reasons, the design concept for the elevation bearing, as shown in Figure 6, is proposed. The scheme is somewhat unusual because of the application of a pair of axially preloaded spherical roller thrust bearings which act as primary radial bearings. However, because of this particular arrangement, which permits a common center of the spherical radius for each set of opposing bearings, nearly equal load sharing as well as freedom of spherical rotation of each elevation bearing assembly is essentially assured. Thus, only a small frictional alignment moment is transferred into the reflector structure by either load flexures of the tower structure in the elevation axis direction or by bearing misalignments.

Because of axial preload requirement, the U-shaped bearing housing becomes rather heavy in proportion to other structural components. However, stiffness is of primary interest in this case and takes preference over weight or size considerations.

Nevertheless, it may well be possible to reduce both size and weight of the bearing assemblies during the final design stage, subject to a trade-off study of stiffness requirements versus system dynamics requirements, as the design shown in Figure 6 was originally prepared for the 300-foot diameter telescope and, therefore, is somewhat oversized.

#### 4. The Reflector Structure, the Spherical Joints and the Panels

(a) The reflector structure (W-Y. Wong Reports 34 and 34A).  
This is the structure which is supported on the elevation bearings; it

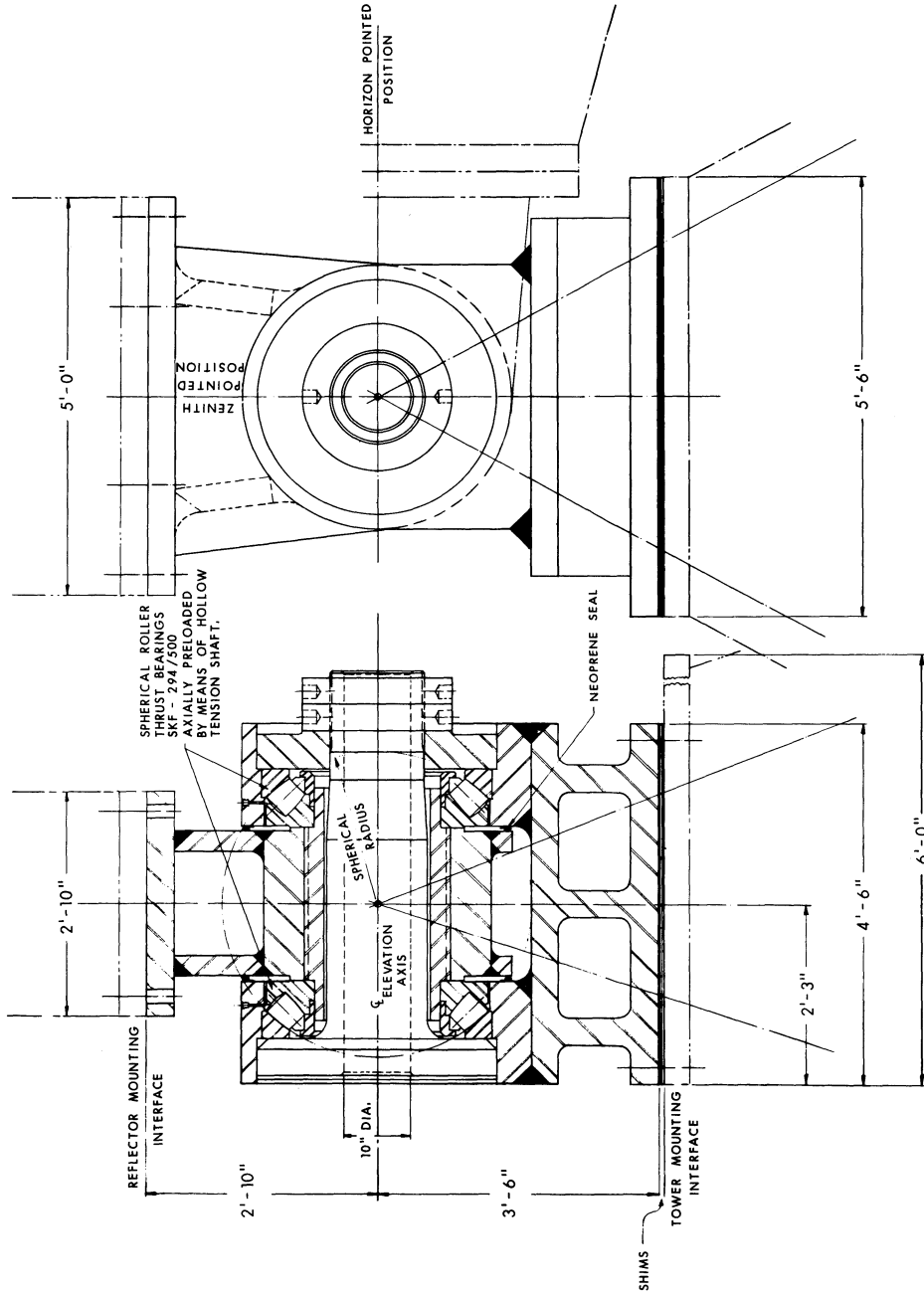


Figure 6. The elevation bearings.

includes the elevation drive wheel structure but does not include the feed support legs. Its function is to give the main support for the reflector surface. This main support is provided at 60 homologous points. These 60 points (which are radially symmetrically placed, see Figure 7) in turn are bridged by the panel structures and finally the surface plates are supported on the panels. This nomenclature should be noted, since the word "panel" is used by some engineers to mean the reflecting surface itself. The panels are described later in this section; here it is only necessary to say that they have linear dimensions of the order of 30 feet and thus are important structures in their own right.

The reflector structure is homologous; as its elevation angle changes the 60 main surface joints always remain very closely on a parabolic surface. The focal length of this surface changes regularly with elevation angle and so also does the departure of the direction of its axis of symmetry from the direction defined by the elevation axis position encoder.

The way in which von Hoerner's method achieves homologous performance has been published (von Hoerner 1967(b) and 1969) and will not be repeated. The application of it to the present design has been straightforward; the following conditions have been included in the design and have been satisfactorily met.

(i) The 60 homologous points must remain at their required position to an RMS accuracy of 0.004 inches (0.10 mm) as the telescope tilts from zenith to horizon.

(ii) All expected dead loads must be applied to the structure in its design. These loads include the surface panel and plate loads and the loads imposed by the feed legs, the prime focus and the vertex equipment rooms. The loads from the elevation drive have been arranged to be small.

(iii) The design must allow for the selection of member sizes, which in as many cases as possible are standard sized tubes or pipes. It must show separately those members which have to be specially fabricated. The effects on homology of this selection must be checked.

(iv) The structural design must include the weights and stiffness of the spherical joints (see Section 4(b)) for their effects on strength and homology.

(v) The structural design must be one which is practical for fabrication and erection.

(vi) The design must produce a structure which meets the survival conditions imposed by high winds and possible snow or ice loading.

(vii) The structure must have adequate stiffness so that its overall and detailed dynamic behavior is satisfactory.

The design and computational work which has been needed to achieve these results is very extensive. The results are summarized in W-Y.

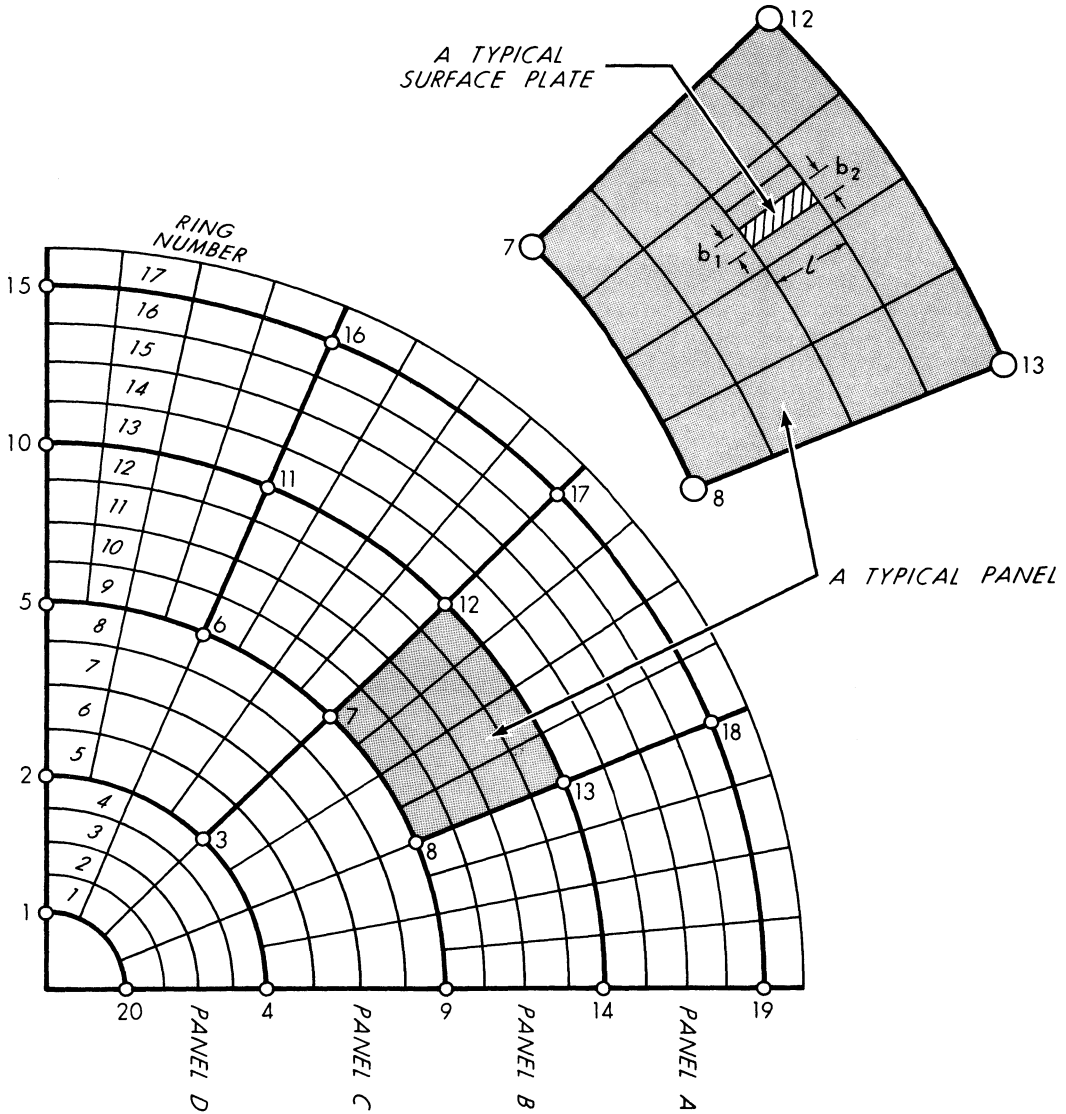


Figure 7. The homologous joints which support the panel structures.



Wong's Reports 34 and 34A. The accuracies to be expected from the reflector design are considered in more detail in Chapter III.

The choice of tubes and pipes is economical for several reasons, but raises the possibility of individual member vibrations induced by even quite moderate winds. This type of vibration is well-known. For the present structure, it has been considered (S. von Hoerner Reports Nos. 24 and 35). Wind-induced vibrations are not critical if the wind velocity which makes the member resonant is above the greatest velocity expected or if the air flow is turbulent. If these conditions are not met, members will vibrate at their natural frequencies so that under this condition the alternating stress in the member must be low enough to avoid fatigue failure even with any number of oscillations. The structure has been checked to ensure that no members are unsafe due to wind-induced vibrations.

The reflector structure is specified in detail in W-Y. Wong's Reports 34 and 34A. These give joint coordinates, member sizes and say which members are standard, which have to be specially ordered and which are to be individually fabricated. The reflector design is shown in Drawings D-111-001, Sheets 1-6.

The designs for both the tower and reflector structure have been made with the intent of using a steel of high yield strength. One such material is Cor-Ten\* manufactured by U.S. Steel. This steel also has good resistance against corrosion. The latter property will be important in that no serious loss of cross-section area (which might be important in some thin-walled sections) can occur due to corrosion of the interior of the members. All exterior surfaces will be protected by paint; this is needed for temperature control. Furthermore, corrosion-resistant steels require painting less often than more normal varieties and thus give a maintenance advantage. Although Cor-Ten is discussed here, the design requirements can be met also by steel of approximately equivalent properties available from other steel producers.

(b) The spherical joints (SDL Report H-10, Chapter 2). The use of tubular members in radio telescopes is well established; both the Parkes 210-foot and the Effelsberg 100-meter instruments use many such members. However, in the present design their use, and the following other factors, require the adoption of a somewhat unusual joint design. For example, in the reflector structure most members connecting at a particular joint are not oriented in common planes, as is the case with most standard space frames, but project from all directions since the joint locations are dictated by the requirements for a homologous deformation solution and not by geometrical considerations alone. Furthermore, in some instances as many as 15 members intersect at one point, which makes it impractical to employ direct or gusset plate joint connection of the tubular members.

---

\* Cor-Ten is a trade-mark of U. S. Steel.

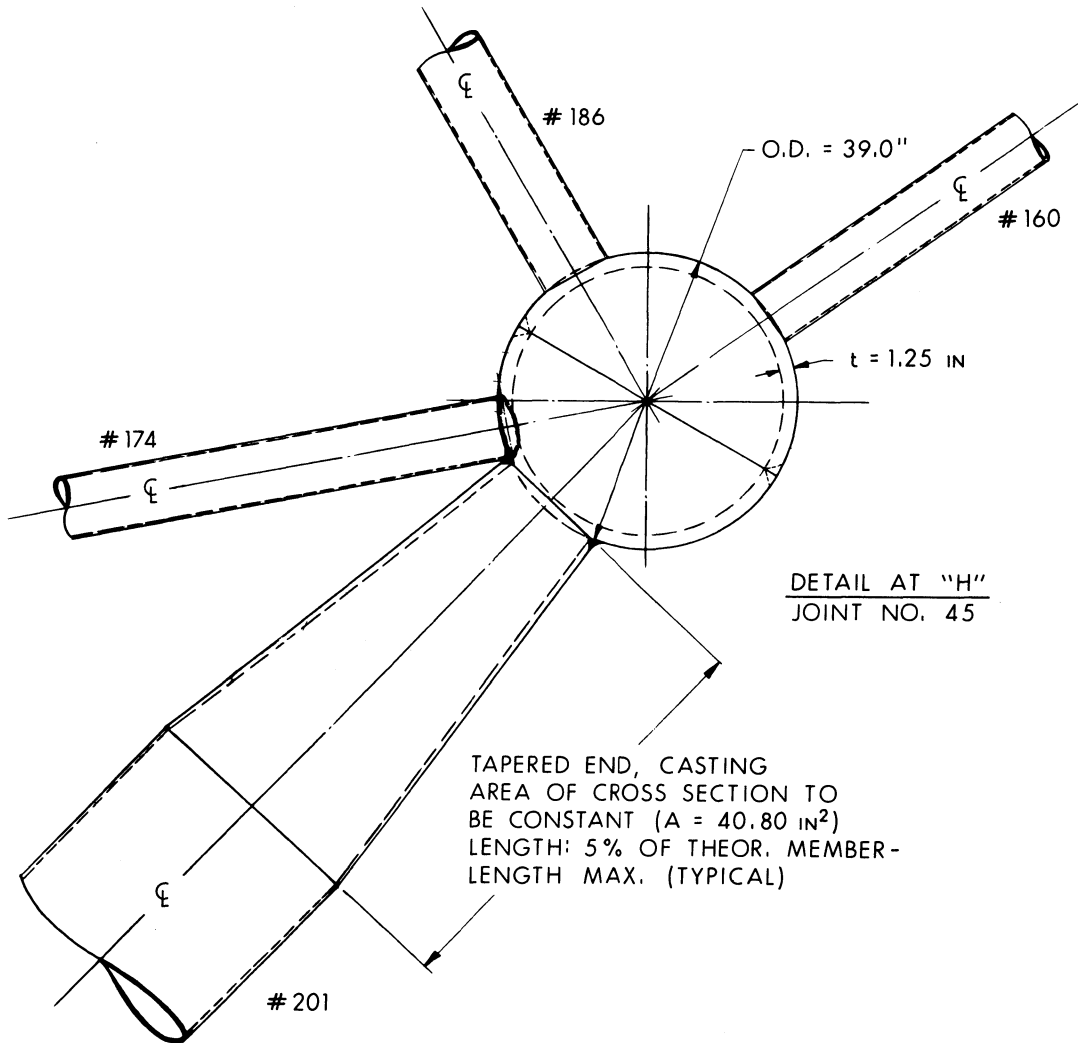


Figure 8. An example of a spherical joint (No. 45) in the reflector.

Also, to ensure that homology was maintained in the reflector design it was necessary that the additional total joint weight be limited to about 3 percent of the total reflector weight and that the average axial stiffness variation of each joint member connection be no more than  $\pm 5$  percent of the theoretical stiffnesses of an idealized structure consisting of full length members and pin joints.

Another requirement was that the axial offset of each member from the theoretical point of intersection be kept as small as possible so as to minimize the effects of secondary moments acting on the joints which could also possibly alter the homologous reflector deformations. Finally, connections and alignments of members must be easy and the joint design should preferably be universal in order to be economical.

The concept of joints which are hollow spherical shells, of correctly chosen diameters and wall thickness, has been adopted and meets the foregoing requirements. Such a concept is not new; one example is to be found in the truss structure for the Japanese built roof of Expo 70's "Symbol Zone".

Two computer programs have been used to determine the geometry, strength and stiffness of the joints. One determined the angles between members and derived the minimum possible sphere diameters. The second program determined the joint stresses, wall thicknesses, stiffnesses and weights.

The joints replace the end parts of the members of the reflector structure, but the knowledge of their weights and stiffnesses, as compared to the same quantities for the pieces of steel they replace, allow for the homology solution to be rechecked. This has been done and the deviations produced are acceptable. The following table summarizes the results of the reflector joint design.

Total number of spherical shells required	:	145
Estimated total shell weight	:	33 tons
Net weight increase, due to replacing member ends with joints	:	20 tons
Maximum stress in joints	:	below 19,000 lbs/in <sup>2</sup>

Figure 8 shows an example of one of the joints for the reflector structure. The tower structure is less complex than the reflector and conventional welded joints are used.

The methods of fabricating the joints have been studied and seem straightforward. The shells will be cast in two halves using Austenetic Manganese Steel (ASTM-A-128-64) which has a yield strength of more than 50,000 lbs/in<sup>2</sup> and which is weldable to Cor-Ten. The two half spheres are welded together and member ends (which will be tapered castings if neces-

sary) are welded to the spheres. Complete joints will be stress-relieved in the fabrication shop.

(c) The panels (Collins Yang and S. von Hoerner, Reports Nos. 40 and 41). The panels bridge the 60 homologous reflector structure points (Figure 7) and in turn each panel carries between 56 and 80 reflector surface plates. The radially symmetric arrangement of the 60 homologous points means that four panel designs only are required--an outer ring of 16 (Panel A, the next ring of 16 (Panel B), the next ring of 8 (Panel C) and the inner ring of 4 (Panel D).

The requirements placed on the panels are quite strict, as the following list shows, and their design was a considerable task in structural design and analysis. The panels must:

(i) Carry the homologous behavior of their 60 support points through to the points of attachment of the surface plates to the panels. This must be realized under the applied loads of their own dead load, the surface plate dead load and the loads imposed on the panels by the reflector structure as it in turn deflects.

(ii) Maintain the accuracy of the surface plate support positions under operating wind conditions.

(iii) Be adequately strong to withstand survival loads due to wind, snow or ice.

Most of the design problems arose in meeting the first of these conditions. Two principles were followed: (1) The dead loads should move the surface plate points by equal amounts in a direction parallel to the reflector axis and (2) the forces exerted on the corners of the panels by the rest of the reflector structure should not move the surface points at all in this same direction. These conditions were met by using the concepts (von Hoerner 1967(a) of "equal softness" for (1) and "pressure-stable cells" for (2). The analysis used in the design was "trial and success" rather than an attempt to use a complete homology program, since the required accuracy could be met by this method. A standard structural analysis computer program was used throughout the analysis, but the final designs were reanalyzed by using frame and truss models, which gave very similar results. Since a truss model assumes a pin-jointed structure and a frame model allows for joint stiffness, their agreement shows that joint stiffness is unimportant.

Figure 9 is an example of one of the results of this process; it shows the geometry of the members which go into each of the 16 "B" panels. Report No. 40 gives the detailed results (in the form of joint coordinates and member sizes) for each of the four types of panel.

The panels will be fabricated from Cor-Ten pipe. No complications are expected for the internal joints; the connections between the panels and the 60 reflector structure points have been given special consideration and a suitable welded connection has been proposed.

The performance of the panels under dead loads, operating wind forces and thermal effects has been evaluated and the results are

THE GEOMETRY OF THE B-PANELS

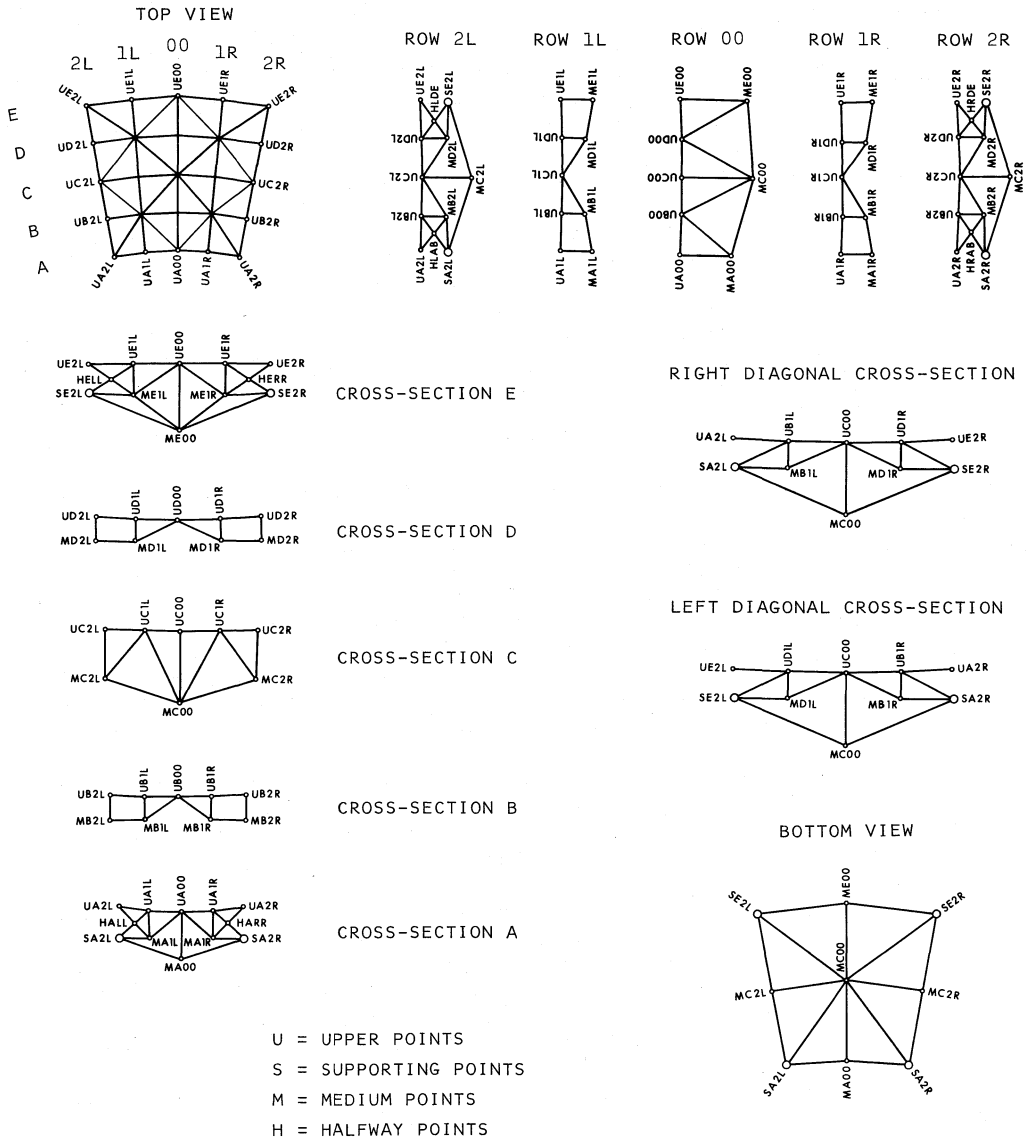


Figure 9. The geometry of the B-panels.

included in Chapter III. It is sufficient to note here that the dead-load panel deflections add an RMS inaccuracy of 0.002 inches (0.051 mm) to the overall surface accuracy. Similarly, the adequacy of the design to meet the survival conditions has also been satisfactorily determined.

#### 5. The Surface Plates, Their Fabrication and Setting

(a) The requirements the plates must meet. The reflecting surface of the telescope is formed by the surface plates, each of which is mounted by adjustable screw jacks to the panel structures. In a highly precise telescope the surface plates must meet a set of demanding requirements.

(i) The individual plates must have a high-reflection coefficient and a very small transmission coefficient for millimeter-wave radio waves.

(ii) The shape of each plate must conform closely to the shape of that part of the parabolic surface it represents. The shape should not deform seriously under operating wind and temperature conditions. The shape may deform under the survival snow, ice, and wind loads, but the plates, after such loading, must return accurately to their original shape.

(iii) The surface plates must be capable of being manufactured at reasonable cost. They must be capable of being transported to the telescope and mounted on their panel support points without undue risk of damage or loss of surface accuracy, nor must these operations be unduly expensive.

(iv) A means must be found whereby the plates can be measured and adjusted after they have been mounted on the telescope to conform to the parabolic reflector surface with the required accuracy. (This is a requirement for an accurate measuring technique rather than for a property of the plates themselves. It does, however, affect some characteristics of the plates.)

(b) Meeting the requirements. The first requirement is easily met if the reflector surface is a good, highly conducting sheet of metal without holes or large gaps. The use of very fine mesh or perforated sheet would be possible, but for millimeter wavelengths the holes have to be so small that no appreciable reduction of wind forces results. Equally, very mild ice or snow conditions easily block such fine holes. Therefore, solid aluminum is selected for the plates. This requires that the corner mounting arrangements must allow for the differential expansion of the surface plate and its steel support structure. This the present design does satisfactorily. To keep radio leakage low, the gaps between the plates, when mounted on the telescope, are kept to about 1.5 mm (0.06 inches). This is adequate to avoid appreciable loss of antenna gain or any noticeable increase of antenna temperature due to ground

radiation reaching the receiving horn through the surface of the reflector.

Meeting the next three conditions has required a considerable amount of work; the performance of the instrument and its cost depend heavily on the success achieved. Therefore, more than one solution has been sought, and in what follows we will describe the two most attractive of these solutions.

To indicate the importance of the problem, we set out in Table 4 below reasonable estimates of the likely contributions to the surface error budget which may be allowed to arise from the surface plates.

Table 4. Estimated Surface Error Budget for the Reflector Surface Plates

Source of Error	Estimated RMS Error
Fabrication and test of surface plates at the manufacturer	$\pm 0.003$ inch $\pm 0.076$ mm
Setting accuracy of the plates on the telescope	$\pm 0.005$ inch $\pm 0.127$ mm
Root sum square value of all other contributions (subreflector, gravity, wind and temperature effects on the plates and structure)	$\pm 0.006$ inch

In Chapter III, we summarize the surface error budget which we expect the telescope to meet, and Table 4 is only presented here to show what small parts of the total are likely to be permissible for the surface plate fabrication and setting. The root sum square of the figures in the last column is 0.212 mm, approximately the design figure given in Table 1, so that the surface plates must be fabricated and set to about the accuracies given in Table 4.

(c) The NRAO surface plate (S. von Hoerner Report No. 38). A design for a surface plate has been made at NRAO and typical plates have been fabricated and tested. The results show that such plates meet the requirements already stated. The work has been extensive and the final results are given in the above-referenced report.

The surface of the telescope will consist of 17 concentric rings of surface plates (see Figure 7); the total number of plates is 2912. Most of the plates have a length of about 74 inches; the four inner rings have plate lengths of about 63 inches; the widths of the plates vary from ring to ring. As the following Table 5 shows, between 32 and 256 plates

fall into each of the 17 groups of plates. The total surface area of the plates is 38,258 sq. feet (3554 sq. meters).

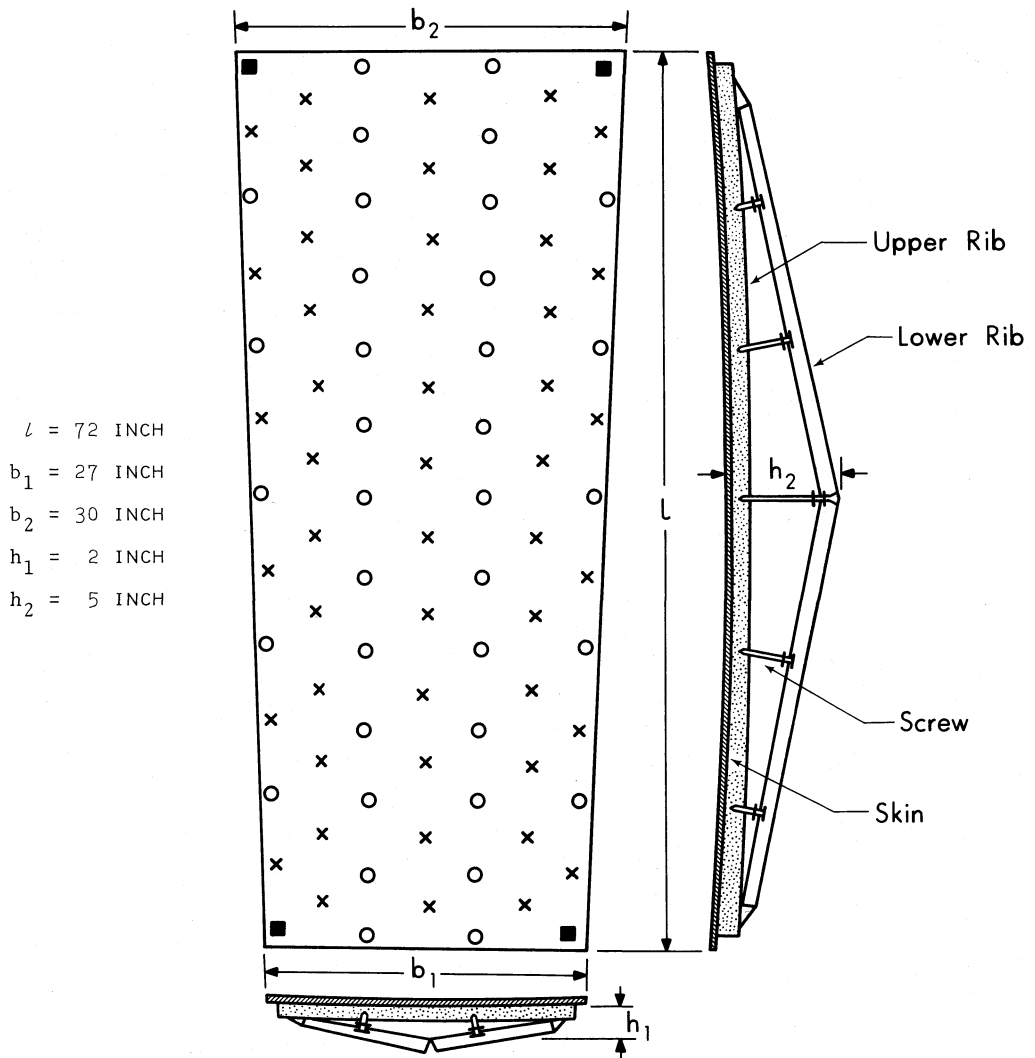
Table 5. The 17 Groups of Surface Plates

Ring Number	No. of Plates in Ring	Length of Plate	Width of Plates in Inches	
			Lower Edge	Upper Edge
1	32	63.08 inches	25.5	37.9
2	64		18.9	31.2
3	64		25.1	31.2
4	64		31.2	37.4
5	128	74.39	18.7	22.3
6	128		22.3	25.8
7	128		25.8	29.4
8	128		29.4	32.9
9	128		32.9	36.3
10	256		18.2	19.9
11	256		19.9	21.6
12	256		21.6	23.3
13	256		23.3	24.9
14	256		24.9	26.6
15	256	26.6	28.2	
16	256	28.2	29.8	
17	256	29.8	31.4	

The design of the NRAO surface plate is shown in Figure 10, and one of the test plates is shown in Plates 2 and 3. The engineering drawing of a test plate (56D00086) is in the Appendices. The plate is made of an aluminum skin, 0.125 inches thick, supported by a series of upper ribs riveted to the skin and then by a system of lower ribs below the skin. All ribs are aluminum. The upper ribs and skin are connected to the lower ribs by a total of 36 adjustment screws; by turning these screws the surface plate is adjusted to conform to the required shape. The skin before adjustment is a routinely manufactured flat sheet. The design has been evolved by various tests made on specimen surface plates with various detailed differences in design. The best design was adjusted and tested as follows:

(i) The adjustment screws were roughly set by bending the surface plate over a rod placed first along its long center line, then along its short center line.





- 4 CORNER POINTS FOR EXTERNAL ADJUSTMENT ON TELESCOPE
- 36 SCREWS FOR INTERNAL ADJUSTMENT IN FACTORY
- × 48 INTERMEDIATE POINTS FOR ADDITIONAL MEASUREMENTS

Figure 10. The NRAO surface plate.



Plate 3. Photograph of the NRAO surface plate.



Plate 2. Photograph of the NRAO surface plate.

(ii) Individual adjustments were made to the 36 screws; the surface was supported at its four corners (arranged to lie in a horizontal plane) and the surface contour was measured using a precise level and vertical scale. The measurement accuracy of this system (RMS value of repeatability) was  $\pm 0.0006$  inches ( $\pm 0.015$  mm). A total of 88 points were measured on the surface (see Figure 10). After adjustment a typical value for the RMS value of the departures from true parabolic shape was 0.0024 inch (0.061 mm). The adjustment screws were locked by an epoxy cement when the adjustment process ended.

(iii) Hysteresis effects due to heavy loads were investigated by having a man walk on the plate. The plate was mounted skin up on its four corners, walked on for a few minutes and measured on its measurement jig. The plate was turned over and the process repeated. The whole cycle was repeated five times. From the skin-up and skin-down measurements, the RMS departure from its original shape was found to be 0.00067 inch (0.017 mm). This showed that for such loads (which exceed 200 pounds per square foot) the plates deform elastically and return very accurately to their original shape when the load is removed.

(iv) Gravitational deformations were measured by applying a known load uniformly over the surface (in the form of heavy steel nuts) and observing the deflections. This information was needed also so that the wind-induced deflections could be calculated. The results of these calculations show that the effect of an 18 miles per hour wind in deflecting the surface plates adds an RMS value of 0.0006 inch (0.015 mm) to the total telescope surface error budget.

(v) Effects of temperature differences on the surface plates were measured. These are described later in Chapter III, Section 4(c).

This design of surface plate appears to be entirely satisfactory. The fabrication costs have been studied. The actual fabrication procedure prior to surface adjustment does not require very close manufacturing tolerances, since the final accuracy is achieved by adjustment. The measuring technique used at NRAO would certainly not be used for setting and testing in a fabricating shop; quite simple automatic direct reading devices can be used to measure the surface contours. Such techniques are well-known in industry. At NRAO, six man-hours were required to adjust and test one surface plate. Even if this were required in quantity production, the cost per square foot of surface would not be excessive. Each plate is about 12.5 sq. feet of surface and weighs about 50 pounds.

As a final note, it is interesting that both the precise 22-meter (72 feet) antennas built in the USSR use a very similar method of setting the surface. The newer antenna, in the Crimea, has about 40,000 screw adjustments operating on its surface, and (see Table 18) achieves an RMS surface accuracy of 0.005 inches (0.12 mm).

(d) Alternative techniques for fabricating surface plates. Despite the success of the NRAO-designed surface plate, the search has continued for other possible means of fabricating the surface. The search was partly prompted by the continued improvement in fabrication techniques and machines used for a variety of tasks in making precisely shaped objects. The aerospace industries have had to meet difficult challenges in making parts for high-performance aircraft and for launch and space vehicles. Large digitally-controlled machines which can shape surfaces in three dimensions are quite common. Techniques of stretch-forming metal sheets, producing bonded metal honeycomb material or mold-forming materials such as fiberglass, are continually being improved. It was therefore desirable and prudent to investigate various other techniques, particularly those which exist in industry, to find what alternative methods for surface-plate fabrication exist.

Accordingly, studies have been carried out under contracts with the Western Development Laboratory Division of Philco-Ford Corporation and the Rohr Corporation to investigate a variety of other possible fabrication techniques. Reports resulting from these contracts are in the Appendices. We will therefore list the fabrication techniques which have been considered and then describe briefly one of the most promising.

The two studies covered the following possible techniques:

- (i) The NRAO design already described.
- (ii) A stretch-formed aluminum skin is attached to a conventional welded aluminum support framework. The skin is thick enough so that the surface (which is within about 1 mm of the correct shape) can be machined to the required tolerance, using a numerically-controlled (N/C) machine tool.
- (iii) An aluminum support frame is fabricated and the upper surfaces of its ribs are machined, using N/C, to the required accuracy. A stretch-formed aluminum sheet is then attached to these ribs.
- (iv) A mold of the required shape to be used as a master pattern is made by using centrifugal force applied to a quick-setting plastic material. (A process of this kind was used some years ago to make small reflectors.) From such a mold fiberglass surface plates with sprayed metal for reflection are produced. An alternative to this technique is to make the molds on an accurate N/C machine.
- (v) A conventional surface plate and support structure is re-surfaced with a thin layer of metal-sprayed fiberglass. The metallized fiberglass surface comes from and has the accuracy of a precisely made mold. The requisite strength comes from the aluminum support structure.
- (vi) The surface plate is fabricated complete from bonded-aluminum honeycomb material.
- (vii) A complete surface plate and support structure is cast from a suitable type of aluminum (A356-T61 for example). The surface is machined to shape on N/C machines.

The studies have shown that several of these techniques are possible; one of the most promising when all factors, particularly cost, are considered is (vii). We therefore describe this in more detail.

(e) The machined-contour surface plate (Philco-Ford WDL Division Report). The first step in this process is to make a casting in aluminum of the entire surface plate and support structure. A typical structure is in Figure 11, where the stiffening ribs below the surface are shown. Such a casting can be made in a sand mold; the costs are not high and adequate dimensional accuracy (for this first step) can be achieved. The technique is widely used; it results in a structure which has high stability for machining and good rigidity. A material such as A356-T61 has excellent characteristics for casting and a yield strength of about 30,000 psi. Dimensional tolerances from the cast run about  $\pm 0.030$  inches ( $\pm 0.76$  mm) and the surface roughness is about 300 micro-inches.

The surface is then machined to the required contour on N/C skin mills. These work to within 0.0005 inch (0.013 mm) of the data recorded on tape and are capable of meeting the required surface tolerance of the plate. They are much used in the aerospace industry; for example, the Boeing Corporation operates machines with work tables 130 feet in length; these machines could work two surface plates at a time.

More esoteric machining methods are used in the industry; electrochemical, electrical discharge or chemical are some examples, but the N/C machines meet the task at not-too-great cost.

(f) Setting the plates on the telescope.

(i) Methods of measuring the surface. The surfaces of large reflector antennas have been measured and set in a variety of ways; for a recent survey see Findlay (1971). Small antennas for millimeter waves have been measured using the machines with which the surface was made, but such methods are not available for dishes of more than about 10 meters in diameter.

Larger antennas must be surveyed after they are built. Such surveys are usually first made with the antenna pointed to the zenith and the methods so far used fall into three classes. Figure 12 shows the principle of these methods.

The most commonly used (the "range-angle" method) has been to measure the angle  $\theta$ , using a theodolite T placed a distance  $h$  above the vertex of the dish. The line VF may be established by sighting on F or, more usually,  $\theta$  is measured by reference to the local gravity vertical. Then, either the distance VP or the distance from V to P along the dish surface is measured with a surveyor's tape. It should be noted in this and in the methods that follow, V and F need not be the exact positions of the reflector vertex and focus, since enough targets are measured to solve, eventually, for the departures in position of the targets from the best-fit parabolic surface and also for the positions of the focal

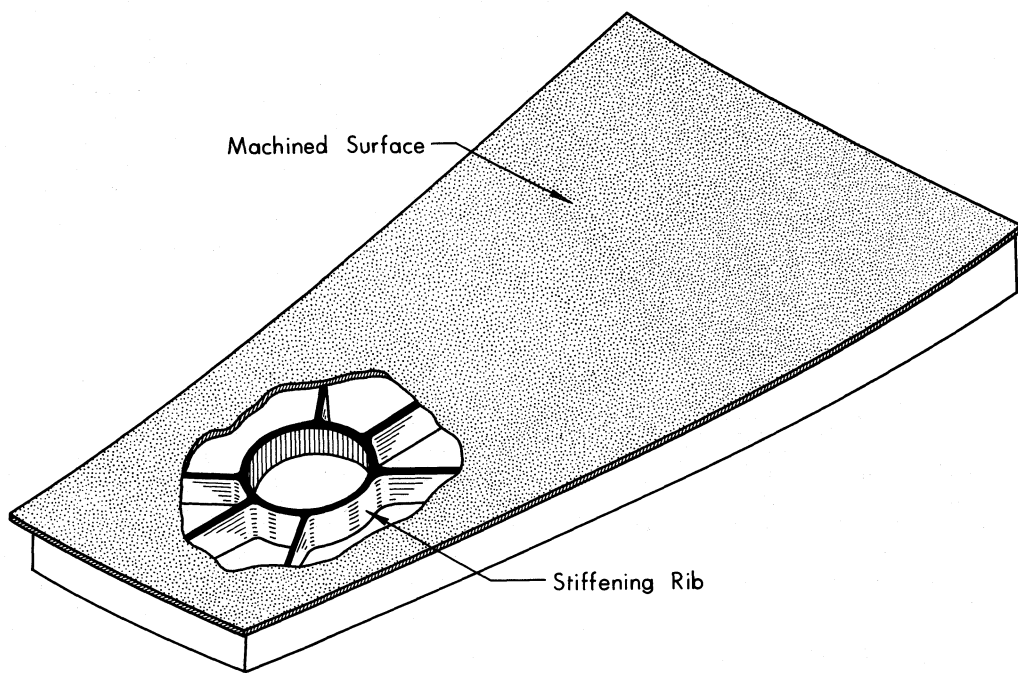


Figure 11. The machined contour surface plate.

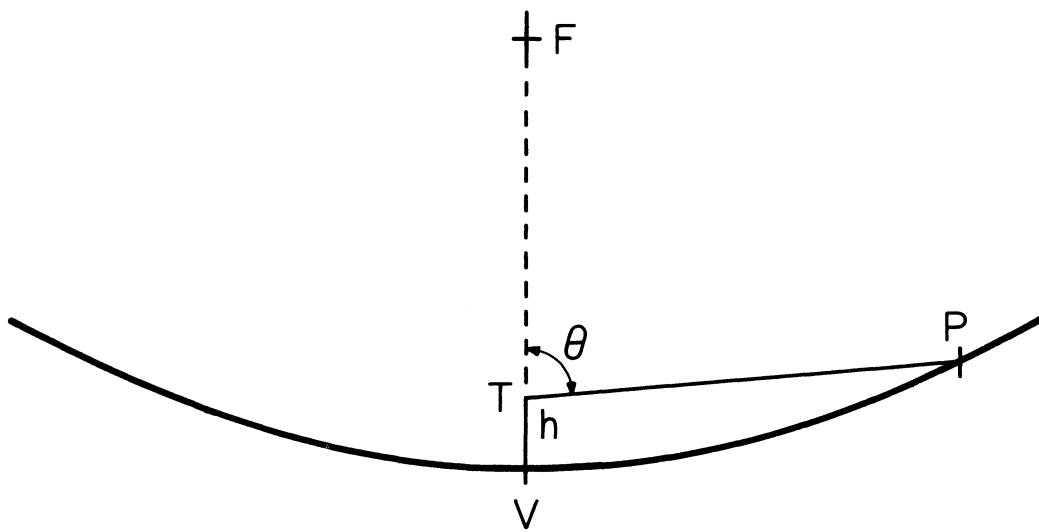


Figure 12. Measurements of the antenna surface.



point and vertex of this paraboloid with respect to the chosen position of V. This technique has been widely used, and at NRAO, for example, using a good theodolite and a contour drilling tape, a measurement accuracy of  $\pm 0.01$  inches ( $\pm 0.25$  mm) has been achieved on the 140-foot reflector.

Another method has been to use two angle measures, one made from T at h and one at a greater height h'. The difference (h'-h) is accurately measured and the range TP deduced. This may be called the "range-finder" method, and it has not been found to be as good as the first.

The third method which only measures distances (the "range-only" technique) measures VP and FP with precise ranging techniques, usually using modulated light-beam range-finders. It has been tested and shows promise (Findlay 1971).

(ii) The methods proposed for the 65-meter telescope. The surface of the telescope will be set by one or both of two methods; the first is an improvement of the range-angle method and the second is a range-only technique. As with all reflector telescopes, the final tests will be the measurement of the gain (aperture efficiency) of the reflector at short wavelengths. This measurement confirms the reflector accuracy, but cannot in its simplest form give information on how to correct the surface adjustments\*.

(iii) Surface setting by range-angle methods. The first stage in setting the surface plates will start when the reflector structure is complete and the panel structures are mounted. (These are the space frames, about 30 feet in linear size, on which the surface plates are to be mounted.) The reflector will be pointing to the zenith at this stage. The 60 homologous points on the 44 panels (refer to Figure 7) will be measured by the range-angle method. This can be done using a tape and theodolite, since an accuracy of about one or two millimeters is required. This measurement is intended mainly to confirm that the structure is geometrically capable of accepting the surface plates and that sufficient adjustment range will be available on each plate. It will also be used, however, to make rough settings of the adjustment jacks for each surface plate, so that when they are erected the surface should be within perhaps two or three millimeters of its required position.

After all surface plates are mounted, targets suitable for range-angle measurements will be mounted on the plates. These targets will be similar to those used at NRAO for 140-foot telescope measurements. They fit into holes drilled into the surface plates; these holes are drilled

---

\* B. G. Clark has suggested using an extension of this technique which will allow the reflector errors to be corrected. It involves measuring the amplitude and phase of a wave reflected by the dish from a point source--in principle it can measure the reflector profile.

using a contour drilling tape laid on the reflector surface, so that the distances of each ring of targets from a central reference point (V in Figure 12) is known. A sketch of a typical 140-foot target is shown in Figure 13; for the 65-meter telescope the reference dots on the target will be replaced by thin engraved lines. One target will be mounted on each one of the surface plates at each corner where four surface plates come together. We deal later with the method by which all four corners are adjusted to this one target.

At this stage the telescope surface has 18 rings and a total of 3168 targets. The range-angle method is next used in a refined form to measure the target positions. The angle measure is made by using the Zeiss pentaprism system (Kühne\*1966). In principle it replaces the theodolite in the conventional method with a quartz pentaprism, a separate pentaprism being used for every elevation angle to be measured. Figure 14 shows the system. The pentaprism is mounted on a rotating table, the axis of which has been optically aligned with the axis of the fixed alignment telescope. This axis becomes the reference axis of the adjusted surface. All targets in a given ring are observed by rotating the prism table. The target face is marked with graduations and the departure of the target position from the angle  $\theta$  is measured by reference to these graduations. Readings can be semi-automatic; the prism table rotation can be programmed. It is not necessary that the prisms be manufactured to precise values of  $\theta$  (which would be very expensive) but the value of  $\theta$  for each prism must be accurately known. Departures of  $\theta$  from the value required are allowed for by making small (known) changes in the distance SV for each prism.

The method has been used on at least two telescopes, the 25-meter dish at Raisting and the 34-meter dish at Werthoven. In neither case was our standard of accuracy needed, but it seems reasonable that the method can have the following measurement accuracy:

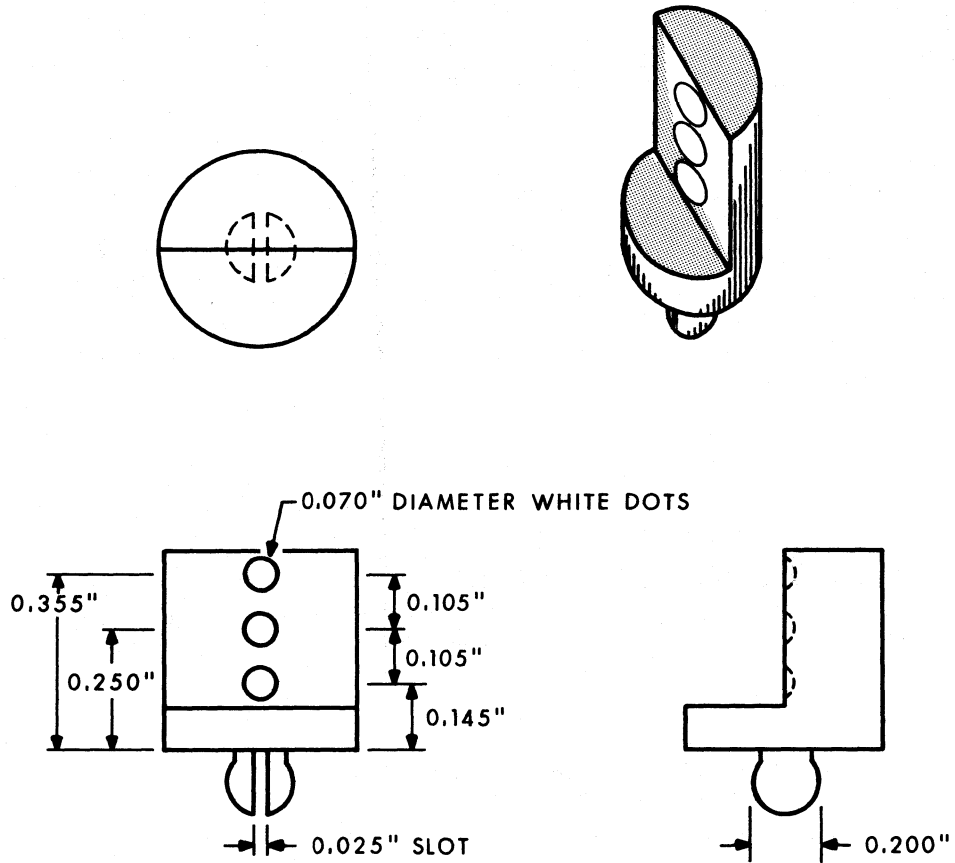
Measurement of distance along the surface from V to P—  
1 part in 125,000 plus a constant error of  $\pm 0.2$  mm.

Measurement of  $\theta$ , including errors of measuring the pentaprisms— $\pm 0.75$  arc seconds.

Kühne's paper gives an expression for the RMS error  $m_n$  of the position of P measured along the dish normal n (Figure 14)

---

\* We are happy to acknowledge the assistance of Mr. Kühne in providing further information about the pentaprism system.



NOT TO SCALE

Figure 13. The targets used for measuring the surface of the 140-foot telescope.

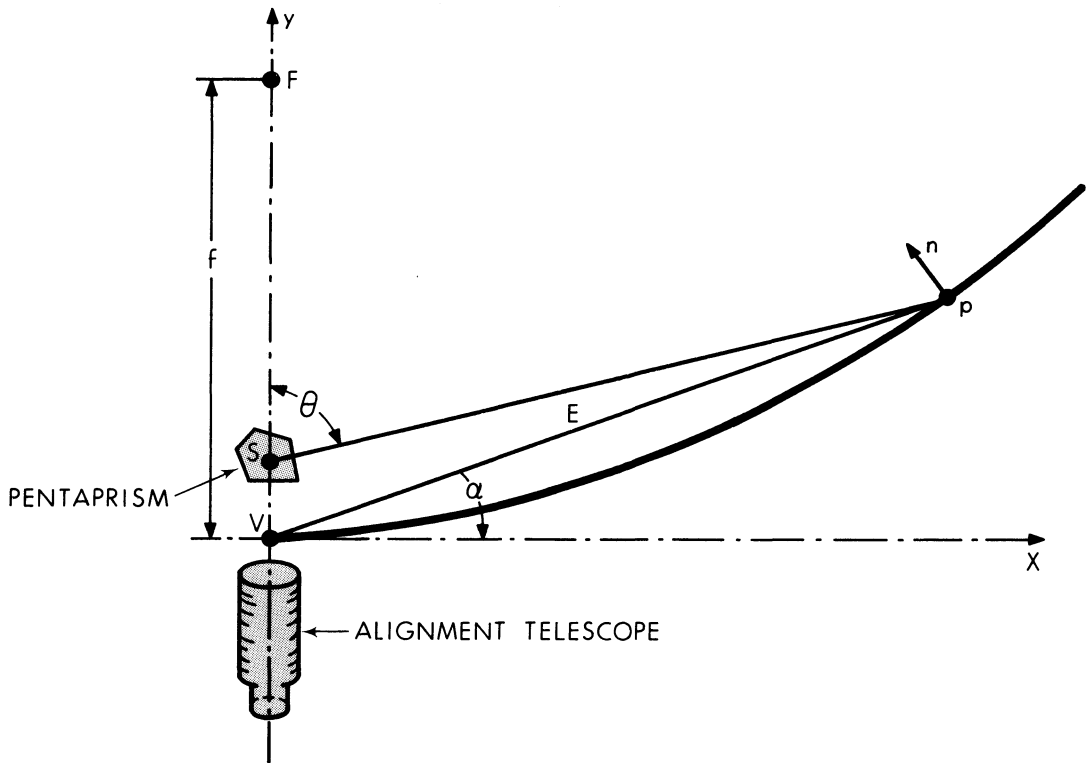


Figure 14. The use of a pentaprism to measure the antenna surface.

$$m_n = E \left\{ \left( \frac{m_e}{4f} \right)^2 + m_\alpha^2 \right\}^{1/2} \quad \text{II(1)}$$

where  $m_e$  is the RMS error in measuring VP (= E) and  $m_\alpha$  is the angular RMS error.

$$\left. \begin{aligned} \text{If we take } m_e &= 0.2 + 8 \times 10^{-6} E \text{ (} m_e \text{ and } E \text{ both in mm)} \\ m_\alpha &= 0.75 \text{ arc seconds (} 3.64 \times 10^{-6} \text{ radians)} \end{aligned} \right\} \quad \text{II(2)}$$

and apply II(1) to our 18 target rings, we get the following Table 6.

Table 6. Measurement Errors in the Pentaprism Method

Target Ring	No. of Targets	E in Meters	RMS Error $m_n$ in mm
1	32	3.3	0.0138
2	64	4.8	0.0204
3	64	6.4	0.0275
4	64	7.9	0.0345
5	128	9.4	0.0416
6	128	11.4	0.0514
7	128	13.3	0.0611
8	128	15.2	0.0711
9	128	17.2	0.0821
10	256	19.0	0.0922
11	256	20.9	0.1032
12	256	22.7	0.1140
13	256	24.5	0.1258
14	256	26.3	0.1375
15	256	28.1	0.1497
16	256	30.1	0.1635
17	256	32.0	0.1775
18	256	33.9	0.1913

Note that there is one more target ring than the 17 rings of plates shown in Table 5. This is due to the fact that target rings occur on the inside edge of the plate ring No. 1 and the outside edge of plate ring No. 17.

From the last column we derive the  $\log$  value of the RMS measurement error when all 3168 targets are measured with their associated RMS errors ( $m_n$ )

$$\begin{aligned} \text{RMS measurement accuracy} &= \left\{ \frac{1}{3168} \sum_i n_i m_{ni}^2 \right\}^{1/2} \\ &= \pm 0.125 \text{ mm (0.0049 inches)} \end{aligned} \quad \text{II(3)}$$

The range-angle method thus seems able to achieve the requisite measurement accuracy. A few practical comments should be made, however. First, at each target we have to adjust the corners of four plates to the single target. This can be done by a simple jig which by reference to gravity using a spirit level carries the required elevation from the one target to the four corners. Second, it will not be possible to measure all the targets in one night. The measurement time per target will be about 30 seconds, so that on one night only a few hundred targets can be measured. Thus the setting process will be referenced on each night's measurement to targets on the plates above the 60 homologous points, and blocks of other targets will be measured with respect to these master targets.

(iv) Setting the surface by range-only methods. A method has been developed by which the surface can be surveyed and adjusted by measuring the distances TP and FP (Figure 12). T is now to be regarded as a fixed reference point near the vertex of the dish, and F is a fixed point near the focal point. The method uses a modulated light-beam distance measuring equipment mounted near V. The distance from the instrument reference plane to P via a mirror at T is one measurement; T is then removed and the distance from the instrument to P via a mirror at F is measured. To discuss the practicality and accuracy, we first consider the properties of distance-measuring systems for the task. It is clear that an accuracy of about 0.1 mm (0.004 inch) is required to achieve our goals. The requirement is less strict for the measure of TP, but is approximately the same for all targets in the measurement of FP.

Modulated light-beam distance measuring systems have been used in surveying for about 20 years, but they have mainly been designed for use over distances of several miles. Their use is described, for example, in the book by Saastamoinen (1967) where the Geodimeter and Tellurometer are discussed in detail. Two instruments made by Zeiss (Leitz 1969) and the Mekometer II (Froome and Bradsell 1966) are also of interest in showing the accuracy of the techniques and the ease with which the instruments can be made to read out automatically in digital form.

The principle involved is simple. A high intensity light beam is amplitude modulated at a frequency which can be a few MHz up to about 500 MHz. This beam is sent over the long path to be measured and

also over a short reference path. Figure 15 illustrates the method. The two returned light signals fall on photodetectors; the two outputs of which are identical waveforms at the modulation frequency  $f$ . The phase difference between these waveforms is accurately measured, usually by mixing each with the same local oscillator to give waveforms at the chosen intermediate frequency. The difference ( $L$ ) in the one-way lengths of the long and short paths can be written

$$L = \frac{1}{2} (n + \epsilon)\lambda \quad \text{II(4)}$$

where  $\lambda$  is the wavelength in air of the modulation frequency  $f$ ,  $n$  is an integer and  $\epsilon$  a fraction less than unity. As an example, suppose  $f$  is 500 MHz,  $\lambda = 60$  cm and for a measurement where  $L$  is already known to a few centimeters,  $n$  is known. The phase difference between the two waveforms measures  $\epsilon$ ; good electronic techniques allow a measurement accuracy of  $\epsilon$  to about 2 in  $10^4$ , so that  $L$  is known to  $\pm 0.06$  mm. Small corrections for the refractive index of air can easily be made when this sort of accuracy is required over paths of up to 100 meters in length. The system is thus capable of making range-only measurements on the telescope to our required accuracy.

The method proposed is to measure with such an instrument mounted near the dish vertex  $V$  (Figure 12) the path lengths  $VTP$  and  $VFP$ . Rotating tiltable mirrors mounted at  $T$  and  $F$  allow of these paths being followed to all targets. The targets themselves have reflecting faces to return the  $TP$  and  $FP$  rays along their own paths. The range indications and target identifications are produced in digital form and stored on tape.

The mirror at  $F$  will only be as stable in position as the feed support allows. Measurements will be made in low wind conditions, thus  $F$  moves only because of slow temperature effects in the feed legs. Readings of groups of targets are taken in blocks of 20-50 (in a total time of about 10 minutes) and each block of readings permits a solution for the target errors and for the position of  $F$ . Thus slow movements of  $F$  can be eliminated from the measurements.

A 550-MHz distance-measuring instrument has been built and tested at NRAO. It has the required stability and accuracy; its output is digital in steps of 0.01 mm. This is achieved by the correct choice of modulation and digit frequencies. Figure 16 is a block diagram of the instrument.

This method has been developed as an alternative or a possible improvement over the range-angle system already described.

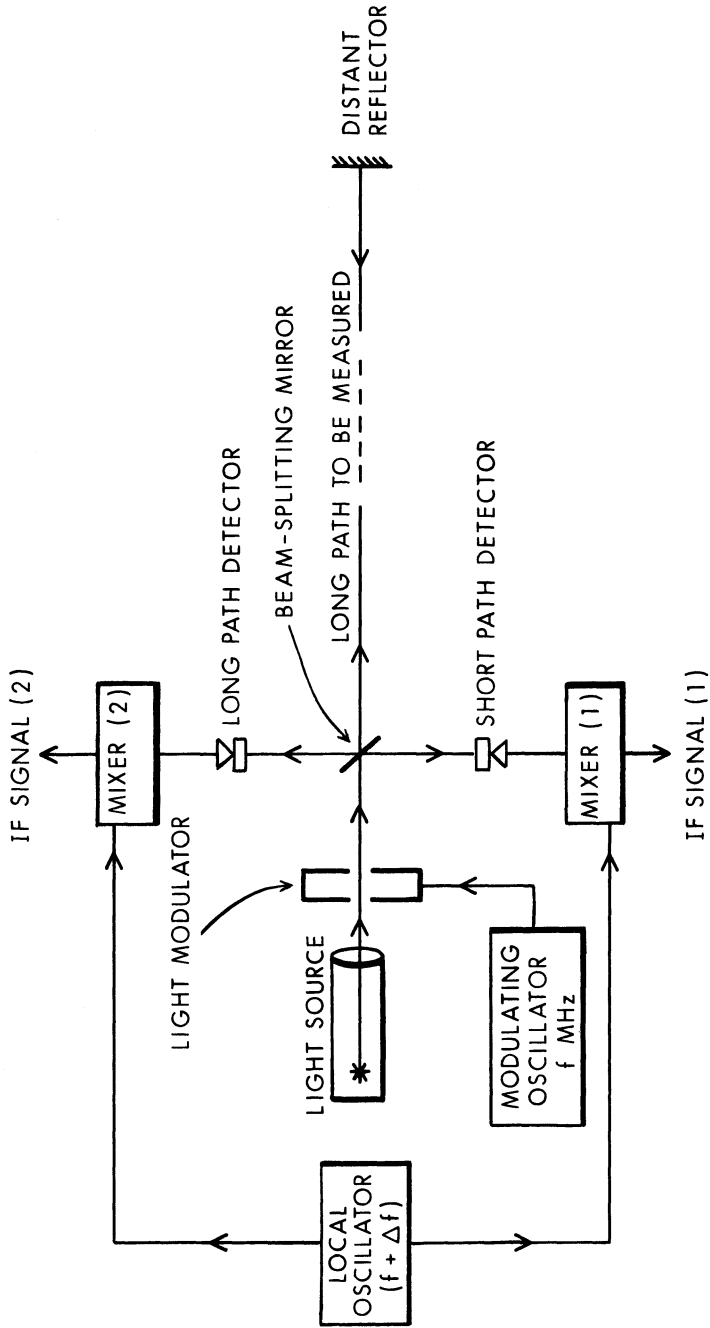


Figure 15. The modulated light beam technique for distance measuring.



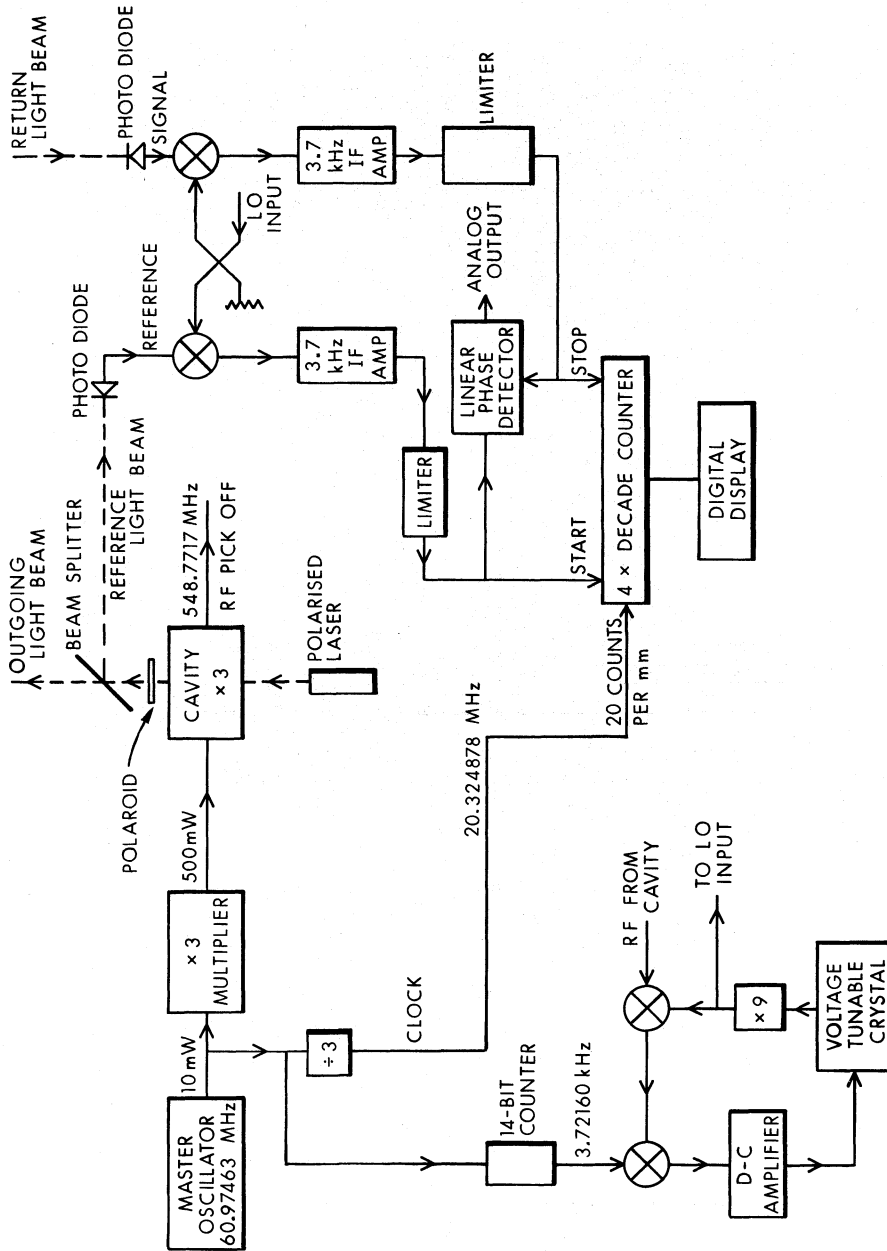


Figure 16. The NRAO modulated light beam system.

## 6. The Cassegrain System, the Feed Support, and the Observing Rooms

(a) The Cassegrain system (S. von Hoerner Report No. 31). The various considerations on which the choice of the parameters of the Cassegrain optical system depend are covered in the above-referenced report. We can summarize them as follows:

(i) The telescope will be used at longer wavelengths as a prime focus instrument, and at shorter wavelengths as a Cassegrain. The choice of the approximate wavelength at which the change takes place affects the choice of subreflector size, the design of the vertex mounted feeds, and these factors in turn are linked with mechanical designs of the instrument cabins and subreflector mount.

(ii) The homologous behavior of the main reflector carries with it the fact that the primary focal length of this reflector changes with the telescope's elevation angle. Also, the reflector axis of symmetry moves somewhat, as the elevation axis changes, with respect to the line joining the vertex of the reflector to the center of the apex of the feed support system. These motions require appropriate movements of the subreflector and feeds to be possible and the requirements for such motions affect the choice of the Cassegrain geometry.

(iii) In the Cassegrain mode, various types of beam switching and beam movement may be required for different observing programs. The telescope beam may be moved by tilting the subreflector so that if more than one feed is placed near the secondary focus the telescope can switch easily from one observing system to another. Periodic tilting or nutating of the subreflector can allow of various "on-off" observing programs which are used to reduce the effects of sky noise. The ability to perform these various beam movements depends on the size and inertia of the subreflector and so affects the choice of Cassegrain geometry.

(iv) The primary reflector focal length was fixed at the focal length/diameter ( $f/D$ ) ratio of 0.426 since this value is standard for all the larger NRAO telescopes. Thus, any front-end equipment used on the Green Bank telescopes will be interchangeable with the 65-meter telescope. This primary  $f/D$  ratio does not harm the Cassegrain performance of the 65-meter instrument, but thought has to be given to the dimensions of the feed horns likely to be used at the secondary focus. This again affects the choice of Cassegrain geometry.

(v) The effective aperture of the whole telescope is blocked by the subreflector and its support structure. The amount of this blocking which can be tolerated must be considered in the choice of geometry.

We will not follow through the method by which a suitable Cassegrain geometry was selected, but will only give the description and characteristics of the system proposed. Figure 17 shows the geometrical optics of the system. Parallel rays from infinity pass through the prime focus of the main reflector in the prime focus mode; in the Cassegrain

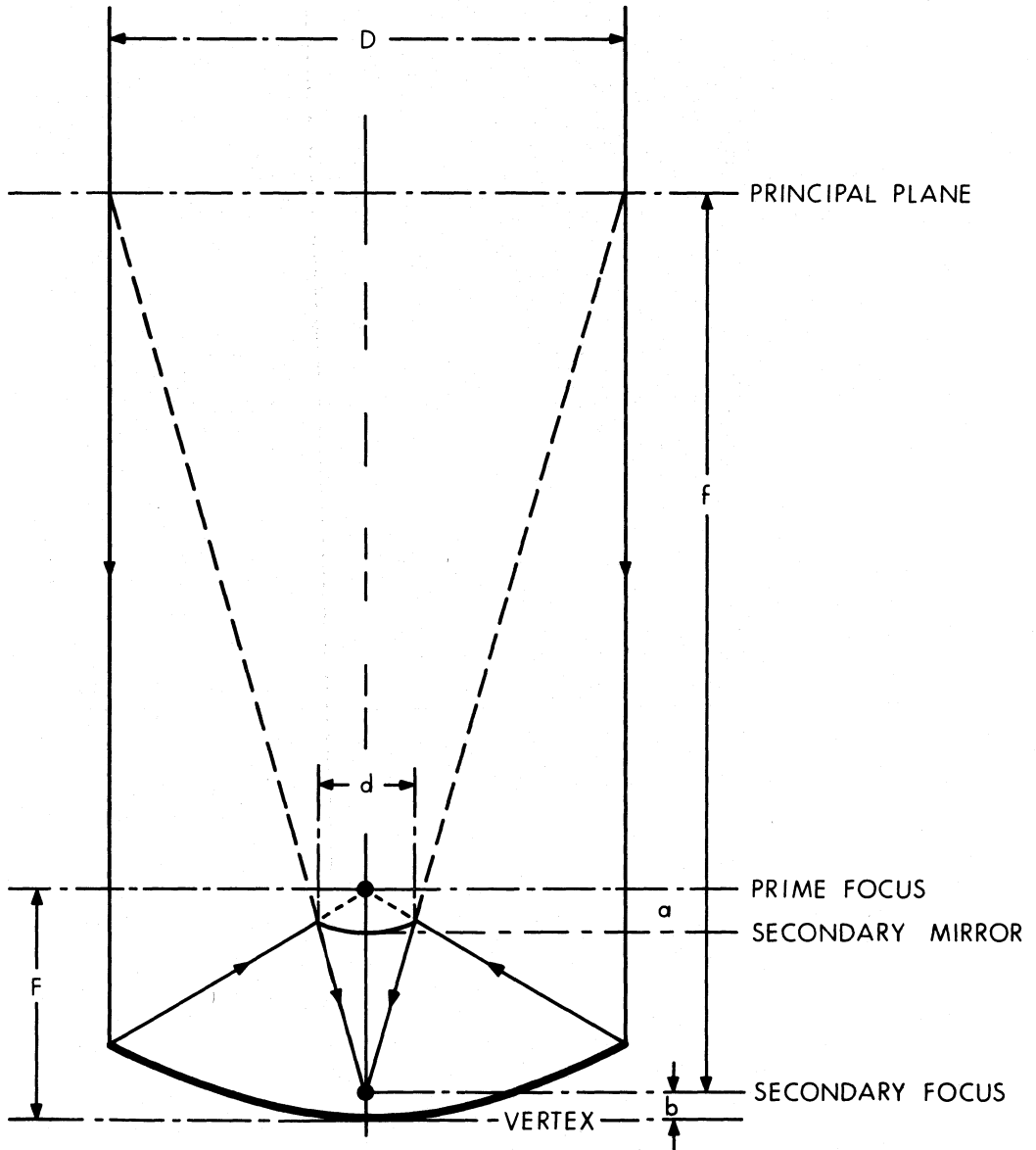


Figure 17. The geometrical optics of the Cassegrain system.

mode they are reflected to pass through the secondary focus. The primary focal length  $F$  is the distance from the primary focus to the main reflector vertex while the secondary focal length  $f$  is the distance from the secondary focus to the principal plane of the system. Thus the Cassegrain system can be considered to be a reflector of diameter  $D$  and a focal length  $f$  which is considerably longer than  $F$ . The ratio  $f/F$  is referred to as the magnification of the system. (Note that Figure 17 is not to scale, and is oversimplified--with such wide-angle optics principal planes become curves.)

The following Table 7 summarizes the dimensions and performance of the Cassegrain system.

Table 7. The Cassegrain System

Property	Value		
Main reflector diameter (D)	65.0 m (213.1 feet)		
Main reflector focal length (F)	27.70 m (90.88 feet)		
Subreflector diameter (d)	3.657 m (12.00 feet)		
Secondary focal length (f)	437.46 m (1435.3 feet)		
Magnification (f/F) or (M)	15.793		
Longest wavelength (lowest frequency) for use as Cassegrain	About 4 cm (7.5 GHz)		
Height of secondary focus above vertex of main reflector	1.524 m (5.00 feet)		
Distance from prime focus to vertex of subreflector (a)	1.559 m (5.11 feet)		
Approximate lengths and aperture widths of secondary feed horns at wavelengths of 3.5 mm and 3 cm	$\lambda$	Horn Length	Horn Aperture
	3.5 mm	34 cm	5.3 cm
	3.0 cm	2.9 m	46 cm
Lateral displacement of feed from secondary focus which is permissible before either the coma becomes objectionable or the spillover limits gain and increases noise seriously	$\lambda = 3.5$ mm	—about 115 cm (3.75 feet)	
	$\lambda = 3$ cm	—about 2 m (6.6 feet)	

The table demonstrates some of the advantages gained from the use of a Cassegrain with a magnification of about 15. The sizes of the feeds at the secondary focus are not unreasonable, yet quite large feed displacements from the vertex (as would be used, for example, if multiple feeds were used) are quite possible. In fact, the number of feeds which can be used for mapping and for short-wavelength surveys will most probably be limited by the cost and complexity of the radiometers and not by the radio telescope.

Finally, the subreflector itself should be considered briefly. It is a hyperboloid, with a focal length (focus to vertex) of 1.559 m (5.11 feet). The surface accuracy must be high; reflectors of this size can be fabricated with RMS surface errors of somewhat less than  $\pm 0.002$  inches ( $\pm 0.05$  mm) and this is the planned accuracy of the reflector. Its weight will be kept low to allow of its being moved rapidly in the modes needed for beam motion.

The subreflector will be mounted in such a way that it can be removed and replaced readily; this allows of rapid change-over between the Cassegrain and prime-focus modes of using the telescope. The mounting allows of a range of controlled movement of  $\pm 1$  inch (2.5 cm) in both the axial and lateral directions; it can be tilted and rotated to give a nutating motion. It can be positioned to an accuracy of  $\pm 0.002$  inches ( $\pm 0.05$  mm) in the axial direction and  $\pm 0.01$  inches ( $\pm 0.25$  mm) in lateral directions.

(b) The feed support (W-Y. Wong Report No. 42). The function of the feed support is to carry the prime focus cabin and all the equipment needed for observing with feeds at the prime focus. It also, in the Cassegrain mode, carries the subreflector. Both these tasks require that the feed support be as stable as possible against deformations due to its own weight and due to the dead loads of the equipment near its focus. It must also not deflect due to wind forces by amounts which would impair the pointing precision of the telescope. The effects of temperature differences between the legs of the feed support will also deform the structure; these effects must be calculated and, if possible, reduced to an acceptable value. The structure must, of course, withstand the survival loads due to wind, ice or snow.

The structure that meets these requirements is shown in Figure 18; its design was essentially determined by the need to keep the structural deformations small. It is a tetrapod, each of the four legs passes without interference through the dish surface. (This section is a tubular member to minimize the problem of clearing the neighboring panel structures.) The connection between this tubular member and the built-up leg structure is braced in four directions to the nearest surface support points. This bracing does not affect the dish surface accuracy to any appreciable extent. The four legs are built-up from tubular members (to minimize wind forces) and each leg is guyed at points near its

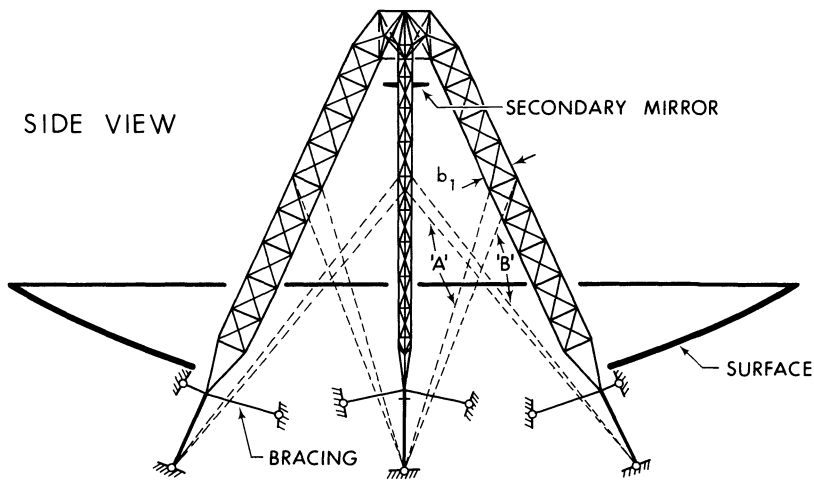
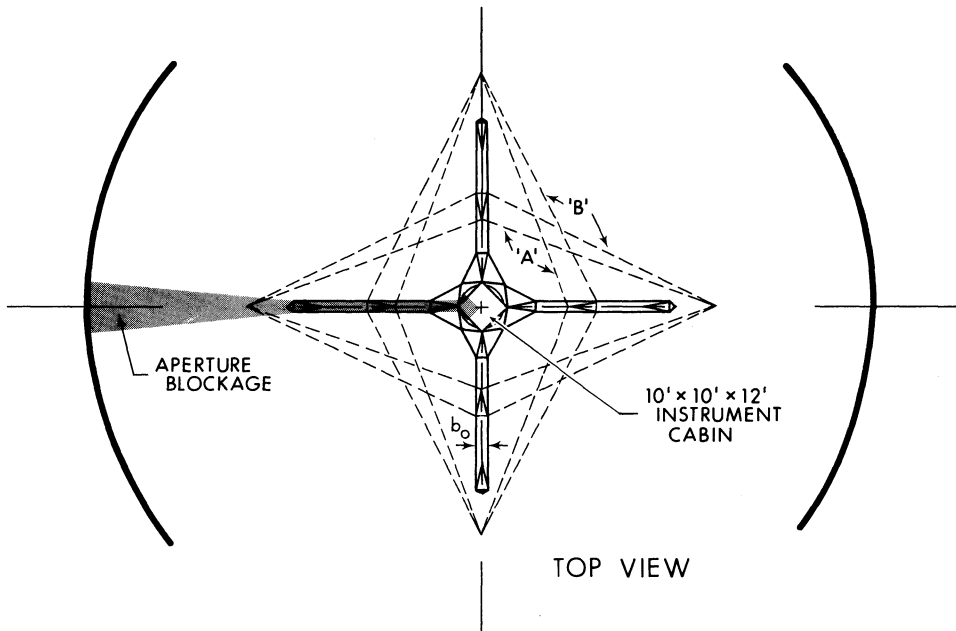


Figure 18. The feed-support structure.

center to increase its lateral stiffness. The guys terminate at the joints in the main reflector structure where the feed legs themselves end. The legs are quite deep structures ( $b_1$  in Figure 18 is 2.5 m or 8.2 feet) but their width ( $b_0$ ) has been kept fairly small (1.0 m or 3.3 feet) to reduce their blocking effect on the aperture.

The deflections of the feed support under gravity and wind loads have been calculated. The gravity deflections, when taken together with the movement of the main reflector axis as it deflects with changing elevation angle, are not serious and are, of course, removed from the overall pointing error budget in the calibration process. A steady 18 miles per hour wind deflects the feed support in such a way as to translate and rotate the subreflector. The beam shifts due to these movements have opposite signs; the resulting beam shift is calculated to be 1.08 arc seconds, and this figure is used in the computation of the total pointing and surface error budgets in Chapter III.

The long feed legs are the most sensitive parts of the whole telescope to the existence of temperature differences. Such differences between the legs influence the telescope pointing. For example, if we assume that the temperatures of the four legs lie at random within a temperature range of  $\pm 1^\circ$  F, the resultant pointing error is 2.0 arc seconds. This figure is used in the error budgets of Chapter III for the case of operation on a clear night. When the sun shines on the legs the pointing is considerably worse, as the error analysis of Chapter III shows.

The dynamical behavior of the feed support, with the loads of the observing cabin and subreflector, have been studied and a natural frequency at 4.2 Hz is found for oscillations about an axis parallel to the reflector axis. This is satisfactory.

The feed support and observing cabin give a total aperture blockage of 6.4 percent. This figure does not include the small effects of the guy cables, but it is quite acceptable.

The feed support is designed to be fabricated from the same type of steel used for the reflector and tower structure.

(c) The observing rooms. The telescope has observing rooms located at both the prime and the secondary focal points. Each is 10 feet square with a length of 12 feet. These rooms house the feed horns and front-end electronic equipment; they are insulated and have good temperature control systems. Each can carry about 10 tons of equipment.

The room just behind the prime focus is connected to the apex of the feed-support structure. It is provided with a mount for the standard-sized NRAO front-end boxes; this mount allows of rotation of the whole box about its axis and also permits the feed to be focussed. These movements are remotely controlled. Such mounts have been in use at Green Bank for several years.

The observing cabin at the secondary focus rotates as a whole about the axis of symmetry of the reflector. It extends about 5 feet (1.53 m) above the main reflector surface, so that its front wall lies approximately in the secondary focal plane. Several feeds can be mounted through this front face of the cabin; its 12-foot length is sufficient to accommodate the longest feeds required in the Cassegrain mode, and the telescope beam can be moved from one feed to another by tilting the subreflector. This arrangement, similar in principle to that used at the Goldstone 210-foot antenna, allows of rapid change-over between observing programs.

## 7. The Position Reference System

The purpose of the position reference system is to determine the direction of the telescope beam in the sky by reference to the usual system of astronomical coordinates. This is done in two ways; there is a coarse position system, which is used only to ensure that the telescope can be moved and roughly controlled at all times, and a precision position system which is precise enough to ensure the accurate pointing required for short wavelength observations.

(a) The coarse position system (SDL Report H-10, Chapter 10). This system uses 17-bit\* angle encoders, one mounted at the azimuth axis and one at the elevation axis. Both are driven by anti-backlash gears. This is necessary for the azimuth encoder, since the shaft center space is required for the passage of cabling. The elevation axis encoder could be axially mounted, but for uniformity it is made the same as the azimuth system.

(b) The precision position system. It is not easy to determine the position of the radio beam with the high precision required by measuring the angular positions of the telescope axes. The difficulties arise because the whole telescope structure, and in particular the towers, deflects under gravitational and wind loads and is deformed by temperature differences in the structural members. Many of these deflections can be arranged not to influence the pointing accuracy of the instrument if the reference position is chosen to be the point in space where the azimuth and elevation axes intersect.

This position is on the reflector structure, behind the reflector surface. (It is close to joint No. 56 and is often referred to in this way.) In order to measure the two angular coordinates of the telescope beam direction from this point it is necessary to carry a reference from the ground up to the axis intersection. This has been done

---

\* One bit corresponds to an angle of 9.89 arc seconds with this encoder.



in three large telescopes already (the instruments at Parkes, Goldstone and Algonquin Park) by building a central tower, shielded from wind or sunlight, from the top of which the direction in space of the reflector axis is determined by an optical system (the master equatorial as it is called).

The present design uses the same principle, but instead of using a central tower the position reference platform is fixed in angular position with respect to the ground by making the platform stay locked in direction to light beams projected onto it from stable light sources on the ground. Figure 19 shows the principle of the method. In practice, the system has been designed to use seven autocollimators firmly mounted around the outside of the azimuth track. (Drawing 111-D-011 shows the layout and the autocollimator mounting.) The seven light beams are reflected back to the autocollimators from a seven-sided mirror on the reference platform. The platform itself is supported from the reflector structure, but the mirror is free to rotate about two perpendicular axes (azimuth and elevation) with respect to the structure. The mirror assembly is driven about these two axes by torque motors and the angular positions of the mirror axis with respect to the telescope structure are measured with 22-bit angle encoders which give a resolution of 0.31 arc seconds. The seven-sided mirror is driven by the torque motors, using error signals from the autocollimators to control the servo-loop, so that the mirror faces remain normal to the light beams no matter where the telescope points.

The foregoing general description should be sufficient to describe the principles by which the precision position system works. Since the whole system is so vital to the performance of the telescope, it has been designed in detail and considerable care has been taken to estimate the probable accuracy of position measurement. In what follows the various parts of the reference platform system are described in more detail.

(c) The autocollimators (SDL Report H-10, Section 10.4). Each collimator must meet the following requirements:

(i) It must be capable of sensing simultaneously in both azimuth and elevation and misalignment of the light reflected from its mirror, as compared to the light projected onto the mirror.

(ii) It must operate in full daylight and at night over the required distance (about 200 feet) with adequate precision.

(iii) It must give error indications over an adequate range of misalignment angles and the error indications should be reasonably linear with angle over the angular range near perfect beam alignment.

(iv) It must sense the intensity of the reflected light so that when a light path becomes obstructed, information from the corresponding autocollimator can be rejected.

The D696 special two axis autocollimator made by Davidson Optronics meets these needs almost completely. Its range of daylight operation is somewhat smaller than is ideal, but this can be increased without much difficulty. The two axes use different wavelength light sources in the form of mercury and neon lamps. The instrument is sensitive to angular misalignments of 0.1 arc seconds and, among other outputs, it gives an error signal which is linear over a  $\pm 27$  arc seconds range of angular error of the mirror being referenced.

Seven such instruments will be mounted on strong supports around the telescope. Error signals from two autocollimators are sufficient to control the stable platform, but seven are needed since the light beams are, from time to time, obstructed by the tower and dish members of the telescope. The autocollimators are in temperature controlled enclosures; the possibility that their foundations may move due to long-term settlement or to more rapid heaving of the ground as the telescope rotates is allowed for by mounting a precise tilt-sensor on each autocollimator.

The effects of the atmosphere on the angular stability of the light path from the autocollimator to the mirror have been carefully studied. A single-axis autocollimator was used in a test at Green Bank lasting several months. The light path used was 185 feet long; one end was at ground level and the other was about 45 feet above ground on the upper deck of the 140-foot telescope foundation. The path was thus about the right length but at a lower elevation angle (about  $14^\circ$ ) compared to the  $31^\circ$  angle the final system will use (see Figure 19). Fluctuations in this lower-angle path can be expected to be greater than in a path of the same length at a higher elevation angle.

The light from the autocollimator was reflected from a mirror whose direction was controlled by a servo loop deriving its error signal from the autocollimator. The characteristics of this servo loop were very similar to those of the servo designed for use with the stable platform.

Thus the test showed the stability of the atmosphere optical path, but it also tested the servo design. The movements of the mirror and the autocollimator error signals could be separately measured to confirm the performance. Means were provided by adding angular disturbances to the mirror shaft, to simulate the effects of disturbances to the reference platform. The atmospheric effects were recorded in the form of measurements of the angular fluctuations of the optical beam. The recording system also derived the RMS fluctuations, and for part of the observations an autocorrelator was used so that the average power spectrum of the angular fluctuations could be measured. The system is described in more detail in reports by J. Payne (July 21, September 8, and November 29, 1970). Figure 20 shows a short section of a record of the angular fluctuations of the beam, and Figure 21 is a typical power spectrum of the fluctuations.

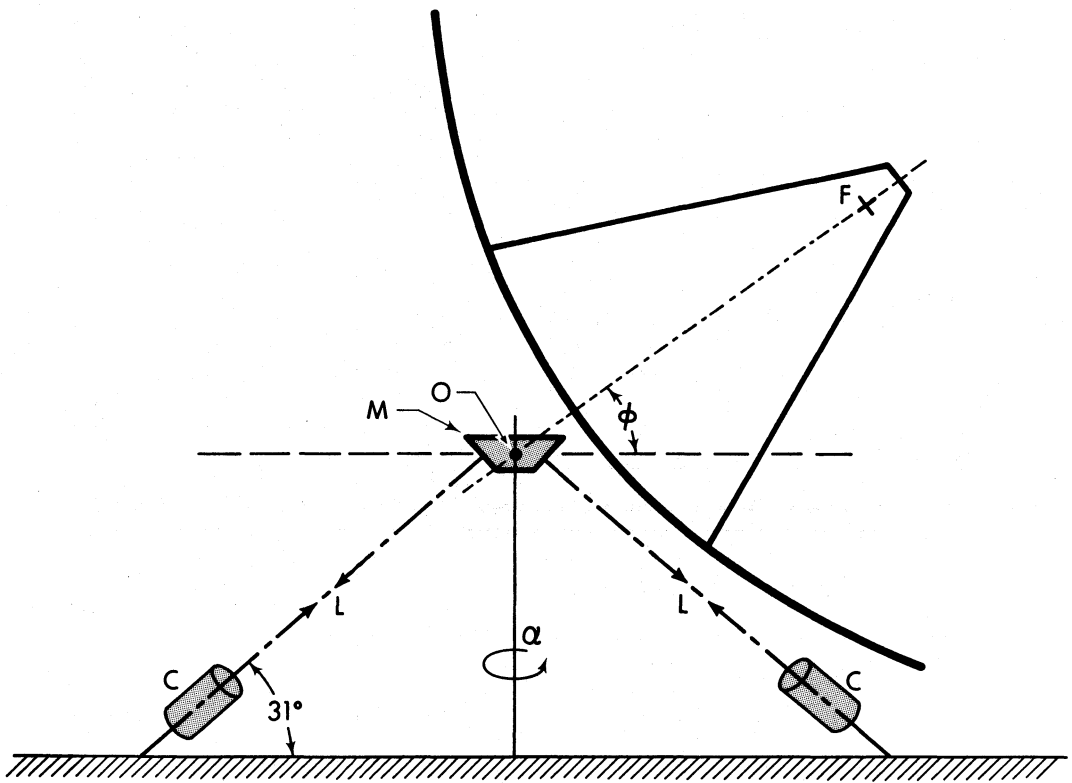


Figure 19. The principle of the stable reference platform.

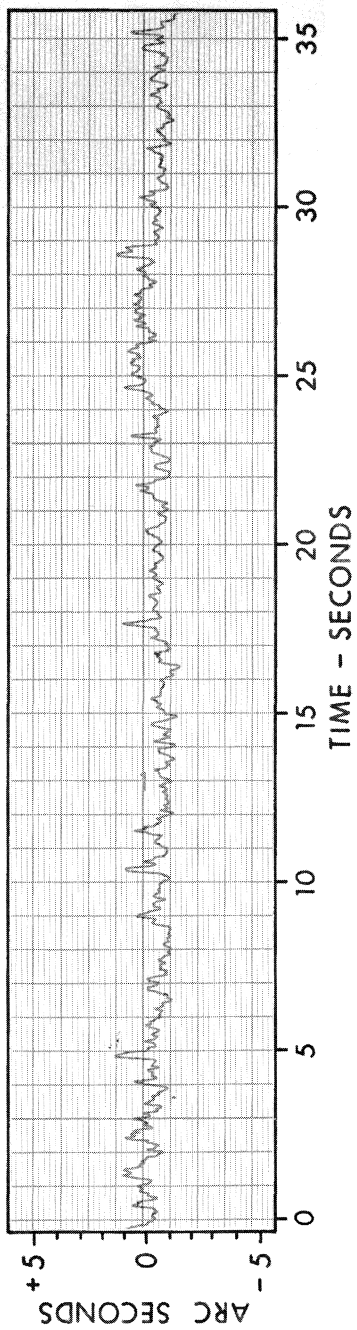


Figure 20. A typical record of the angular fluctuations of the optical path used in the reference platform tests.

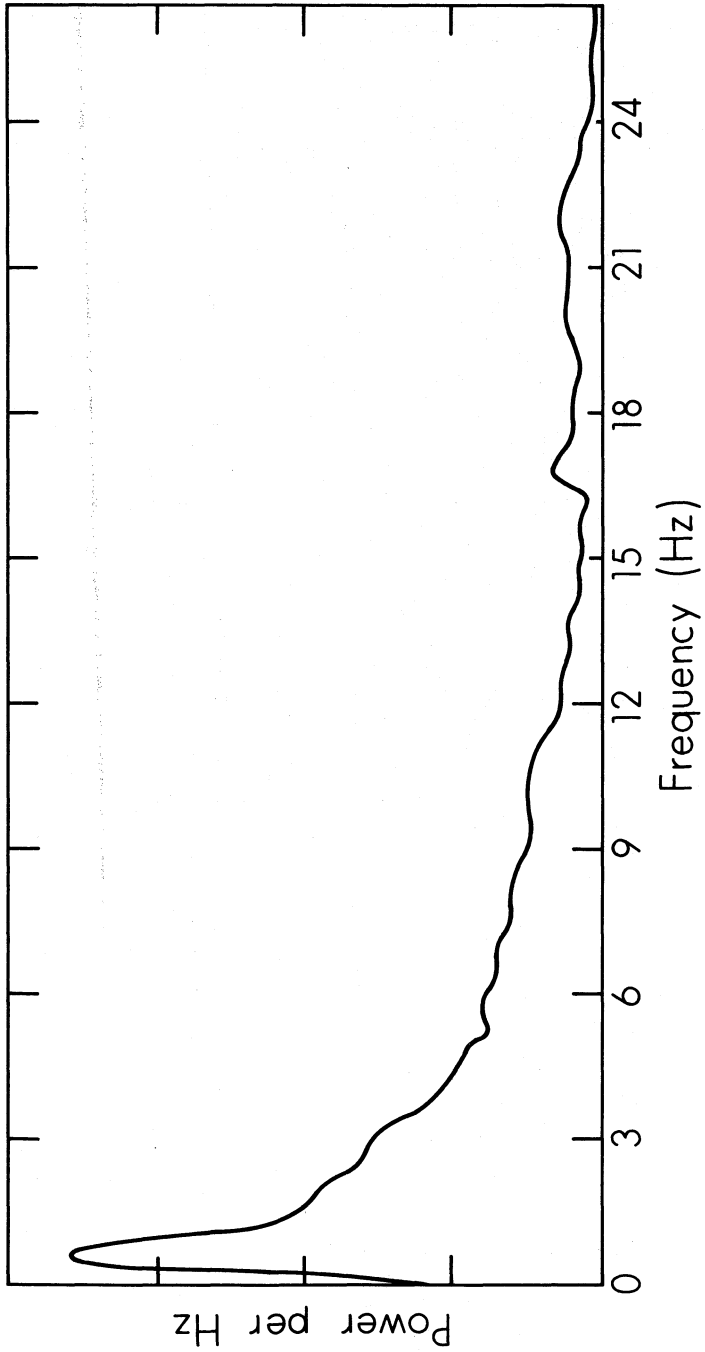


Figure 21. Power spectrum of the angular fluctuations of the optical path used in the reference platform tests.

The results of these tests show that the RMS error introduced into the reference platform servo will be  $\pm 0.60$  arc seconds under the atmospheric conditions which for other reasons still permit precise use of the telescope. This value is used in the error budgets of Chapter III.

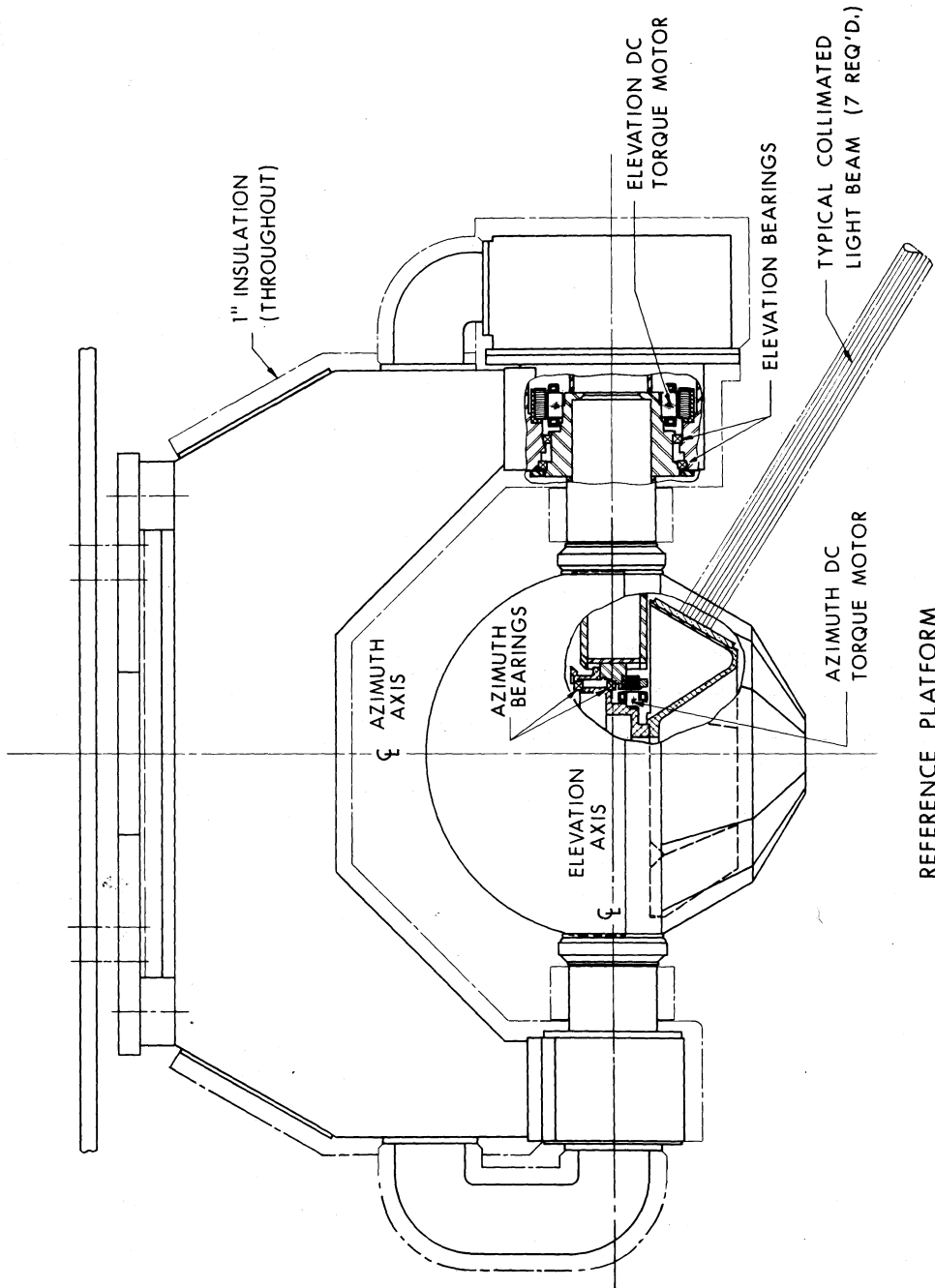
While the test experiment was in progress, the report of a similar experiment conducted at Marshall Space Flight Center became available (Kurtz and Hayes 1966). They made similar measurements over paths of 3200 meters and 165 meters at elevation angles of  $4^\circ$ . They produced very complete results for the atmospheric effects, which, when allowances are made for the different elevation angles, agree with the NRAO results.

(d) The stable reference platform (SDL Report H-10, Section 10.3). The detailed design is shown in Drawings 111-D-012, Sheets 1-6, and Figure 22 is a general view of the platform. The heart of the system is the seven-sided mirror assembly from which the seven autocollimator light beams are reflected. This is made from a precision machined aluminum casting onto which the seven Pyrex mirrors are bonded.

This mirror assembly is rotated in azimuth and elevation by torque motors; its position with respect to the main telescope member joint No. 56 is referenced by accurate 720-pole inductosyns, and tachometers (to give the velocity component required by the servo) are also shaft mounted. The whole platform operates in a carefully controlled environment and a plastic radome with 12 glass windows covers the mirrors. The light beams enter the radome through these windows, so they are made of precision-ground glass. Two radome designs have been made. In the first, the radome rotates with the azimuth rotation of the telescope; in the second the radome remains fixed with respect to the mirrors. The second design is preferred.

The design of the platform has been developed in detail, both because it is such a vital element and also because it is important to have good knowledge of the inertia of moving parts, friction forces and spring constants for the servo design. The wind forces and moments also have been calculated since these are also needed for the servo design. The details of the thermal control, which keeps all components at  $(100 \pm 1)^\circ$  F, have been developed. The method of mounting to joint No. 56 has also been devised in some detail and consideration has been given to the way the platform will be aligned on the telescope.

The components required in the platform are all of high-precision, but all are either available or can be made to the required accuracy. The two position encoders are identical, but they deserve special mention. The contribution to the total overall pointing errors of the telescope from the encoders can be kept fairly small, since 22-bit encoders are commercially available. A detailed encoder specification was prepared and sent to possible suppliers. As a result, 720-pole inductosyns (Fecker Systems Division of Ownes-Illinois) were chosen for inclusion in the design. These encoders have been used in other precise systems--



REFERENCE PLATFORM

Figure 22. A general view of the stable reference platform.

perhaps the most remarkable being their use by the U. S. Naval Observatory on the 6-inch transit circle.

One further question needs to be considered in the reference platform optics. The motion of the reference point on the telescope structure as the telescope moves is mainly rotation in azimuth and elevation. Nevertheless, small movements of this point in space will occur since it may rise and fall or move laterally as a result of temperature differences in the structure, wind-induced deformations or irregularities in the azimuth track.

These lateral movements have been estimated and the size of the mirrors and collimator beams have been so chosen that the expected movements will not interfere with the performance of the system. The angular accuracy of the system is, of course, not impaired by these small linear translations of joint No. 56.

(e) The platform servo system (SDL Report H-10, Chapter 10.7). In principle, the control of the reference platform to keep the seven-sided mirror held with its axis normal to the autocollimator beams is a straightforward task. However, in practice, there are a number of considerations to be met in order that the full angular accuracy of the system is achieved. For example:

(i) At any time several of the autocollimators will be providing error signals in each of the azimuth and elevation axes. These signals must be averaged before they are used as the input position errors to the platform servo.

(ii) As the telescope structure rotates, some autocollimator beams become obstructed and some become clear; unobstructed beams must be selected and a smooth average must be produced.

(iii) The platform servo should, as far as possible, smooth out the angular fluctuations of the collimator beams due to atmospheric irregularities. It should also reduce as much as possible the effects of wind torques on the reference platform.

(iv) The platform servo in its turn is a vital element in the main telescope drive and control system, in that the platform provides the position of the telescope which is then (by comparison with the demanded telescope position) used to derive the error signals to control the main telescope drive. Thus, in simple terms, the platform servo and the main drive servo must work properly together.

(v) Small corrections must be applied to the autocollimator error signals if the tilt-sensors on the autocollimators indicate that ground movement has materially altered the collimator beam direction.

The servo-design proceeded in a straightforward manner. The reference platform has the following natural resonant frequencies:

Elevation axis	-	Torsional mode 200 Hz
	-	Bending mode 170 Hz



Azimuth axis	-	Torsional mode 200 Hz
--------------	---	-----------------------

and the following frictional torques:

Elevation axis	-	0.08 foot pound
Azimuth axis	-	0.06 foot pound

From the frictional torques and the smallest acceptable angular hysteresis errors acceptable (0.5 arc second) the open-loop gain was derived. Tachometer compensation is used. The analysis shows that the torque motors are correctly chosen and that both servo loops (azimuth and elevation) will be stable and will have zero gain at a frequency of about 50 radians/second (8 Hz). This is satisfactorily below the lowest platform mechanical resonance frequencies and yet well above the zero-gain frequency of the main telescope drive servo.

(f) The overall reference platform system. Figure 23 shows in block diagram form the overall reference platform system. Most elements of it have already been described. The collimator selection is made using analog signals derived from the intensity of the collimator light beams; when a beam becomes obscured the signal from that collimator is removed from the averaging process. The collimator selector also, of course, receives the error signals from each collimator in digital form and passes these, after correction for tilt and after selection, to the error averaging block. The errors are generated simultaneously and separately in azimuth and elevation at a rate of 400 digital words per second.

The overall control of these elements of the platform system and the operation of the collimator selection and error averaging are functions of the main telescope control computer (this Chapter, Section 9).

## 8. The Drive and Control System

(a) General requirements. The means by which the telescope is driven and controlled must meet the following general requirements:

(i) The telescope must be capable of being smoothly driven in azimuth and elevation over the whole range of speeds necessary for accurate observations of radio sources in the sky. This implies a drive with good accuracy near zero velocity for both axes; the azimuth drive also needs adequate accuracy at high speeds so that the telescope can be used near the zenith.

(ii) The telescope motion must be controllable for a variety of observational programs either from commands supplied by the telescope computer or by manual control by an operator. The working coordinate system may be one of several sets of astronomical coordinates.

(iii) The telescope beam position, in astronomical coordinates, must be continuously measured and supplied, as a function of time, to

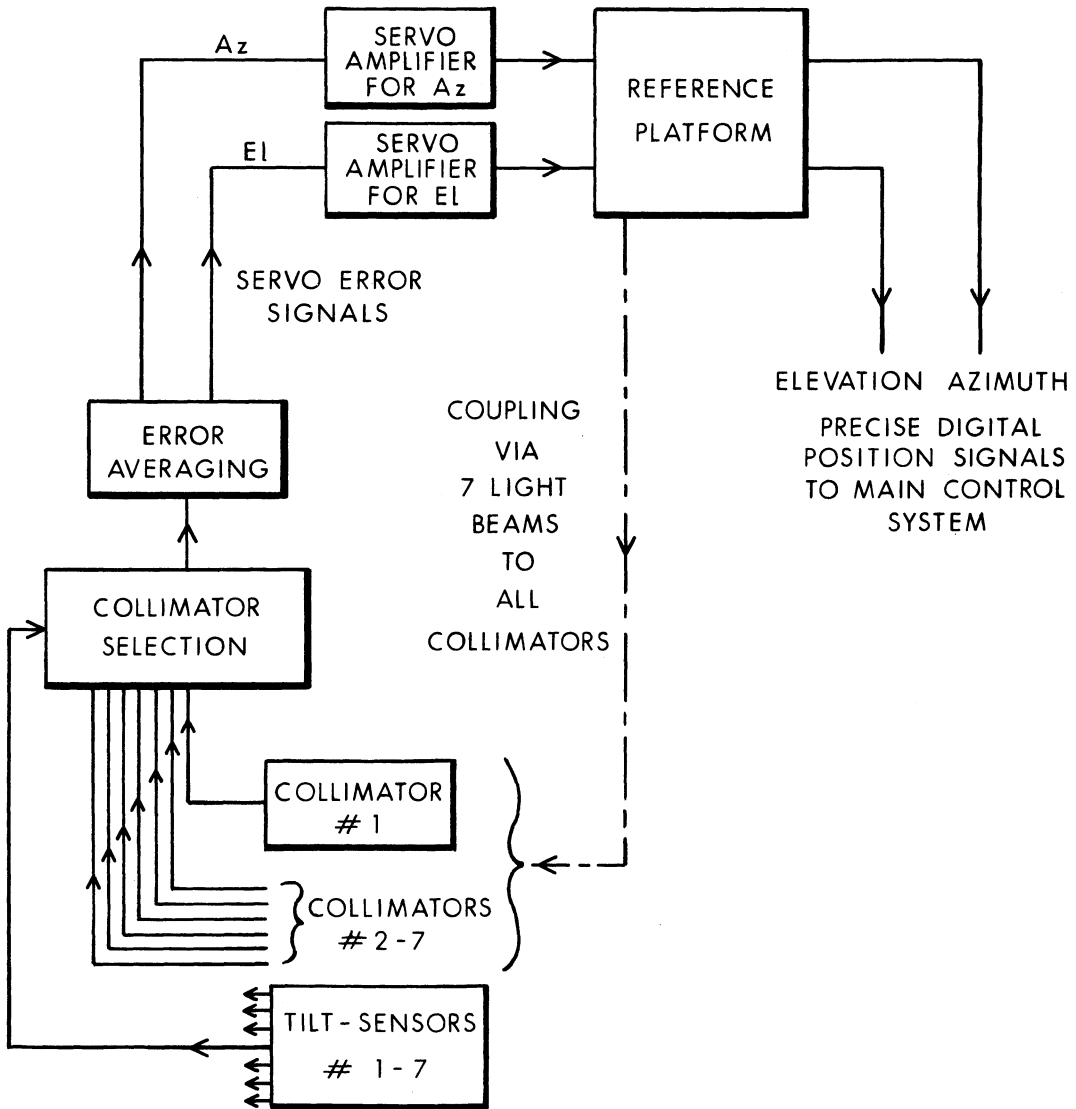


Figure 23. Block diagram of the reference platform control system.

the manual control console and to the telescope data recording system.

(iv) The telescope must move at slew speeds about both axes to go quickly from one position in the sky to another. This ability must be provided at all times and under all weather conditions up to these limiting conditions where the telescope must be driven to its stowed position. The slewing rates need not have any high positional or velocity accuracy.

The drive and control system has been designed to meet these requirements. More specifically it provides:

- (i) A maximum drive rate of 20 degrees per minute at each axis.
- (ii) The telescope can be driven to the stow position in winds up to 45 miles per hour.
- (iii) The telescope will track any desired point in the sky (which is moving at or about the sidereal rate) with an angular accuracy (1 $\sigma$  RMS) of 3 arc seconds, in winds up to 18 miles per hour. There is a cone of avoidance near the zenith where tracking is not possible; its semiangle is about one degree.

(b) The main drive components (SDL Report H-10, Chapters 7 and 11). Both the azimuth and elevation drive systems are electrical. The drive motors are air-cooled DC servo motors, driving through gear boxes. Both control servo loops employ velocity feedback and the main power drive is generated by solid-state amplifiers. There are 16 drive units for the azimuth drive and four for the elevation drive. The principle of using half the drive units to oppose the others ("bucking") to avoid backlash is used in both drive systems when they are used for precise driving. When used for slewing, all drive units supply torque in the required direction. Other methods of drive have been considered and none seem as good (either because of cost or performance) as the one selected.

The following two tables show the quantities which are used in selecting the main drive system and the components chosen.

Table 8. Azimuth Drive Parameters

Property	Value
Moment of inertia at azimuth axis	6.1x10 <sup>9</sup> in.lb. sec <sup>2</sup>
Maximum wind moment (18 miles per hour wind) for precise tracking	1.0x10 <sup>6</sup> ft. lbs.
Maximum acceleration moment during tracking	0.89x10 <sup>6</sup> ft. lbs.
Maximum friction moment during tracking	0.177x10 <sup>6</sup> ft. lbs.

Table 8, continued

Property	Value
Maximum rolling friction moment	$0.083 \times 10^6$ ft. lbs.
Drive-to-stow moment (45 miles per hour wind plus friction)	$7.0 \times 10^6$ ft. lbs.
Maximum slew speed	19.7 degrees per minute
Number of drives	16
Mean radius of azimuth turntable	123.00 feet
Diameter of drive wheel	36.0 inches
Gear ratio of drive train	189.5:1
Overall drive ratio (input-shaft to azimuth axis)	15,538:1
Maximum speed of input shaft	850 RPM
Static efficiency of gear train	95%
Dynamic efficiency of gear train	98%
Spring constant of a single gear train at the input shaft	$3.6 \times 10^3$ in. lbs./radian
Moment of inertia of gear train at the the input shaft	0.125 in. lb. sec <sup>2</sup>
Horsepower of a drive motor, its frame and type	5 HP at 850 RPM. Frame 286D, 240 V-DC fan cooled, totally enclosed GE compensated DC servo motor.
Type of drive system	Anti-backlash (8 driving, 8 bucking except when slewing)

Table 9. Elevation Drive Parameters

Property	Value
Moment of inertia at elevation axis	$1.6 \times 10^9$ in. lb. sec <sup>2</sup>
Maximum wind moment (18 miles per hour wind) for precise tracking	$1.0 \times 10^9$ ft. lbs
Maximum acceleration moment during tracking	$0.23 \times 10^6$ ft. lbs.
Maximum friction moment during tracking	$0.066 \times 10^6$ ft. lbs.
Drive-to-stow moment (45 miles per hour wind plus friction)	$6.5 \times 10^6$ ft. lbs.
Maximum slew speed	22.4 degrees per minute
Number of drives	4
Pitch radius of ring gear	794
Pitch diameter of drive pinion	13.60 inches
Gear ratio of drive train	117.18:1
Overall drive ratio (input shaft to elevation axis)	13,683:1
Maximum speed of input shaft	850 RPM
Static efficiency of gear train	95%
Dynamic efficiency of gear train	98%
Spring constant of a single gear train at the input shaft	$2.32 \times 10^4$ in. lbs./radian
Moment of inertia of gear train at the input shaft	1.9 in lb. sec <sup>2</sup>
Horsepower of a drive motor, its frame and type	20 HP at 850 RPM. Frame 368 D, 240 V-DC fan-cooled, totally enclosed GE compensated DC servo motor
Type of drive system	Anti-backlash (2 driving, 2 bucking, except when slewing)

Both drive systems require gear reducers, and these must meet requirements both for transmitting the maximum torque required to move the telescope in winds and also for adequate stiffness to give a high spring constant to the total structural resonance. The azimuth gear trains have been specially designed (Drawing 111-D-008, Sheet 3). For the elevation drive it has been possible to select gear boxes (Western Gear No. 44125-RI) which have been designed for antenna applications and have high efficiency, low inertia, good stiffness and small size. Brakes are mounted on each gear box.

The tachometers needed for the velocity feedback loop of the servo are mounted on all the 16 azimuth and 4 elevation drive units.

The remainder of the azimuth drive components have already been described, so that only a brief further description is needed of the elevation drive and the bull gear.

To preserve the homologous behavior of the reflector structure, it is important that no large loads (greater than about  $\pm 5000$  pounds) be applied radially to the elevation wheel by the elevation drive. Also, to keep the lowest natural resonant frequency of the reflector structure high, it is most desirable that the mass of the elevation drive assembly not contribute to the reflector structure moment of inertia. These two requirements have been met by (1) floating the elevation drive on the elevation gear, (2) balancing the weight of the drive assembly by spring-tension devices, (3) arranging that the spring-tension cylinders are critically damped. The elevation drive arrangement is shown in drawings Nos. 111-D-005, Sheets 1-4, and a further detailed description is in SDL Report H-10, Chapter 8.

The main elevation gear has a pitch radius of 66 feet 2 inches, a 1.25 inch pitch and a face width of 8 inches. The gear support girder is shown on drawing No. 111-D-001, Sheet 3.

(c) The design of the control system. The telescope drives are fed with power from the servo system in such a way that whenever there is an error between the actual telescope position and its required position the servo supplies drive torques to correct this error. The general requirements for such a servo system are that it should give a stable and accurate drive. The conditions that are taken into account in making such a design may be outlined as follows:

(i) The dynamical properties of the structure to be driven must be known. Any well-built elastic structure will be capable of oscillations in a variety of modes, and usually these modes show very little damping. Thus the modes must be discovered and their natural frequencies determined so that the drive can be designed to avoid exciting any of the possible oscillations. (The dynamic analysis of the present structure is treated in more detail in Chapter III, Section 2.)

(ii) The main mechanical disturbances which can influence the accuracy of the drive system are frictional torques and the varying

torques on the structure due to wind. The servo must thus deliver sufficient drive torque to overcome frictional torques when the positional error of the telescope is small compared with the required tracking accuracy. Also, the servo must be capable of responding to positional errors induced by wind; this requires that the range of frequencies over which it performs well should cover most of the frequency range within which the wind can induce pointing errors.

Of course, analysis and experience is used in the overall telescope design to ensure that the servo can meet its requirements. For example, the structural and mechanical design of the present telescope was initially required to yield no oscillatory modes with natural frequencies below 1.5 Hz. This figure is related to the frequency range of the wind-induced torques which begin to fall off in magnitude at about 0.02 Hz and fall quite rapidly above 0.3 Hz. It is a good working rule that the servo frequency bandwidth can extend from zero frequency up to one-third or one-fourth of the lowest structural frequency. Similarly, the frictional forces (both static and rolling) of the azimuth and elevation movement were estimated early, so that the servo design would be able to handle the resulting frictional torques.

(d) Design method and results. With these considerations in mind, let us look in rather more detail at the steps which the servo design has followed. (See Figure 24 for a block diagram of a simple servo loop.)

The steps followed in the design are:

(i) The magnitude of the error signal, in millivolts, which corresponds to a one-bit (0.31 arc seconds) telescope position error, is determined and arranged to be adequate when compared to the electronic noise at the preamplifier input.

(ii) The gain of the amplifier chain must be sufficient so that this error signal can produce a torque at the drive motor shaft sufficient to overcome friction and operating wind torques at that point. Since these torques and the motor characteristics are known, the amplifier gains are determined. A check is then made to ensure that sufficient motor voltage can be supplied to drive at full motor speed.

(iii) Using the transfer function of the servo motor and tachometer feed-back, the transfer function of the compensation network required to give a stable servo system is derived.

At this stage, for example, the azimuth axis drive design had an open-loop gain of 47 dB and a phase margin of  $35^\circ$  at the frequency of 4.5 radians per second (0.7 Hz) where the open-loop gain becomes equal to unity. These values satisfy the requirements of stability and of satisfactory performance in the presence of friction. This latter point was, however, analyzed in more detail, and so also was the performance of such a servo loop in the presence of wind disturbances.

The analysis of the effects of friction was quite detailed (SDL Report H-10, Chapter 11, Sections 9 and 10). Two effects were discussed:

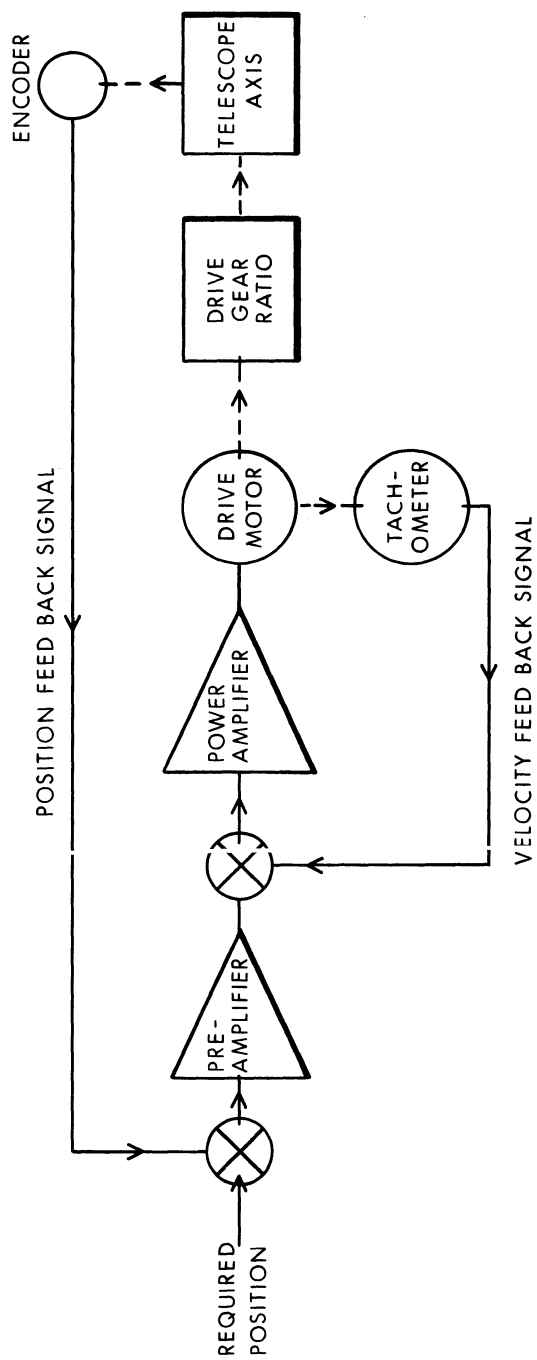


Figure 24. A block diagram of the servo drive for one axis of the telescope.



"stick-slip" and "limit cycling". Stick-slip is the phenomena which occurs because static friction is normally greater than rolling friction; there is thus the possibility that the drive will go in a succession of jumps in position at low speeds. A servo with velocity feedback may show limit cycling, which means that the telescope position may oscillate about the required position as the instrument moves. This effect also depends on the sliding-rolling friction difference.

The results of the analysis showed that both effects will occur, but that they result in pointing errors of about 0.5 arc seconds occurring at frequencies about 0.3 Hz. (More precise figures are included in the pointing error budget in Chapter III.) Errors of this magnitude are quite acceptable.

The final stage in the design was the choice of the various main components, e.g., amplifiers, motors and tachometers, to be used in the servo-system. No difficulties were experienced in this task since the realization of the system falls within the state of present-day practice.

(e) The operational control. Figure 25 shows in a simplified form one element of the drive and control system, as, for example, would be employed to drive two of the four elevation drive pinions. The main commands come from the computer (which is described in the following paragraph), but they may also be commands by an operator at the control console. The command is compared, in the digital subtractor, with either the error-corrected precise telescope position derived from the reference platform or with the coarse position from the axis encoder. The error signal goes via a torque equalizer (whose task is to ensure that all drive units contribute approximately equally to the drive load) to the drive-buck difference control. This control sets the right difference between the torque developed by the motor which is driving in the required direction and the motor which is cancelling backlash by opposing the drive. (In slew, this control drives both motors together.) Each motor and its associated tachometer has its own servo amplifier and drives its own gear reducer. The output shafts of the two reducers drive (and buck) the drive to the telescope axis.

This system is typical of both the azimuth and elevation drives. In azimuth, there are eight such pairs of drive motors driving 16 wheels; in elevation two such pairs drive four pinions on the elevation bull gear.

## 9. The Telescope Computer

There are many tasks for the telescope computer; in this section we will outline these and give some indication of their complexity. The telescope computer will not, however, handle the observational data from the telescope, as that will be the task of the data-handling and process-

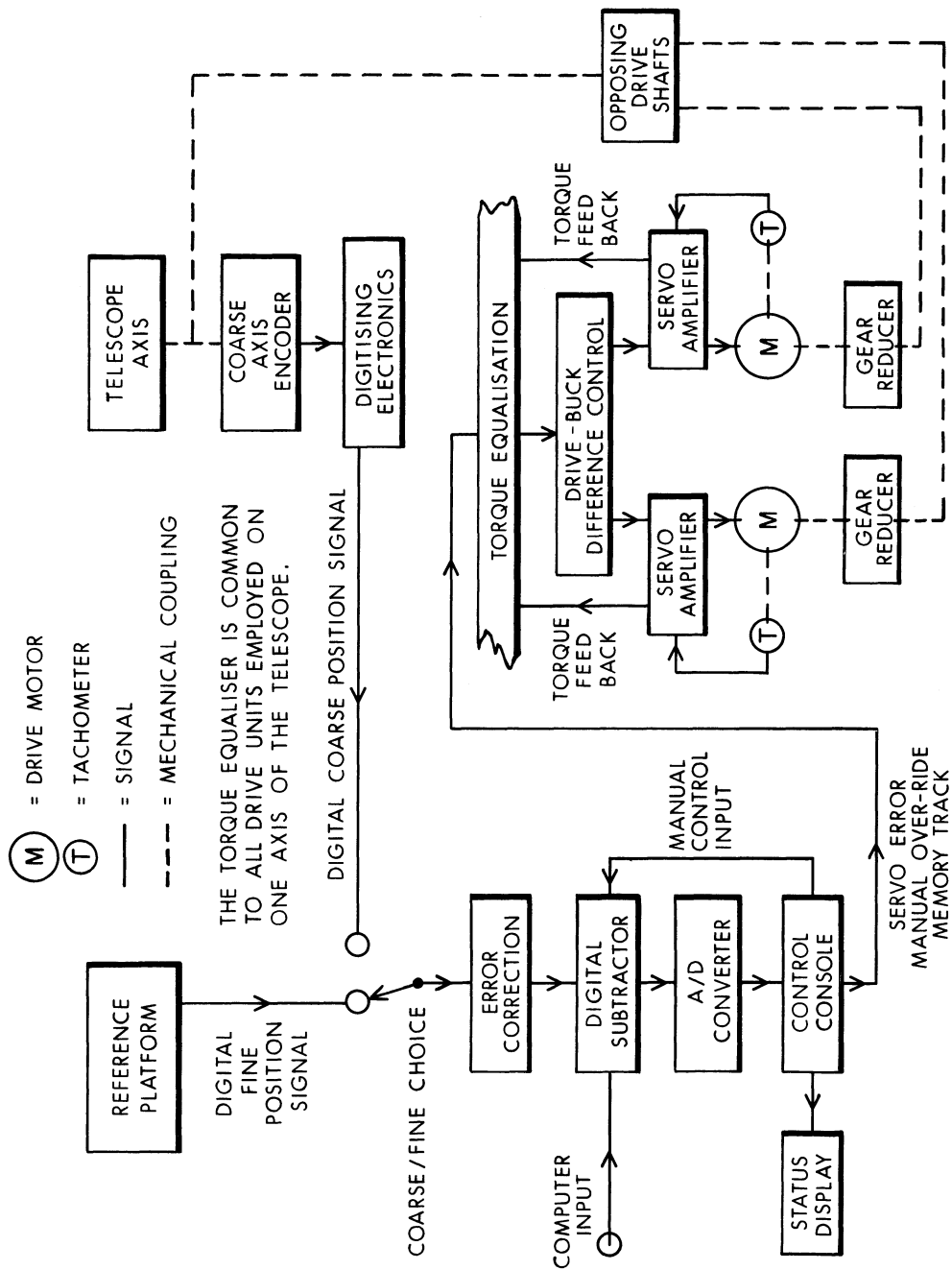


Figure 25. Block diagram for one unit of the drive and control system.

ing computer. The two computers will communicate with each other, but this separation of functions is very desirable and, owing to the development of several good, small-sized computers, not expensive. It means that the telescope computer can be programmed, tested and set into operation and then not be subject to changing requirements. The data-processing computer will require quite considerable flexibility to cope with changes in observing methods and different scientific tasks. This separation of function also allows us to reserve the choice of the data-handling computer to a late stage. It is therefore not considered further here; its cost will be included in the cost of the electronic observing equipment for the telescope.

The following are the chief computer tasks:

(a) Reference platform orientation. The computer will continuously calculate the orientation of the stable reference platform. This orientation provides the basic coordinate system for the telescope; source positions or required beam positions of the telescope are transformed into this coordinate system and compared with the telescope position to generate the error signals for the drive. The orientation of the platform is also required as an input to the platform servo to maintain the platform angular stability. This computer task may be further described as the following subtasks:

(i) Setting up and inverting the matrices relating the active autocollimator outputs (there will be between 4 and 14 outputs active at any one time) and deriving the least squares solution for the platform altitude and azimuth.

(ii) Performing the matrix multiplication needed to solve for the platform orientation given the autocollimator outputs.

(b) The telescope position. The computer will calculate continuously the desired telescope position in the reference platform coordinate system. Such a calculation is a spherical transform, and can be made without excessive effort for a variety of coordinate systems. The desired telescope position will be the input; it will be possible to insert it in any of the following coordinate systems:

(i) Altitude and azimuth.

(ii) Hour angle and declination.

(iii) Right ascension and declination.

(iv) At any epoch after 1850 in equator and equinox coordinates.

(v) Ecliptic coordinates.

(vi) Galactic coordinates (old and new).

The results of this calculation goes via a buffer to the digital comparator where it is compared with the stable platform encoder outputs.

(c) Pointing corrections. The computer will apply pointing corrections which are known to exist, from prior calibrations of the telescope, and those due to atmospheric refractivity. For this latter calculation the computer is supplied with measurements of ground-level

temperature, barometric pressure and relative humidity. The pointing corrections due to the structure are slowly-varying functions of the elevation angle and are easily dealt with. The computer will provide an output to adjust the subreflector or prime focus feed position as a function of elevation angle so that the changing focal length of the telescope as it tilts can be allowed for.

The rapidly varying (but small) reproducible errors inherent in the precision encoder system are compensated in the electronics associated with the encoders and not in the computer.

(d) Other tasks. The following various tasks will be handled by the computer:

(i) It may be desirable to display telescope coordinates in a system different from the one chosen as computer input. The computer must make the transform and send the coordinates to the display in the correct form (angles must be in degrees, minutes and seconds, for example).

(ii) The computer will calculate the parallactic angle for the telescope beam in the sky. This is needed for polarization observations, and may in fact be used either to control the orientation of the telescope feed or to provide as output data the relation between feed orientation and the source orientation in the sky.

(iii) Already, in (b) above, the computer has control of the telescope position and can command it to follow a variety of tracking or scanning demands. However, it must also be possible for the operator to insert manually a position change in case he wishes to make a manually controlled scan in any coordinate system. The computer meets this task, which is not met by the existing ability to transfer full control from the computer to the telescope operator.

(e) Other control system modes. The computer would be capable of carrying out the following two functions, although the present design of the control system does not require it to do so:

(i) The computer could calculate the velocity required for any change in the telescope position and supply this as a velocity signal to the servo loop. This mode can be an improvement over the more straightforward provision of velocity information derived from the tachometers.

(ii) The comparison of actual-demanded telescope position could be made digitally in the computer rather than in the digital comparator and the positional error processed digitally. This could make it simpler to achieve the desired network response in the servo-loop.

Each of the above computer tasks has been used to give an estimate for its running time and frequency of operation. These estimates have been based on a 2 microsecond core cycle and an instruction set typical of small 16-bit computers. The required input-output devices have also been listed.

There will also be programs for acquisition of reference platform lock (for use after the shut-down, for example), a variety of programs to test and exercise the main and platform servos and other similar tasks.

The general intent is that, after test and debugging, all programs would be coded into read-only memory and the computer inhibited from executing instructions from the remaining core scratch pad. The computer would thus be protected from destroying its own program memory, and its operating instructions would consist only of turning it on.

#### References

- Findlay, J. W. 1971, Ann. Rev. of Astron. and Astrophys., 9, 271-292.
- Froome, K. D., and Bradsell, R. H. 1966, J. of Sci. Instruments, 43, 129-133.
- Kühne, C. 1966, in "Design and Construction of Large Steerable Aerials", Institution of Electrical Engineers (GB) Conference Publication No. 21, pp. 187-198.
- Kurtz, R. L., and Hayes, J. L. 1966, "Experimental Measurement of Optical Angular Deviation Caused by Atmospheric Turbulence and Refraction", NASA Technical Note TN D-3439, National Aeronautics and Space Administration, Washington, D. C.
- Leitz, H. 1969, "Two Electronic Tacheometers by Zeiss", translated into English from Allgemeine Vermessungs-Nachrichten, 76, pp. 73-79.
- Saastamoinen, J. J. 1967, Surveyors Guide to Electromagnetic Distance Measuring, University of Toronto Press, Toronto, Canada.
- von Hoerner, S. 1967(a), Astron. J., 72, 35-47.
- von Hoerner, S. 1967(b), J. Struct. Div. Proc. Amer. Soc. Civil Engrs., 93, 461-485.
- von Hoerner, S. 1969, in "Structures Technology for Large Radio and Radar Telescope Systems", James W. Mar and Harold Liebowitz, eds., MIT Press, Cambridge, Mass., pp. 311-333.

## CHAPTER III

### THE TELESCOPE PERFORMANCE

#### 1. Introduction

In this chapter we shall review the various factors which determine how well the telescope may be expected to perform. The results of this review then permit estimates to be made of the way the instrument can be used under various climatic conditions.

#### 2. The Dynamic Behavior of the Telescope Structure

As has been said already in the section on the drive and control system, the ability to point the telescope and its performance in winds depend on its structural dynamics. Thus, the structural design was made with the intent that it should have both good static behavior (i.e., it should satisfy the conditions for homology and strength) and also good dynamic behavior. The analysis of its dynamics could only be made when the design was reasonably complete; in this section we describe the dynamic analysis and give its results.

(a) The dynamic analysis requirements. The structure is massive and elastic. It can obviously vibrate in a wide variety of oscillatory modes at various natural frequencies. The fact that there will be quite low damping associated with such oscillations is clear from simple principles--steel at normal working stresses shows very small elastic loss and welded joints are similarly behaved. Losses can be expected to exist in the air damping of the structure, in the gears of the drive gear-boxes and in the movement of the ground under the concrete foundation, but these effects are small.

The dynamic analysis must identify the main oscillatory modes, particularly those at the lowest natural frequencies. This emphasis on the low-frequency modes arises from the fact that wind turbulence is mainly effective in exciting the lowest frequencies. For a structure of this size both theory and experiment show that energy exchange from the

wind to the structure begins to fall in importance at about 0.02 Hz and drops rapidly above about 0.3 Hz. The lowest structural natural frequency should be well above these values; experience says that it should be about 1.5 Hz and this value was the target chosen during the design.

In addition to the large-scale or body-vibrational modes, it is important to consider possible vibrational modes in individual components of the structure. Most of these are at high frequencies, weakly coupled to the total structure and are of no importance. The vibrations of individual members may, however, be important. In Chapter II, Section 4, we have discussed the possibility that wind-induced vibrations (due to von Karman vortices) could affect the survival of the tubular members, and we have concluded that this is safely avoided. Nevertheless, the method of dynamic analysis of the structure must also recognize and allow for the existence of vibrations in the long tower members since these might reduce the lowest system resonances; the present analysis does this.

(b) The method of dynamic analysis (SDL Report H-10, Chapter 9, Simpson, Gumpertz & Heger Report No. 9333) The analysis was conducted in two stages. First, the reflector structure was treated. The reflector, feed support legs and elevation wheel, including the applied masses of the surface and the observing cabins, were analyzed to determine the dynamic characteristics as seen by the elevation bearings. The results of this detailed analysis, which was made by Simpson, Gumpertz & Heger, can be represented by treating the whole reflector as a body with fixed mass and fixed moments of inertia supported by infinitely stiff bearing and drive points. This mass-inertia system was then associated with six degrees of freedom, each of which had a particular stiffness. This dynamical equivalent to the reflector was then applied to the tower and the second stage of the analysis, the inclusion of the tower stiffness and inertia, was made. The result was the modes of oscillation of the combined tower-reflector system.

The analysis of the tower proceeded as follows. The tower structure was modeled assuming its individual members to be pin-jointed at their ends but with appropriate masses and equivalent member stiffnesses concentrated at the member centers and also (to allow for the heavy joints) with masses at the joints themselves. This model reproduced the natural oscillatory modes of the tower, including the effects of individual members. There are further equivalent springs in such a system; bearings, gears, the azimuth trucks and rail and even the concrete foundation all contribute springs to the system, and appropriate values were supplied for these quantities.

With this input, a digital computer structural dynamics program, developed by the Space and Re-entry Systems Division of the Philco-Ford Corporation at Palo Alto, was used to make the dynamic analysis. Two reflector positions were used, when it was pointing towards the zenith

and also at  $45^\circ$  from the zenith. This latter position is known to be close to the situation which gives the lowest natural frequency for the structure.

The analysis was tested for sensitivity to various parameters. For example, it was rerun with the values of reflector mass and inertia increased first by 10 percent and then by 20 percent. A similar pair of runs was made with the stiffnesses reduced by 10 percent and 20 percent. A run in which the tower structure joints were rigid rather than pinned was made and the solution shown to be insensitive to this change.

(c) The results. The dynamic analysis of the reflector alone was carried out with two sets of boundary conditions; for each of the two the elevation bearings were taken as fixed points. In the first analysis, joint No. 58 was taken as fixed as far as tangential gear movements were concerned, and in the second analysis joint No. 54 was similarly treated. These two conditions well-describe the telescope in the zenith and at  $45^\circ$  from the zenith. One analysis was performed with antisymmetric conditions along the (x,z) plane. (See Figure 26 for the coordinate system.) The results of these analyses showed the first ten possible vibration modes. The lowest frequency revealed was 2.56 Hz and the mode with this frequency was the simple rotation of the reflector about the x-axis. The simple rotation mode of the reflector about the elevation axis (the y-axis) had frequencies of 2.87 Hz (zenith position) and 2.68 Hz ( $45^\circ$  position). For full details see the Simpson, Gumpertz & Heger Report No. 9333.

These reflector results, when combined with the tower structure, trucks, gears and foundations, showed the dynamic modes for the whole telescope. The six modes having the lowest natural frequencies are sketched in Figure 26 and are described in words in the following Table 10. The first reflector modes already described are included in the table as modes Nos. 5 and 6, although these are modes of the reflector only and not of the whole structure. It should be realized that modes 3 and 5 are coupled, so are modes 2 and 6; the frequencies given for modes 2 and 3 include the effects of these couplings.

### 3. The Accuracy of the Homologous Performance

(a) The sources of variation (S. von Hoerner Report No. 33). Although in principle the solution to the problem of obtaining truly homologous behavior of the reflector support structure should be limited only by the computational accuracy of the computer, in practice there will be a number of causes contributing to a less-than-perfect deflection pattern for the reflector surface. In this section we examine these causes and calculate their effects on the resulting accuracy of the reflector surface. The actual reflector structure will deviate



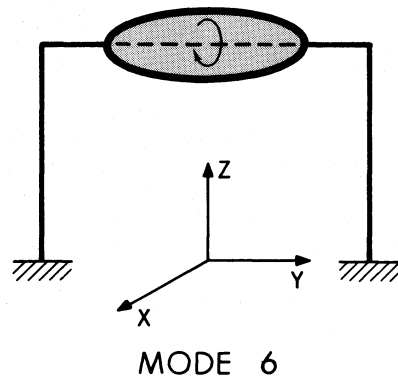
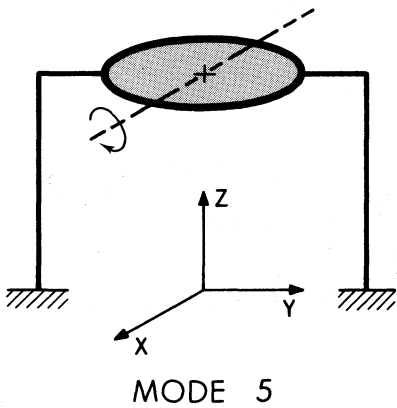
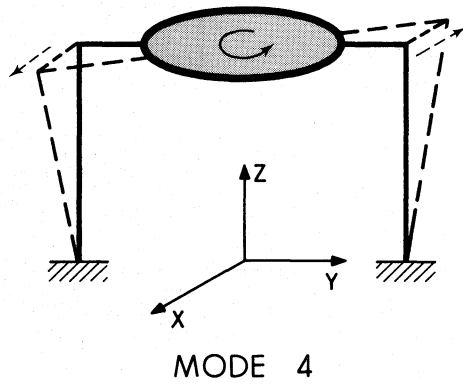
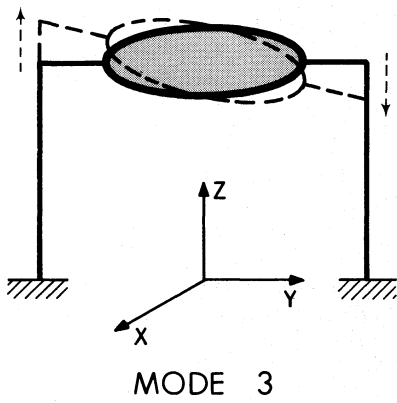
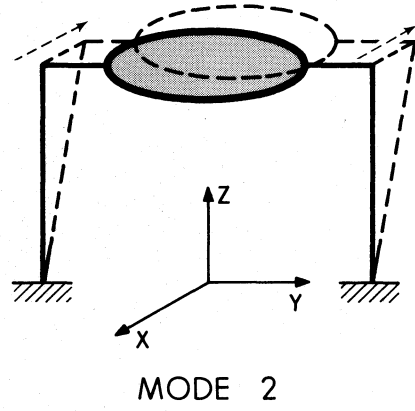
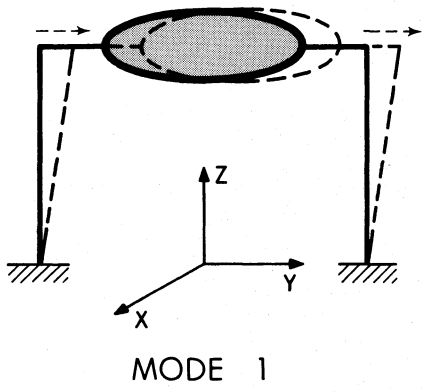


Figure 26. The main modes of oscillation of the telescope.

Table 10. Six Main Modes of Oscillation of the Telescope

Mode No.	Description	Frequency* for Reflector Position	
		Zenith	45°
1.	The tower tops rock backward and forward along the line of the elevation axis	1.61±0.05 Hz	1.52±0.06 Hz
2.	The tower tops rock together in phase along the line perpendicular to the elevation axis and approximately parallel to the ground.	1.92±0.04 Hz	1.61±0.06 Hz
3.	The tower tops rock one up, one down in antiphase in the vertical direction.	2.31±0.11 Hz	1.67±0.07 Hz
4.	The tower tops rock in antiphase, otherwise as in Mode 2. This mode rotates the reflector about the vertical azimuth axis.	2.44±0.01 Hz	2.00±0.05 Hz
5.	Rotation of the reflector about an axis perpendicular to the elevation axis and parallel to the reflector aperture.	2.56 Hz	2.56 Hz
6.	Rotation of the reflector about the elevation axis.	2.87 Hz	2.68 Hz

\*The ± values correspond approximately to the range of values when the reflector stiffness or inertia is changed by 10 percent.

from the structure developed by the homology program for the following reasons:

(i) The members used to build the telescope will have bar areas which differ somewhat from the design area. This will arise because as many members as possible will be made from commercially available pipes or tubes, and the bar areas of these will not be exactly correct. Also, for these members and for the members which are specially made, fabrication tolerance will cause stiffness differences.

(ii) The spherical joints add weight to the structure. They also replace small lengths of the member ends and thus modify the total stiffness of any given member.

(iii) The linear dimensions of the structure as built will differ slightly from the design dimensions. This in turn means a departure from homology since both the geometry and the member stiffness change somewhat.

(iv) Forces can be applied to the reflector structure from other parts of the telescope as it moves. For example, lack of perfect level of the azimuth track can apply forces from the tops of the towers to the elevation bearings.

There are other effects which might cause departures from homology; variations of Young's modulus or of thermal expansion coefficient between various members might occur. Such effects are, however, small for run-of-the-mill steel of good commercial quality.

(b) Expected variations in bar areas (S. von Hoerner Report No. 33, W-Y. Wong Report No. 34(A)). Most of the reflector support structure members are steel tubes or pipes, with areas of cross-section between 0.5 sq. inch up to 16 sq. inches. In choosing these members, various criteria have to be met. Adequate radius of gyration to avoid buckling must be supplied by giving an adequate length/radius ratio. The wall thickness must be sufficient to allow of easy welding, yet below 0.4 inches to keep thermal lag small. The frequency of any wind induced vibrations must be kept above about 2.5 Hz and fatigue must be avoided by either avoiding vibration or keeping the alternating stress small enough.

When all these requirements are met, it is found that most of the members can be supplied by using tubes or pipes which are of standard manufacture. Some, however, must be specially fabricated from steel plate by rolling and welding. For all types of member, the departures of the actual bar areas from the required area were found. Departures of about 1 percent were permitted in selecting members from the suppliers' lists. Manufacturing tolerances were found to be about 5 percent in most instances, although in a very few cases it may be necessary to select actual pipes or tubes to keep the area tolerances below 5 percent.

With this information it is then possible to estimate the total expected RMS departure from the design bar area, and, as Report No. 33 shows, this average departure will be on the average 2.3 percent of the bar area.

(c) Variations in weight and stiffness of the joints. The homology calculations give the stiffnesses of members connecting the points where the members intersect. In the practical structure, these points are the centers of the spherical joints and the members are shorter than the distance between these points by the sizes of the joints. The effects of the joints on the homology solution is thus to replace a short

length of the member; this in turn changes the weight and the stiffness of the member by small amounts, and then the homology condition is no longer exactly satisfied.

In the first design of the joints the condition was imposed that the change in weight due to the joints (the difference between the joint weights and the weights of the member lengths no longer needed) should be no more than about 5 percent of the total structure weight. Similarly, it was planned that the average percentage stiffness change should be less than about 3 percent. These figures were chosen with a reasonable knowledge of what their effects on homology might be.

The first design process for the joints could not produce a detailed optimum design for each joint; this task remains to be done in the detailed design of the telescope. Thus the changes in weight and stiffness which result from the first design can be regarded as upper limits, capable of some further improvement.

The changes may be described as follows:

(i) The weight of each of the reflector structure members is changed. The average change in weight, expressed as a percentage of the member weight, is  $\overline{\Delta W}$ .

(ii) The individual values  $\Delta W$  for the members deviate randomly about  $\overline{\Delta W}$ ; this deviation is described by the RMS value of  $(\Delta W - \overline{\Delta W})$ , and expressed as a percentage.

(iii) The stiffness of each member changes and as for the weights, the average stiffness change  $\overline{\Delta K}$  is expressed as a percentage of  $K$  and the deviation of the stiffnesses from  $\overline{\Delta K}$  is described by the RMS value of  $(\Delta K - \overline{\Delta K})$  expressed as a percentage.

The average weight and stiffness changes, and the individual variations about these average values both contribute to departures from homology.

The first joint design resulted in the following values:

$$\begin{array}{ll} \overline{\Delta W} = +2.5\% & \text{RMS } (\Delta W - \overline{\Delta W}) = \pm 2.0\% \\ \overline{\Delta K} = -3\% & \text{RMS } (\Delta K - \overline{\Delta K}) = \pm 2.0\% \end{array}$$

(d) Dimensional accuracy and azimuth track irregularity. The reflector structure must be built to a good, but not excessive, dimensional accuracy. We specify that this accuracy, expressed as the RMS deviation of each of these three coordinates of a point on the structure from its required position, should be 0.25 inch (6.4 mm). This specification will require a well-controlled erection procedure; for example, dimensional errors in the reflector structure should be reasonably random and should not develop any large-scale consistent pattern.

Undulations in the azimuth tracks will be the chief source of distorting forces applied to the reflector structure. The specifications for this (including truck, rail and foundation distortions under working loads) suggest that the maximum vertical movement of the tower bases will result in a lateral force on the reflector structure at the elevation bearings of 50 tons.

(e) Estimates of the effects on the reflector surface. In order to estimate the total departures from homology due to all the above effects, the following set of computations was made. Three representative reflector support structures were chosen, each of which showed good homologous performance ( $\Delta H_0$ , the RMS deviation of the surface points, from a true paraboloid, was small). Changes were then made to each of these structures in separate runs for each of the quantities whose effect on homology was to be found. The changes were introduced as random numbers with their mean values and deviations equal to the desired amounts. The structures, so modified, were then reanalyzed and the new departures from homology ( $\Delta H_c$ ) was found. The additional deviation

$$\Delta H = \left\{ (\Delta H_c)^2 - (\Delta H_0)^2 \right\}^{1/2}$$

was calculated. In all, 16 such experimental calculations were performed. The results are summarized in the following Table 11.

(f) Discussion. The total RSS departure from homology is thus seen to be acceptably small. It should be noted that items 1-6 in the table all depend on the elevation angle (i.e., the value of  $\Delta H$  is that corresponding to a movement of the telescope from zenith to horizon) and therefore could, if so desired, be still further reduced if the telescope surface were set (say) at  $30^\circ$  from the zenith and used mainly over the zenith to  $60^\circ$  depression angle range. (See Report No. 33 for further discussion.) However, no such reduction in  $\Delta H$  is made before using  $\Delta H$  in the telescope error budget (Chapter III, Section 5).

#### 4. Effects of Wind and Temperature on the Telescope Performance

(a) Introduction. The most serious effects on the performance of the telescope arise from the influence of wind and of temperature differences and changes on various members of the structure. Both these influences bend and deflect the structure. Note that it is differences of temperature and fairly rapid changes of temperature with time which degrade accuracy. When all the telescope is at the same temperature, its performance is not degraded.

The telescope loses accuracy for both these causes in two ways. First, the reflector surface departs from its true shape, and thus

Table 11. The Deviations from Homology

Change Applied to the Structure	Resulting $\Delta H$	
	inches	mm
1. None -- the value of $\Delta H$ for the "perfect" homology solution	0.002	0.051
2. Apply the average $\overline{\Delta W} = +2.5\%$ $\overline{\Delta K} = -3\%$ for the spherical joints	0.0012	0.030
3. Apply the deviation in stiffness due to joints RMS $(\Delta K - \overline{\Delta K}) = \pm 2\%$	0.0017	0.044
4. Apply the deviation in weight due to joints RMS $(\Delta W - \overline{\Delta W}) = \pm 2\%$	0.0017	0.043
5. Use standard pipes, include fabrication tolerances of bar areas $\Delta A = \pm 2.3\%$	0.002	0.051
6. Permit xy and z coordinates of points to vary $\pm 0.25$ inch	0.0013	0.033
7. Permit a track irregularity of $\pm 0.25$ inches	0.0009	0.023
RSS value of $\Delta H$	0.0042	0.107

becomes less efficient at short wavelengths. Second, the ability to point the radio beam of the telescope is degraded since wind and temperature differences can deflect the radio beam without causing the positioning mechanism to sense and correct these beam deflections. We shall call these two effects (i) degradation of surface accuracy and (ii) degradation of pointing accuracy and in this section describe the magnitudes of the effects.

(b) Permissible magnitudes. Ideally, neither loss of surface accuracy nor of pointing accuracy is permissible. However, we have adopted throughout the criteria that the following can be permitted and still result in a satisfactory instrument at its shortest operating wavelength:

(i) The RMS surface accuracy may, in total, be degraded to  $\lambda_{\min}/16$  ( $\lambda_{\min}$  is the shortest usable wavelength).

(ii) The RMS precision for tracking may be degraded to one-fifth of the HPBW at  $\lambda_{\min}$ . (HPBW is the half-power beamwidth.)

These criteria represent a significant departure from perfection. The  $\lambda_{\min}/16$  surface accuracy results (if the deviations are random) in a gain reduction of the instrument to a value of 0.54 of its full gain for a perfect reflector. In practice this means that the aperture efficiency would drop from about 60 percent (perfect reflector) to 32 percent at  $\lambda_{\min}$  with the imperfect reflector. The tracking precision of one-fifth of the HPBW implies that the signal from the source would be reduced by a factor of 0.90 when the beam is at its 1 $\sigma$  deviation from the true direction.

It is generally accepted that "perfect" performance for a radio telescope results when the surface accuracy is  $\lambda_{\min}/32$  and the tracking accuracy is one-tenth the HPBW at  $\lambda_{\min}$ . The gain loss factors then are 0.86 (for surface irregularity) and 0.97 (for pointing).

(c) Temperature effects (Report No. 37, S. von Hoerner and V. Herrero). Although effects of temperature and wind will act together on the telescope, it is convenient to discuss them separately. Two main questions have to be answered in describing the temperature effects. (1) What temperature differences are likely to be experienced by the structure? (2) What will the effects of these be on the surface and pointing accuracies?

The first question is best answered by experience and experiment. The telescope structure will be painted with a well-tested thermal control paint. This has been used on all NRAO telescopes and on the Goldstone 210-foot, as well as on many others. It has high reflectivity in the visible light range, yet radiates well in the long infrared. Thus, direct heating by sunlight is reduced and yet any temperature differences can radiate themselves away.

(i) Measurements of temperature differences and changes: A series of measurements has been made on the NRAO telescopes (particularly the 140-foot, a spare 140-foot panel, the 36-foot on Kitt Peak, and on one 85-foot), and on a test surface plate for the present telescope. Study of work by JPL on the Goldstone telescope confirms the nature and magnitude of the results; so also do measurements and calculations of the temperature changes in typical components of the telescope structure. These measurements are discussed and analyzed in S. von Hoerner and V. Herrero's Report No. 37 in some detail.

The quantities whose values are needed may be summarized as follows. We are chiefly concerned with the magnitudes of the effects on clear, calm, sunny days and on clear, calm (or nearly calm) nights, since these conditions demonstrate the most and least severe effects of temperature

on performance. Temperature differences existing vertically across the structure are the largest in practice and thus the most important. They are referred to here as  $\Delta T^\circ \text{ F}$ . Since telescope members of different sizes respond differently with time to changes of temperature (i.e., their thermal lag is different), we need also to know the values of  $dT/dt$  or  $\dot{T}$  (degrees F per hour) where  $T$  is the ambient air temperature. In deriving the values for  $\Delta T$  and  $\dot{T}$  to be used in the thermal analysis from observations, the 95 percent level of the distributions of  $\Delta T$  and  $\dot{T}$  were used--this means that the calculated thermal deformations will be greater than the actual deformations for 95 percent of the time.

The results of measurements of  $\Delta T$  and  $\dot{T}$  are listed in the following Table 12. From this the further Table 13 was derived, giving the values to be adopted for the thermal deflection analysis.

(ii) The thermal deflection analysis. This analysis must be carried out for all the important parts of the structure carried on the elevation bearings. The reference platform pointing system removes from consideration thermal effects on the tower. The thermal effects on the panels and on the support structure were analyzed by computation. The effect of  $\Delta T$  on a surface plate (NRAO type) was measured. A test plate was adjusted while at a uniform temperature and then exposed outside on a clear day. The temperature difference between its upper surface and a rib behind the surface was measured. The contour of the surface was measured (at 37 points) when  $\Delta T$  was  $-6.95^\circ \text{ F}$  and again when  $\Delta T$  was  $+2.10^\circ \text{ F}$ . (This change occurred as the plate came out of the shadow of a building into full sun.) From these measurements the expected contributions to the RMS surface accuracy could be calculated. They are shown in Table 14 of Section 5.

The analysis of the panel structure was straightforward. Both  $\Delta T$  and  $\dot{T}$  have to be considered although the thermal lag contribution is in fact small except at dawn and dusk. The analysis was made in the computer by assigning changed lengths to members in accordance with the temperature regime. The chief thermal effect is a degradation of the surface accuracy; there is only a small contribution to the pointing accuracy errors. The results of the analysis are given in Tables 14 and 15 of Section 5.

The support structure analysis was made by computing the deformations of the surface points and of the subreflector support legs under the various thermal loads. The results here are both a loss of pointing accuracy and the degradation of surface accuracy. A part of this surface accuracy degradation is due to the support structure deformation, but a part also comes from the movement of the subreflector; both effects are combined to give the total surface degradation.

The thermal analysis, when applied to the support structure, shows that the main contributions to the pointing errors come from temperature differences between the subreflector support legs. The detailed design



Table 12: Summary of Measurements of  $\Delta T$  and  $\dot{T}$  on Various Structures (95% level)

Description of Measurement	Applicable to:	$\Delta T$ °F		$\dot{T}$ °F/hour	
		Clear Night	Noon Sun	Clear Night	After Sunset
$\Delta T$ measured on 140-foot spare panel	Surface panels		14.0		
$\dot{T}$ for 1 year at Sugar Grove	Panels, structure				8.5
Heavy members of 140-foot corrected for lag	Panels, structure		12.0		
Tower members and legs of 85-1 telescope at Green Bank	Structure		5.4		
140-foot reflector support structure	Panels, structure	2.2			
Surface to support structure of 36-foot on Kitt Peak	Surface, panels, structure		12.5		
Surface to support structure on 36-foot on Kitt Peak	Surface, panels, structure	1.9			
Test surface plate for 65-meter telescope at Green Bank	Surface	2.0	9.2	1.5	8.6

Table 13. Values for  $\Delta T$  and  $\dot{T}$  Adopted for the Thermal Deflection Analysis

Component part of the 65-meter Telescope	Adopted Values			
	$\Delta T$ °F		$\dot{T}$ °F/hour	
	Clear Night	Noon Sun	Clear Night	After Sunset
Reflector surface plates	2.0	12.0	1.5	8.6
Panels	1.5	9.0	1.5	8.6
Reflector support structure	1.5	9.0	1.5	8.6

and analysis of the subreflector support legs is given in Report No. 42 by W-Y. Wong. Since the most critical requirements arise at the shortest wavelengths, where the telescope will be operated with Cassegrain optics, this is the case which is analyzed in detail. The results show that temperature differences between the legs are very important. If there is a 1° F temperature difference randomly distributed between the four legs of the feed support, the RMS contribution to the pointing error is 2.0 arc seconds.

It can thus be concluded that the main contribution to pointing error due to structural temperature differences arises from the legs which support the subreflector (the feed-support legs). The changes of length of these legs both rotates and translates the subreflector and it is these motions which primarily affect the pointing.

(d) Wind effects (S. von Hoerner and V. Herrero, Report No. 39). The use of a stable reference platform mounted at the axes intersection removes from consideration a number of the effects of wind on the telescope. The following effects, however, remain and their magnitude has been determined.

(i) Steady or irregular winds will distort the reflector. This will degrade the reflector surface accuracy and will introduce pointing errors.

(ii) Steady or irregular winds will deflect the subreflector support legs. This results mainly in pointing errors but may also cause a gain reduction due to the displacement of the subreflector from its required position with respect to the surface and to the feed system.

(iii) Irregular winds will produce torques about both telescope axes. Although, in principle, the servo system used in the azimuth and elevation drives can sense the pointing errors due to these imposed torques, and can thus correct them, this is only true for disturbances

whose frequencies fall within the range where the servo system is operative. The remaining pointing errors due to the higher-frequency gusts still remain.

To evaluate these effects due to wind, properties of the wind itself and its spatial and temporal structure have to be known. In addition to quite extensive information in the literature, a lengthy set of observations were made at Green Bank on a tower 150 feet high to confirm that the figures used in the wind analysis were satisfactory. Report No. 39 by S. von Hoerner and V. Herrero summarizes the wind information which has been used in the analysis and also gives the calculations of the wind-induced deformations of the telescope structure (excluding the feed-support legs). Report No. 42 by W-Y. Wong studies the wind deformations of the feed support legs. The assumptions and calculations made of these effects have been checked by having independent studies made by Simpson, Gumpertz & Heger. In discussing the wind-induced pointing errors due to the drive system, the results of SDL Report No. H-10 are used.

We now summarize the results of these various studies.

(i) Effects of wind on the reflector structure. Various pressure distributions which arise from wind forces on the reflector have been analyzed. The reflector surface was divided into a number of areas, one for each of the surface joints where the panels are held, and the force due to the wind pressure acting on the area was concentrated at the joint.

The joint displacements were then computed and a program determined the best fitting paraboloid and computed: (a) RMS surface error. (b) Defocussing gain losses expressed as an equivalent RMS surface error. (c) The total equivalent surface error resulting from (a) and (b). (d) The angular pointing error.

The results of this analysis for a wind mean speed of 18 miles per hour showed that the contribution to the RMS surface error was 0.076 mm and the average contribution to the pointing error was 3.2 arc seconds.

(ii) Effects of wind on the feed support legs. The principal effect here is the pointing error which results from the wind on the feed legs and focal point cabin producing a lateral displacement of the sub-reflector. (As in the case of temperature effects, the Cassegrain mode is the one most likely to suffer from these effects.) The analysis (W-Y. Wong Report No. 42) shows that an 18 miles per hour wind produces a pointing error of 1.1 arc seconds.

(iii) The effects of wind on the performance of the drive and control system. Wind acting on the antenna will cause errors in the servo-controlled pointing system, since the wind can produce varying torques on the structure about both the azimuth and the elevation axes. To counteract these torques the servo drive must develop a position error signal at its input. When the rate of fluctuation of the wind torque is

slow enough, compared to the response of the servo, these position errors are corrected. The servo response (its gain as a function of frequency) must, however, be limited at higher frequencies since the drive must not be able to give energy to the structure at any frequencies approaching the dynamical resonances of the structure. Thus, if there are wind torques with components in this frequency range outside the servo response, they will produce pointing errors. The spectrum of wind torques acting on large antennas is quite well established, both from direct measurement and from calculations based on wind structure. Thus, when the servo response is known, the positional errors can be calculated. Two such calculations are made in SDL Report No. H-10 (Chapter 11.7) and show that, at 18 miles per hour, the RMS position error due to this effect is 0.4 arc seconds.

(e) Summary. All these effects are summarized in the following Section 5 in the form of surface accuracy and tracking error budgets. The thermal and wind effects provide limitations to the telescope performance which are about the same in magnitude as other limitations; from this it may be concluded that the design is roughly balanced; i.e., all the various possible limitations appear to have about the same magnitude for a telescope of this size.

## 5. The Surface and Tracking Accuracy Budgets

(a) General. The two most important quantities on which the telescope performance depends are the overall reflector surface accuracy (including the subreflector) and the pointing precision. In this section we summarize the various contributions to these two quantities in the form of error budgets. In such a budget, it is usually conservatively correct to assume that the various contributions are mutually independent, and thus to add them by taking the root of the sum of the squares (RSS) of the individual contributions.

We express the surface accuracy by taking the root mean square (RMS) value of the departures of many approximately equally spaced surface points from a true parabolic surface. We choose for this reference surface that paraboloid which best fits the surface points; its focal length, axis direction and vertex position are permitted to vary. We do not, however, as is sometimes done, weight the points according to the illumination pattern of the reflector.

We measure pointing accuracy by the quantity which is often called tracking accuracy, and define it as follows. We assume that the telescope has been well-calibrated over all the useful sky insofar as its repeatable pointing errors are concerned. We then set it to track a point which is moving in the sky at about the sidereal rate. (At the equator and on the meridian this is a rate of 15 minutes of arc per

minute of time.) The RMS value of the angular departures of the center of the telescope beam from its required position in the sky is the tracking accuracy, and it is measured in seconds of arc.

As has already been discussed in Section 4 of this chapter, the telescope will be considered as performing satisfactorily at its shortest wavelength  $\lambda_{\min}$  if:

$$\text{surface accuracy} = \lambda_{\min}/16$$

$$\text{tracking accuracy} = 1/5 \text{ (half-power beamwidth at } \lambda_{\min} \text{)}$$

(b) The reflector surface accuracy. In the following three-part table are listed the various factors which contribute to the overall surface accuracy. We have separated those factors which do not depend on wind or on temperature, and given references to the sections of this report where the magnitudes of the quantities are discussed in more detail.

Table 14. The Telescope Surface Accuracy Error Budget

(i) The surface accuracy under conditions of no wind and constant uniform temperature.

Table 14(i)

Source of Error	Reference to this Report	Magnitude ( $1\sigma$ value)
Departure of main reflector structure from true homologous behavior	Chapter III, Section 3	$\pm 0.004$ inch $\pm 0.107$ mm
Departures of panels from true homologous behaviour	Chapter II, Section 4	$\pm 0.002$ inch $\pm 0.051$ mm
Fabrication tolerances of individual surface plates	Chapter II, Section 5	$\pm 0.003$ inch $\pm 0.076$ mm
Gravitational deflections of individual surface plates	Chapter II, Section 5	$\pm 0.0014$ inch $\pm 0.035$ mm
Setting accuracy of the surface plates on the telescope	Chapter II, Section 5	$\pm 0.0049$ inch $\pm 0.125$ mm
Total subreflector surface errors (fabrication and gravitational)	Chapter II, Section 6	$\pm 0.002$ inch $\pm 0.051$ mm

The RSS of the last column =  $\pm 0.0080$  inch or 0.200 mm.

(ii) The effect of wind on the surface accuracy. The following additional errors result from a gusty wind of 18 miles per hour mean speed at the level of the reflector center.

Table 14(ii)

Source of Error	Reference to this Report	Magnitude (1 $\sigma$ value)
Total surface errors due to wind on reflector structure, including equivalent error due to reflector defocussing	Chapter III, Section 4	$\pm 0.0029$ inch $\pm 0.076$ mm
Effect of wind deforming the panel structure	Chapter II, Section 4	$\pm 0.0008$ inch $\pm 0.020$ mm
Effect of wind deforming the surface plates	Chapter II, Section 5	$\pm 0.006$ inch $\pm 0.015$ mm
Effect of wind on sub-reflector support, including tilting, and lateral transition--translated to equivalent surface error	Chapter II, Section 6	$\pm 0.0002$ inch $\pm 0.005$ mm

RSS of last column = 0.0032 inch or 0.080 mm.

(iii) The effect of structural temperature differences and changes on the surface accuracy. Two temperature regimes are chosen for display here; in both these the telescope performance depends on (1) the vertical structural temperature difference  $\Delta T$  and on (2) the rate of change of ambient temperature with time,  $\dot{T}$ . Table 14(iii) gives the contributions to the surface error corresponding to various  $\Delta T$  and  $\dot{T}$  values. The values chosen are typical for a sunny day, and will only be exceeded on 5 percent of all clear nights. (See Section 4 of this Chapter for more details.)

(c) The telescope tracking accuracy error budget. The following three-part Table 15 summarizes the tracking accuracy, first under the conditions of no wind and uniform constant temperature; then wind and temperature effects are added.

Table 14(iii)

Source of Error	Temperature Regime	Error Magnitude (1 $\sigma$ )	Combined Error (1 $\sigma$ )
Reflector support structure	<u>Clear sunny day</u>		
	$\Delta T = 9.0^\circ \text{ F}$ $\dot{T} = 8.6^\circ \text{ F/hour}$	$\pm 0.0123 \text{ inch}$ $\pm 0.31 \text{ mm}$	
Panel structure	<u>Clear sunny day</u>		
	$\Delta T = 9.0^\circ \text{ F}$ $\dot{T} = 8.6^\circ \text{ F/hour}$	$\pm 0.0056 \text{ inch}$ $\pm 0.14 \text{ mm}$	$\pm 0.0169 \text{ inch}$ $\pm 0.430 \text{ mm}$
Surface plates	<u>Clear sunny day</u>		
	$\Delta T = 12.0^\circ \text{ F}$ $\dot{T} = 8.6^\circ \text{ F/hour}$	$\pm 0.0102 \text{ inch}$ $\pm 0.26 \text{ mm}$	
Reflector support structure	<u>Clear night</u>		
	$\Delta T = 1.5^\circ \text{ F}$ $\dot{T} = 1.5^\circ \text{ F/hour}$	$\pm 0.0021 \text{ inch}$ $\pm 0.054 \text{ mm}$	
Panel structure	<u>Clear night</u>		
	$\Delta T = 1.5^\circ \text{ F}$ $\dot{T} = 1.5^\circ \text{ F/hour}$	$\pm 0.0009 \text{ inch}$ $\pm 0.020 \text{ mm}$	$\pm 0.0028 \text{ inch}$ $\pm 0.072 \text{ mm}$
Surface plates	<u>Clear night</u>		
	$\Delta T = 2.0^\circ \text{ F}$ $\dot{T} = 1.5^\circ \text{ F/hour}$	$\pm 0.0017 \text{ inch}$ $\pm 0.043 \text{ mm}$	

Table 15. The Telescope Tracking Accuracy Error Budget

(i) The tracking accuracy with no wind and uniform constant temperature.

Table 15(i)

Source of Error	Reference to this Report	RMS Error ( $1\sigma$ ) arc second
<u>Drive and Control System</u>	Chapter II, Section 8	0.9
Hysteresis and limit cycling errors.		
Tracking and acceleration errors.		0.6
<u>Stable Reference Platform System</u>	Chapter II, Section 7	
Platform hysteresis and encoder errors		1.0
Autocollimator errors		0.9
Atmospheric effects on light beams		0.6
System noise		0.5

RSS of last column = 1.9 arc seconds.

(ii) The tracking accuracy in the presence of wind. The following additional errors arise in the presence of gusting wind of average speed 18 miles per hour at the reflector center.



Table 15(ii)

Source of Error	Reference in this Report	RMS Error ( $1\sigma$ ) arc second
Disturbance to drive, control and position reference sys- tem.	Chapter II, Section 8	0.4
Deflections of reflector sup- port structure due to steady and gusting wind components.	Chapter III, Section 4	3.2
Deformations of panel and surface plates.	Chapter III, Section 4	0.3
Deflections of subreflector support system.	Chapter II, Section 6	1.1

RSS of last column = 3.4 arc seconds.

(iii) The tracking accuracy in the presence of temperature differences and changes. The temperature regimes corresponding to a clear, sunny day and a clear night are again used in this table.

Table 15(iii)

Source of Error	Temperature Regime	Error Magnitude (1 $\sigma$ ) arc seconds	Combined Error (1 $\sigma$ ) arc seconds
Reflector support structure	<u>Clear sunny day</u> $\Delta T = 9.0^\circ \text{ F}$ $\dot{T} = 1.5^\circ \text{ F/hour}$	2.4	
Panel structure and surface plates	<u>Clear sunny day</u> $\Delta T = 9.0^\circ \text{ F}$ $\dot{T} = 1.5^\circ \text{ F/hour}$	Negligible	8.5
Subreflector support system	<u>Clear sunny day</u> $\Delta T$ between legs = $4^\circ \text{ F}$ $\dot{T} = 1.5^\circ \text{ F/hour}$	8.2	
Reflector support structure	<u>Clear night</u> $\Delta T = 1.5^\circ \text{ F}$ $\dot{T} = 1.5^\circ \text{ F/hour}$	0.40	
Panel structure and surface plates	<u>Clear night</u> $\Delta T = 1.5^\circ \text{ F}$ $\dot{T} = 1.5^\circ \text{ F/hour}$	Negligible	1.1
Subreflector support system	<u>Clear night</u> $\Delta T$ between legs = $0.5^\circ \text{ F}$ $\dot{T} = 1.5^\circ \text{ F/hour}$	1.0	

## 6. The Estimated Performance of the Telescope Under Various Climatic Conditions

(a) The effects of the atmosphere on radio astronomical observations at millimeter wavelengths. The main atmospheric effects on observations are the absorption of radio waves in the atmosphere and the radiation from the warm and wet atmosphere of radio noise into the radio telescope radiometer. A possible further effect is that lack of uniformity in a horizontal plane in the refractive index of the atmosphere can cause phase irregularities on the incoming wave front and thus reduce the effective gain of the instrument. (The refraction of the uniform atmosphere is important, but it does not degrade performance. It can be allowed for by measuring at ground level the atmospheric temperature, pressure and relative humidity.)

(i) Atmospheric absorption. Figure 27 shows typical values for the absorption of radio waves passing once vertically down through the atmosphere. The main contributions come from oxygen and water vapor; of these the water vapor contribution is the variable. Two water-vapor curves are shown, one for a dry atmosphere ( $W_V = 3.4$  mm) and one for a rather humid atmosphere ( $W_V = 21$  mm). ( $W_V$  is the total precipitable water in the whole atmospheric depth, i.e., if all the water vapor in a vertical column were liquified it would have a depth of  $W_V$ .)

Figure 27 shows that good ground-based millimeter wave observations can be made in and near the atmospheric windows. It also explains why the present telescope is planned to work up to 86 GHz, so as to take advantage of the window there. The dry atmosphere has an absorption of about 8 percent at 86 GHz at the zenith, and observations are not seriously influenced by such absorption. It should perhaps be noted that Figure 27 cannot be interpreted as saying that no work can be done outside the windows. Spectral-line observations are often possible close to the absorption lines; for example, the CO line at 115.27 GHz ( $\lambda = 2.6$  mm) lies close to the oxygen absorption peak at 118.75 GHz, yet it has been easily observed with the NRAO 36-foot telescope.

(ii) Atmospheric noise. Radiated noise from the atmosphere can be troublesome at all wavelengths shorter than about 10 cm. However, under clear sky and dry air conditions millimeter-wave observations have been made with good precision. This subject is considered in more detail in Chapter IV on the site for the telescope.

(iii) Irregular refraction. The effects of irregular atmospheric refraction on the gain and pointing precision of large reflector telescopes at millimeter waves are not yet directly known, but there is good evidence from interferometer measurements and some other observations that these effects will not limit the performance of the present instrument (See Findlay 1971).

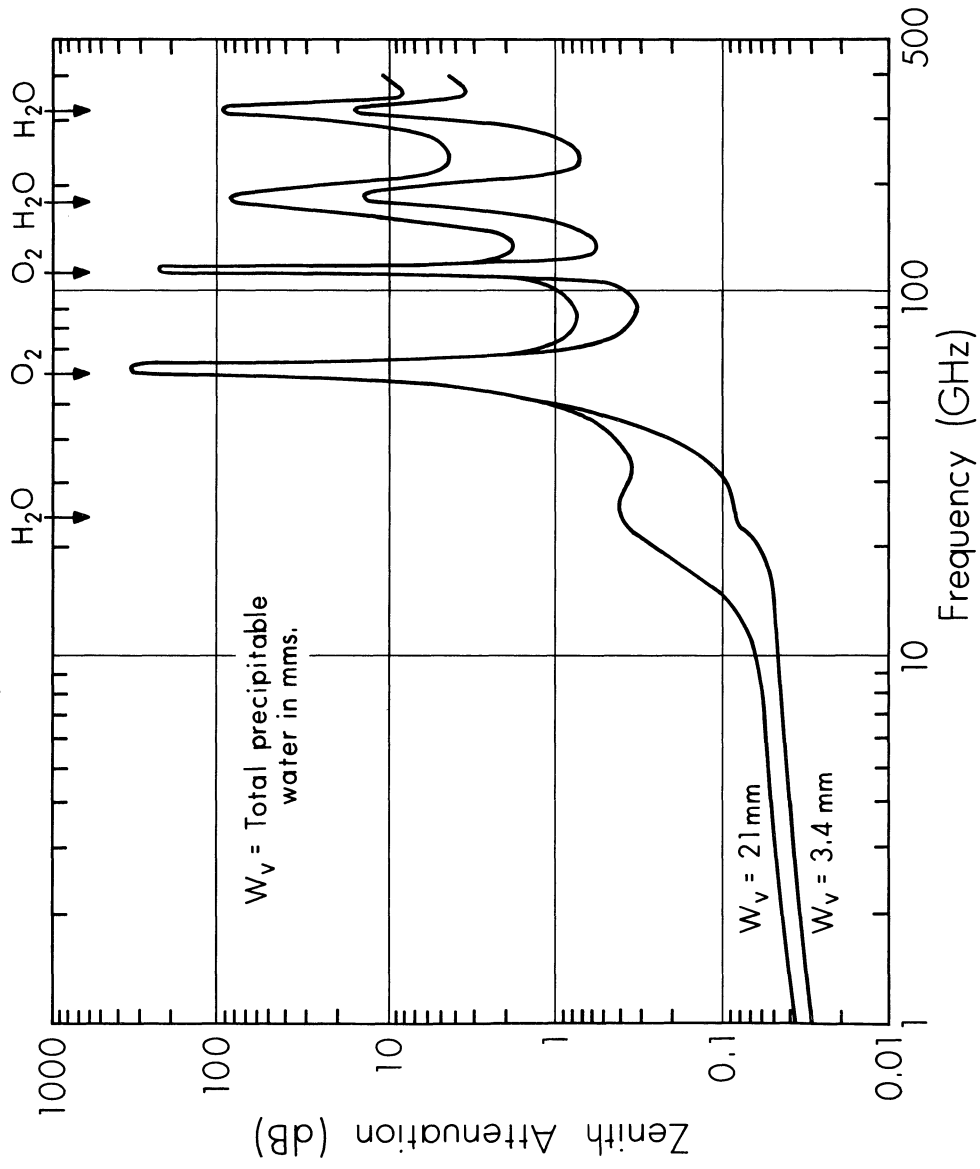


Figure 27. One-way zenith absorption of radio waves in the atmosphere.

(b) Performance under various climatic conditions. Let us summarize the information in the error budgets of Tables 14 and 15, and attempt to show how the telescope will perform under some typical atmospheric conditions. We will discuss, as a measure of its performance, the short-wave limit of the telescope  $\lambda_{\min}$ . This limit is set either because the reflector surface accuracy deteriorates or because the tracking accuracy deteriorates. We continue to use the criteria:

$$\lambda_{\min} = 16 \times \text{RMS Surface Accuracy}$$

or

$$\text{HPBW at } \lambda_{\min} = 5 \times \text{Tracking Accuracy.}$$

We now attempt to collect the values of surface and tracking accuracy under various weather conditions. The sunny day and clear night cases have been discussed, so has the effect of a steady wind. When we try to estimate what will happen when wind and temperature effects are combined, the problem becomes more difficult. In Report No. 36 von Hoerner has attempted to estimate how the combination affects accuracy insofar as the reflector surface is concerned. He made temperature measurements on the surface and on a supporting rib of the NRAO surface plate under conditions of a flow of air across the plate. Two air velocities were used, and for the plates he derived an expression for  $\Delta z$ , the deformation of the surface plates:

$$\Delta z \text{ in full sunshine} = \frac{8.3 \times 10^{-3}}{1+v/3.8} \text{ inches} \quad \text{III(1)}$$

$$\Delta z \text{ at night} = \frac{1.8 \times 10^{-3}}{1+v/3.8} \text{ inches} \quad \text{III(2)}$$

where  $v$  = wind speed in miles/hour.

If we can assume the same form for the variation of temperature effects with wind, we can compile the following expressions:

(i) Surface accuracy with wind acting--clear night and sunny day. The contributions to the surface accuracy budget are:

$$\begin{aligned} &+ 0.200 \text{ mm (Table 14(i) -- no wind or temperature)} \\ &+ 0.080 (v/18)^2 \text{ mm (Table 14(ii) -- assuming contribution} \\ &\quad \text{varies as } v^2) \\ &+ \frac{0.072}{1+v/3.8} \text{ mm (Table 14(iii) -- for a clear night)} \end{aligned}$$

or

$$\pm \frac{0.430}{1+v/3.8} \text{ mm (Table 14(iii) -- for a sunny day).}$$

(ii) Tracking accuracy with wind acting--clear night and sunny day. The contributions to the tracking accuracy budget are:

$$\begin{aligned} & \pm 1.9 \text{ arc seconds (Table 15(i) -- no wind or temperature).} \\ & \pm 3.4 (v/18)^2 \text{ arc seconds (Table 15(ii) -- assuming contri-} \\ & \quad \text{bution varies as } v^2) \\ & \pm \frac{1.1}{1+v/3.8} \text{ arc seconds (Table 15(iii) -- clear night)} \end{aligned}$$

or

$$\pm \frac{8.5}{1+v/3.8} \text{ arc seconds (Table 15(iv) -- sunny day)}$$

We can now use the error contributions (by forming the RSS values) to arrive at Table 16, which estimates the telescope performance under various conditions.

(c) Conclusion. We must stress that the simple methods used to mix the effects of wind and temperature to arrive at Table 16 can only give a rough answer. We believe, however, that the estimates of performance with the climatic factors unmixed are reasonably good.

The telescope will be at its best on clear nights when a wind of a few miles per hour is blowing. Under such conditions its RMS surface accuracy is  $\lambda/16$  for a wavelength of 3.2 mm and its tracking accuracy is 2.15 arc seconds, which is 1/7 of the HPBW of the telescope at 3.2 mm wavelength.

At its worst (with no wind on a sunny day) it will work at 9 mm wavelength (33 GHz).

## 7. The Performance of Some Other Telescopes

(a) General. The present 65-meter telescope will not be the largest fully-steerable reflector in the world, but when its size is considered together with its planned shortwave performance, it becomes an instrument some steps ahead of all others in its requirements for accuracy. Thus it is not possible by considering existing instruments and their performance to give full experimental evidence from these telescopes that the 65-meter will work as well as planned. Nevertheless, there are a number of experimental facts about the measured performance of existing telescopes which give some support to the calculations and predictions made in this Report. We will in this section list these facts, again emphasizing that they, in themselves, are not advanced as proof of the 65-meter design.

The quantities which are of greatest interest are the surface and tracking accuracies (as already defined in Chapter III, Section 5), and

Table 16. Performance of the Telescope Under Various Climatic Conditions

	Wind Velocity Miles/Hour	Surface Accuracy (1 $\sigma$ ) mm	Tracking Accuracy (1 $\sigma$ ) arc seconds	$\lambda$ min (mm)		$\lambda$ min mm (GHz)
				Surface	Tracking	
Clear Night	0	0.215	3.2	<u>3.45</u>	2.35	3.45 mm (87)
	6	0.200	2.0	<u>3.20</u>	2.15	3.20 mm (94)
	12	0.205	2.4	<u>3.30</u>	2.55	3.30 min (91)
	18	0.215	3.9	3.45	<u>4.20</u>	4.20 mm (71)
Sunny Day	0	0.475	8.7	7.60	<u>9.30</u>	9.30 mm (32)
	6	0.260	3.8	<u>4.15</u>	4.05	4.15 mm (72)
	12	0.230	3.1	<u>3.70</u>	3.30	3.70 mm (81)
	18	0.230	4.2	3.70	<u>4.50</u>	4.50 mm (67)

we concentrate on measurements of these for existing telescopes. Surface accuracy can be measured by high-class surveying, but also, once a telescope is working, it can be determined by using antenna tolerance theory (Ruze 1966). Results of the two methods agree well. Tracking and pointing accuracy can also be measured, since by now a number of small diameter radio sources are known in absolute position to errors of rather less than one arc second. The actual measurements, however, represent not only the errors in the radio telescope but also errors introduced because the noise power received from the source is often only one or two orders of magnitude more than the radiometer noise fluctuations. This causes errors in position measurements, whose magnitude depend on the telescope beamwidth and on the signal/noise ratio in the observations. Also, measures of tracking accuracy also include any irregular atmospheric refraction which is added to the telescope errors. With these restrictions in mind, we list experimental information from a number of telescopes.

(b) The 210-foot Goldstone telescope. This instrument, built by the Rohr Corporation for the Jet Propulsion Laboratory, is of particular interest since it is a well-designed and well-built telescope of the size we are describing (210 feet is 64 meters). The telescope has been working as part of the Deep Space Instrumental Facility since 1966; a considerable number of radio astronomers have used it and the antenna group at JPL and others have made many careful measurements of its performance. Information about the 210-foot has been most useful in the present design, but the single important fact to note here is its excellent tracking performance.

To measure this, the telescope was set to track a strong radio source, but with the source not in the center of the telescope beam but on the side of the beam. In this situation, small angular tracking errors show up as signal level changes, and after a simple calibration and calculation the result can be used to measure the angular tracking accuracy. In one such experiment (Bathker 1969) the  $1\sigma$  RMS tracking accuracy was measured to be 3.6 arc seconds. This is an extremely good result and considerably exceeds the original telescope specification. It is relevant to the 65-meter, since the dynamical properties and servo design parameters of our telescope and the JPL telescope are similar, but ours has, of course, a much higher angular resolution in its encoders.

(c) The 210-foot Parkes telescope. This is one of the oldest large fully-steerable telescopes; it was built at a low cost with the intention of its working well at 21-cm wavelength. In fact it has been used down to 5 cm and the central 100 feet has been tested at 22 GHz (1.4 cm) and shown to have useful gain. This telescope has good tracking accuracy, as is demonstrated by a long series of observations of positions of 750 radio sources (CSIRO staff 1969) where the RMS ( $1\sigma$ ) source positions were found to 10 arc seconds in RA and 12 arc seconds in declination. The observations were made at night, but include read-out



errors and errors due to radiometer noise, so they show that the telescope behaves well over the significant periods of time between the source and calibration source observations.

(d) The NRAO 300-foot transit telescope. The NRAO 300-foot telescope was not built with any expectation of high positional accuracy, but since its resurfacing and subsequent use at shorter wavelengths it has been possible to measure its pointing performance. Two reports by M. M. Davis (September 14 and October 25, 1971) give the RMS pointing errors as follows. (These errors are the RMS departures in position from the telescope calibration curve and so are equivalent to what we have called tracking errors for the 65-meter telescope.)

Table 17. Pointing Errors of the NRAO 300-foot Telescope

Type of Observation	RMS Angular Error ( $1\sigma$ )
Elevation measurements Day and Night	$\pm 9$ arc seconds
Right ascension measurements Daytime (mainly sunny)	$\pm 9.7$ arc seconds
Nighttime	$\pm 2.1$ arc seconds

It should be noted that all the observations contain the errors due to radiometer noise and the elevation measurements include the read-out errors (the digit interval on the encoders is 10 arc seconds). The RA measurements show clearly the effects of sunshine and show also excellent structural stability at night. In particular, they give good support to our 65-meter tracking error estimates insofar as they confirm structural integrity and repeatability at night. They also demonstrate that critical items, such as the feed support, do not on the average experience troublesome temperature differences at night.

(e) The NRAO 36-foot telescope. This telescope has, of course, proved itself to be the most useful millimeter-wave instrument in the world. It is used in an astrodome, but the 40-foot wide dome opening does in fact expose the telescope to some wind and temperature effects during observations. Its RMS tracking accuracy is 5 arc seconds, including radiometer noise and read-out errors (the 1 bit angular encoder interval is 1.24 arc seconds). The RMS surface accuracy is 0.005 inches (0.144 mm) as determined from an aperture efficiency of 50 percent at 85 GHz.

(f) Other millimeter-wave telescopes (Findlay 1971). The following table shows the tracking and surface accuracies of some other telescopes.

Table 18. Tracking and Surface Accuracies of Some Other Telescopes

Property	USSR Crimean RT-22	Aerospace Corp.	U. Texas	U. Calif., Berkeley
Diameter in meters	22.0	4.57	4.87	6.10
Tracking accuracy in arc seconds	9.0	7.2	7.2	9.6
RMS surface accuracy in mm	0.12	0.05	0.10	0.15

(g) Conclusion. This brief survey confirms that, although the 65-meter telescope is an instrument of higher performance than any so far built, there is supporting experimental evidence to show that the tracking and surface accuracies expected of it are not too advanced over those already achieved in some other telescopes.

#### References

- Bathker, D. A. 1969, Radio Frequency Performance of a 210-foot Ground Antenna: X-Band, JPL Technical Report 32-1417, Jet Propulsion Laboratory, Pasadena, California.
- CSIRO Staff 1969, Aust. J. Phys. Astrophys. Suppl. No. 7.
- Findlay, J. W. 1971, Annual Review Astron. and Astrophys., 9, 271-292.
- Ruze, J. 1966, Proc. Inst. Elec. and Electronics Engrs., 54, 633-640.

## CHAPTER IV

### TELESCOPE SITES

#### 1. Criteria for Site Selection

(a) A logical approach. There is a logical approach possible to the task of choosing the most suitable site for a radio telescope. This approach starts by defining criteria the site must meet. These criteria are often, for convenience, separated into two main classes--"primary" requirements which must be satisfied and "secondary" requirements, usually dealing more with practical matters of access, living conditions and so on, where adjustments can be made between the degrees to which the various requirements are met.

The various criteria can be assigned weights, expressed preferably in numbers. Then the site search locates those sites which rate highly according to the various criteria; number values are assigned to the degree of success various sites show in meeting the criteria and a final numerical mix of criteria weights and site scores gives the most desirable site.

The apparent certainty which such a process gives does, however, disguise its disadvantages. These are:

(i) Although it is easy to choose the primary and secondary criteria, to assign correct weights to them is often only a matter of judgment. In an expanding field of science it may be very difficult to make such a judgment with a high chance of its being correct.

(ii) Even when specific sites which look good are identified, the detailed information about them is often insufficient to allow of a reliable quantitative assessment being made of their relative goodness. And again, in a rapidly growing science, it may not be possible to devise site testing procedures which can make the site measurements which would be suitably definitive.

In the present site survey, therefore, although we shall use the framework of this approach, we shall not dignify it by the addition of a numerical system. We shall grade criteria in order, as far as we can, and give reasons for this ordering. We shall also attempt to put in some order the way in which sites meet the criteria.

(b) Primary site criteria. These criteria are all chosen because they affect the performance of the telescope as measured by its ability to make good observations, particularly at the short-wave end of the radio spectrum. We therefore adopt:

(i) Site latitude (A)\*. There are no firm limits set for the latitude range in which the telescope should be placed, but the following reasons all argue strongly for a location as close to the equator as possible in view of other requirements.

- Many of the most interesting short-wave observations will be made on sources within our own galaxy; the galactic center is of particular importance. The further south the site is the better are such observations since the galaxy is seen higher in the sky and more of it is visible. (See paragraph 3(e) (ii) for a further note on the advantages of a site south of the equator.)

- Planetary observations also are better from sites near the equator, since planetary orbits lie near the plane of the ecliptic.

- A site fairly close to the equator has available to it a larger fraction of the total celestial sphere than can be observed from higher latitudes.

(ii) Freedom from clouds (A). Millimeter-wave observations can be seriously degraded by all kinds of cloud. This is a subject on which detailed quantitative experience is lacking, but experienced observers, using the NRAO 36-foot telescope on Kitt Peak, classify the absence of cloud as being of the highest importance in choosing a millimeter-wave telescope site.

In view of the fact that the telescope will work best at short wavelengths only at night, this criterion should be stated as:

- The site should have the maximum possible number of cloud-free (say less than 3/10 average cloud cover) nights per year. Its daytime cloud cover should also be reasonably low.

(iii) Low and stable atmospheric water vapor (B). Radio-wave absorption by water vapor has already been discussed in Chapter III, Section 6 so that the need for as dry an atmosphere as possible has been explained. We can state the criterion more sharply by agreeing (somewhat arbitrarily) that by "dry" we mean an atmosphere whose total precipitable water vapor ( $W_v$ ) is 3 mm or less. Figure 27 of Chapter III shows that, at this level of dryness, the radio windows are very useful. We add the need for as much good observing time per year and arrive at:

- The atmosphere above the site should have  $W_v < 3.0$  mm for a large fraction of nights throughout the year.

---

\* We are classifying the primary criteria with letters. A is a criterion to which the greatest weight must be given.

The criterion for a dry atmosphere is not too heavily stated, or weighted, since other factors, particularly the variability of the atmosphere, confuse the simple picture. A completely uniform dry ( $W_v = 3$  mm) atmosphere at a uniform temperature of  $10^\circ$  C contributes an absorption factor of about 7 percent at 85 GHz and adds about  $20^\circ$  K to the radiometer noise. These are not harmful figures. But now let the total water vapor vary in amount with time (as will occur, for example, in the presence of atmospheric turbulence). A variability of 0.1 mm with  $W_v$  even as low as 3 mm gives 0.17 degree change in the radiometer temperature; this change usually has a noise-like variability with time, and thus can quickly become the limitation to the telescope performance. For special observations, this "sky-noise" can be reduced by techniques such as beam-switching or frequency-switching, and the 65-meter telescope is designed so that such techniques can be used. Nevertheless, since there are some observations where sky-noise cannot be removed or reduced, its existence must be recognized and minimized by good site selection.

Even now, the whole story of atmospheric irregularity has not been told. The variability of the atmosphere makes changes in the optical path length for a radio wave reaching the telescope. If the path differences are themselves different across the telescope aperture, the pointing of the telescope may be changed or its apparent gain reduced. These effects are very important in interferometry and have been studied experimentally and theoretically (see Hinder and Ryle 1971 for a recent survey). To show the importance of low variability in water content, we will quote two results only. If  $W_v$  differs by 0.05 mm for ray paths from a point source entering the atmosphere 65 meters apart, then the apparent direction of that source varies by 1 arc second at 86 GHz. If  $W_v$  varies over small distances of a few meters by more than 0.02 mm, the gain of the telescope will begin to suffer.

This subject of measuring atmospheric variability with time and across rather small distances in space is difficult. Observations of phase stability with interferometers suggest that the sort of  $W_v$  differences being discussed here are not exceeded with a dry and fairly stable atmosphere. But it appears not to be possible to state a measurable requirement on atmospheric stability, and so we make the reasonable assumption that a low value of  $W_v$  will be associated with low variability of  $W_v$ , and accept a low  $W_v$  as the main criterion.

(iv) The radio environment (C). The chosen site should be as free as possible from harmful radio interference. This may come from a variety of man-made sources; these in turn are of two kinds: (1) Radio transmitters on the ground, in the air, or in space. All such sources in the USA operate in frequency bands assigned and controlled by official organizations (the Federal Communications Commission or the Office of Telecommunications Policy). Internationally frequencies are allocated by agreements made in the framework of the International Telecom-

munications Union. (2) Unlicensed and unregulated sources of radio noise, such as electrical machinery, automobile ignition systems, some kinds of lighting systems and so on.

The worst effects of the licensed transmissions are avoided by observing in those bands of the spectrum protected for radio astronomy. Such bands exist (with more or less actual protection) throughout the spectrum but the following should be noted as being of interest in the frequency range where the telescope will be most used, i.e., frequencies above 1400 MHz.

Table 19. Frequency Bands Above 1.4 GHz Allocated (to some extent) to the Radio Astronomy Service

Frequency Band	Degree of Protection Provided
1400-1427 MHz	Worldwide allocation
1611.5-1612.5 MHz	Protection requested by footnote
1660-1670 MHz	Primary allocation but shared
1720-1721 MHz	Protection requested by footnote
2670-2690 MHz	Protection requested by footnote
2690-2700 MHz	Worldwide allocation
4825-4835 MHz	Protection requested by footnote
4990-5000 MHz	Primary allocation, some sharing
5750-5770 MHz	Protection requested by footnote
10.60-10.68 GHz	Mainly primary, shared allocation
10.68-10.70 GHz	Mainly worldwide allocation
14.485-14.515 GHz	Protection requested by footnote
15.35-15.40 GHz	Worldwide allocation, some sharing
22.21-22.26 GHz	Protection requested by footnote
23.6-24.0 GHz	Worldwide allocation, some sharing
31.3-31.5 GHz	Worldwide allocation, some sharing
36.458-36.488 GHz	Protection requested by footnote
86-92 GHz	Worldwide allocation
115.16-115.38 GHz	Protection requested by footnote

Table 19, continued

Frequency Band	Degree of Protection Provided
130-140 GHz	Worldwide allocation
230-240 GHz	Worldwide allocation

This table shows, in simplified form, the allocations most important to the USA made at the 1971 World Administrative Conference for Space Telecommunications. Experience has shown that good protection can be obtained in a country such as the USA within many of the bands allocated to radio astronomy. Nevertheless, a new telescope capable of being used over a wide frequency range should also be sited where the present (and if possible the future) density of licensed radio transmitters is low.

The unregulated radio noise is very directly dependent on the concentration of people living and working near the site. Fortunately, automobile interference power density falls off quite rapidly at the higher frequencies (above a few GHz). Shielding by ranges of mountains is also advantageous in reducing interference from ground-based sources.

Thus we can state a radio-environment criterion:

- The site should be as free as possible from interference generated either by licensed and controlled transmissions or by other radio noise sources. Some shielding by mountains may be desirable.

(v) Meteorological factors (C). We have discussed atmospheric effects on the radio performance; the other meteorological effects of importance are the effects of wind and temperature on the performance of the telescope and the possible high loading of the structure in strong winds, large snow or hail storms or by ice loading. We therefore state two meteorological criteria, one dealing with operating conditions and one with survival:

Operating Criteria

- To make the telescope work at full accuracy the wind at the 100-foot level on the site should be below 18 miles per hour (29 km per hour) for as much time per year as possible.

- The rate of change of ambient air temperature on clear nights should be below 1.5° F per hour for a large part of the night.

Survival Criteria

- The extreme climatic conditions must not exceed the following more than once in 100 years:

Winds at the 100-foot level--90 miles per hour (145 km per hour)

Snow load deposited in 3 hours on a horizontal surface--20 lbs. per sq. foot (97.7 kg per sq. meter).

Ice load deposited in a single ice storm on a horizontal surface--20 lbs. per sq. foot (97.7 kg per sq. meter).

(c) Secondary site criteria. The secondary criteria are the obvious ones which, if followed, lead to a site which is reasonably easy of access, not expensive to develop and which provides satisfactory living conditions near the telescope for staff and visitors. We will not discuss the criteria in detail but merely list them. (No priority order is stated or implied in the listing.)

(i) A good construction and working site. Level or gently rolling ground, good subsurface conditions for azimuth track foundation, no serious surface or subsurface water problems. Easy water supply and sewage disposal.

(ii) Good access and utility supply. Not too far from a good highway (but not within 10 miles of a heavily travelled highway). Good power line (500-1000 KVA) available within a few miles. A major jet airport should be within 100 or so miles.

(iii) Reasonable living conditions. Within about 30-40 miles (or 45 minutes by car) of adequate schools, shops, hospital and medical facilities, some recreation.

(iv) Freedom from natural hazards. Avoid major earthquake zones, areas where there is a high probability of tornados or hurricanes. Avoid natural gas or oil producing areas (actual or potential).

(v) Land acquisition and local government. If possible, locate in area with surrounding land already controlled (national or state forest). Land acquisition costs should be low. Local government should be helpful; willing to control adjacent land use by zoning, for example.

## 2. Sources of Information on the Primary Criteria

Having established the criteria, we will discuss briefly the information which is available and which can be used to judge various sites according to the criteria. The requirement for a low latitude is obvious. The second, for low cloud cover, is not so easy to determine in detail.

(a) Information on cloud cover.

(i) General information. General information on cloud cover over the United States can be derived from several sources, but detailed knowledge of cloud climatology is not good. An excellent survey (McDonald 1958) with the title "Cloudiness Over the Southwestern United States and Its Relation to Astronomical Observing", makes this point and gives references to several general studies.

We rely first on these studies, choosing one which McDonald regards as good (U. S. Department of Agriculture 1941 Yearbook of Agriculture, Climate and Man). Figure 28 is taken from that publication



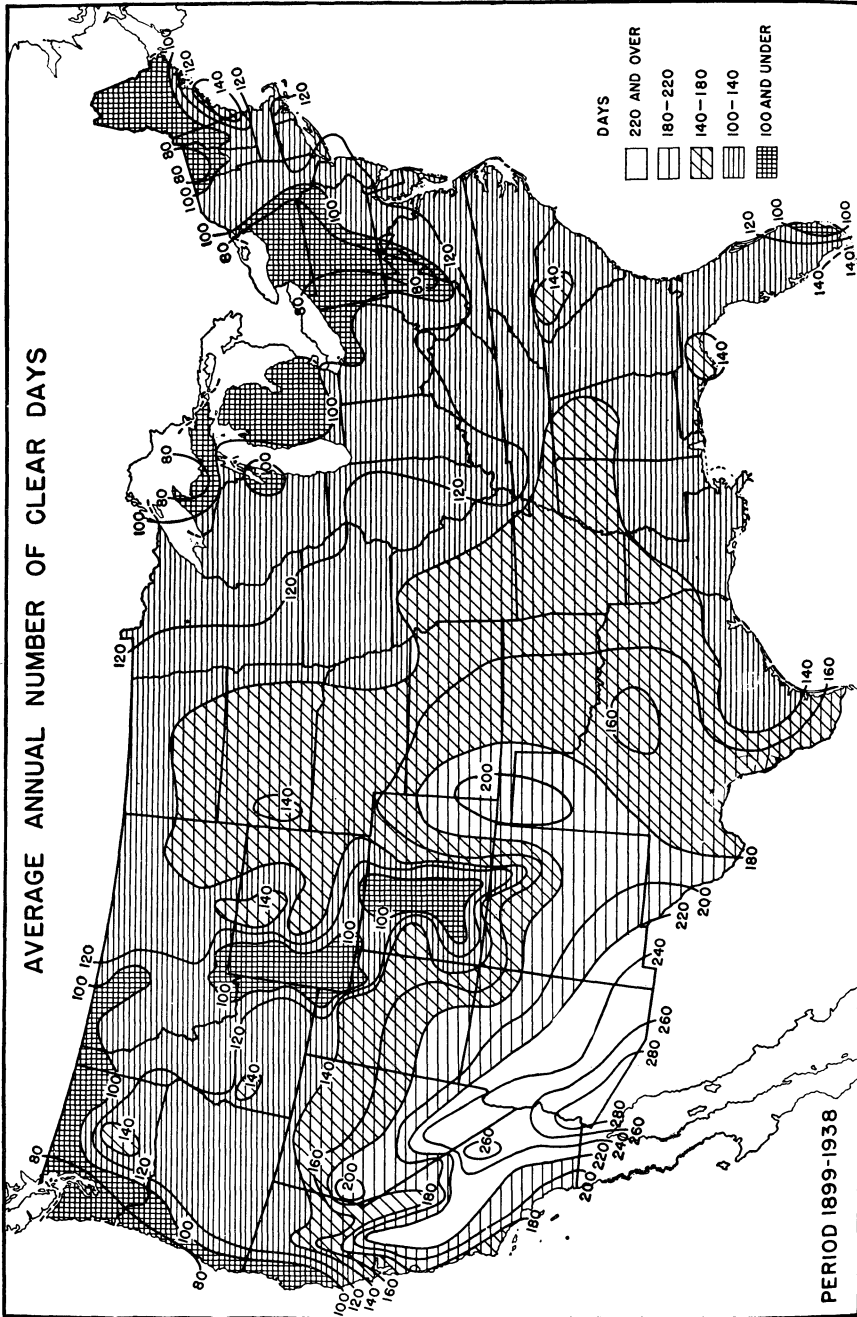


Figure 28. Nationwide pattern of clear days.

and shows the average annual number of "clear" days for the United States over the period 1899-1939. By "clear" is meant days when the average cloud cover was less than 3/10, and we must also remember that Figure 28 refers to days and not to nights. We will return later to the problem of obtaining good cloud information at night over large areas of the country. McDonald was able to compare the cloud cover as shown in Figure 28 with careful studies made over Arizona, and although there are detailed differences, Figure 28 seems to be broadly correct. A similar conclusion seems possible from the cloud-cover information used by Kuiper (1970).

(ii) Cloud cover in more detail. Observations of the earth from meteorological satellites have been made since Tiros 1 was launched in April 1960, so there should be a wealth of data available on worldwide cloud cover (at least for daylight hours). However, a good published summary of satellite information has appeared only as this report was in its final stages of preparation. This is the "Global Atlas of Relative Cloud Cover 1967-70", a joint production of the U. S. Department of Commerce and the Air Force (Washington, D. C., September 1971). This atlas shows the average statistics of clouds over very large areas of the earth; the unit area is a square of 40 km on the side. It thus will be invaluable for comparisons of average cloudiness on about the right scale of detail for estimating the value of sites for a radio telescope, and the information in it will be used before a final site selection is made.

Estimates of night-time cloud are usually only available from astronomical observatories in the sort of detail which is of value for site cloudiness comparisons. When such estimates can be found, they are of considerable qualitative value and should be used.

One project is at present being carried out which will produce some very valuable night cloud comparisons. This is a survey of possible sites for a large infrared telescope, being undertaken under the leadership of Prof. J. A. Westphal of the California Institute of Technology\*. We shall refer to this survey again, since its results are relevant to the search for low precipitable water and to the measurement of atmospheric stability. The survey uses fully automatic infrared telescopes (in the 8-14 micron range) to observe fluctuations of apparent sky brightness. This is done by switching the telescope beam rapidly between two small areas of sky about 10 minutes of arc apart and measuring the difference of sky brightness between them. This is a good measure of sky noise for the infrared astronomer. It is not certain that this observation is directly related to the millimeter-wave sky noise, but it seems likely that low infrared sky variability will go

---

\* The site survey is being supported by the Planetary Astronomy Section of NASA's Office of Space Science and Applications.

along with a stable millimeter-wave atmosphere. The infrared observations are very sensitive to clouds, and so the Westphal site survey will, when complete, give a year's comparison of night-cloud between the sites under study. Nine identical installations are being used, at the following locations:

White Mountain, California  
 Kitt Peak, Arizona  
 Mount Lemmon, Arizona (2 installations)  
 McDonald Observatory, Texas  
 Mauna Kea, Hawaii  
 Palomar Mountain, California  
 Cerro Diablo, Baja California  
 Cerro Tololo, Chile

In addition to the telescopic observations, daily measurements are being made (when the sun is visible) of the total precipitable water in the atmosphere. This is done by measuring the absorption of the solar infrared radiation by water vapor in the 1.87 micron absorption line.

(b) Atmospheric water vapor

(i) General distribution of  $W_v$ . Total precipitable water vapor ( $W_v$ ) in the atmosphere can be measured by sampling the atmosphere throughout the elevation range from the ground to the level where the water vapor has become negligible. This is at about 40 to 50 thousand feet (12 to 15 km) and so meteorological radiosonde observations can be used with reasonable accuracy, even though they often do not extend above the 25,000 foot level. The general distribution of  $W_v$  across the country and throughout the year can thus be found; the fine detail of  $W_v$  is however not determinable because radiosonde observations are only made at fairly widely spaced intervals and are averages over the horizontal track of the instrument. The report by G. P. Kuiper already referred to shows some  $W_v$  values calculated in this way from the basic data contained in the "Atmospheric Humidity Atlas--Northern Hemisphere" (Gringarten et al. 1966). The following Table 20, extracted from Kuiper's Table I, gives values of  $W_v$  for various sites, expressed in millimeters of water. Values corresponding to the 5 and 50 percent levels in the  $W_v$  distribution are given; these may be read as the "average best" and the "median" values. As Kuiper is careful to explain, such general information cannot lead to a reliable choice of the driest and best site, but it indicates the general trend in any area.

The following general conclusions can be drawn about the values of  $W_v$ .  $W_v$  will be low in those areas where the ground-level relative humidity is low.  $W_v$  falls as the ground elevation rises (the effective tropospheric scale height for water vapor is about 2 km).

Table 20. Precipitable Water (mm) in a Vertical Column Over a Number of Sites

Site	Elevation (meters)	January		April		July		October	
		5%	50%	5%	50%	5%	50%	5%	50%
Mt. Palomar (Calif.)	1706	1.8	3.4	1.9	4.4	3.5	9.5	2.6	6.1
White Mt. (Calif.)	4340	0.44	1.1	0.49	1.2	1.1	1.9	0.7	1.3
Kitt Peak (Ariz.)	2064	1.7	4.4	1.8	3.7	5.5	10.9	2.3	7.1
Mt. Lemmon (Ariz.)	2800	1.0	2.7	1.3	2.8	5.0	9.1	1.8	5.0
Pikes Peak (Colo.)	4300	0.40	1.0	0.7	1.3	1.6	4.2	0.81	1.9
Baja California (Mexico)	2830	1.2	2.6	1.35	2.8	3.5	8.2	1.9	4.7
Mauna Kea (Hawaii)	4215	1.2	1.5	1.0	1.8	1.3	2.0	1.2	2.3
Green Bank (W.Va.)	823	1.2	4.3	2.6	8.0	12	20	3.4	10

(ii) Specific information of  $W_V$ . To be more specific about values of  $W_V$  to be expected requires measurements to be made at the sites of interest. Such measurements can be made, on clear days, by using the infrared absorption meters already described. They could, in principle, be made by measuring the radio emission from the atmosphere in one of the water-vapor absorption lines. (Equipment for this purpose has been built and used at Green Bank in the attempt to correlate atmospheric water vapor with interferometer performance.) Vertical profiles of absolute humidity up to 2000 m have been measured by observing Raman scattering of a powerful laser beam (Cooney 1971). As has been noted, the Westphal survey is making  $W_V$  measurements at a number of sites. In the site survey for the Very Large Array (VLA Report Volume III, Chapter 4) measurements of  $W_V$  were made at three sites over a 30-month period. Thus there is some detailed information on  $W_V$  for sites of particular interest to be used in comparisons.

(c) The radio environment. Good general information on the radio environment insofar as licensed or controlled radio transmitters are concerned can be obtained. In recent years, for example, the Electromagnetic Compatibility Analysis Center of the Department of Defense has been collecting data on the location and operating characteristics of a variety of communications and electronic equipments. This data is stored and referenced in a Univac 1108 computer and thus may be retrieved and used in a variety of ways. As an example of the information which can be extracted, topographic data is stored so that path-loss calculations over transmission paths from one place to another can be made (Fuhrmann and Scott 1970).

The environment for man-made noise can be estimated broadly from a survey of nearby operations likely to generate noise and from information about automobile traffic near the site. Fortunately, no very detailed information is needed here for radio observations above a few GHz in frequency, but care is needed to avoid the possibility of later damaging developments.

Before a final selection of a site, it is wise to make radio noise measurements on the site, although it can be very difficult to make such measurements to the very low power levels that sensitive radiometers will reach.

(d) Meteorological factors. Records of wind, temperature, relative humidity and precipitation are available from many weather stations. They are adequate to answer the broader meteorological questions that the site criteria pose. In detail, however, it is often difficult to compare sites with precision. For example, the average distribution of wind velocity is not always known, and thus a judgment has to be made on the basis of an average value of the wind rather than on a knowledge of the percentage of time that the wind is below a given speed.

### 3. Specific Sites

(a) General. One consideration which has not been included in the site criteria obviously has to be given careful attention when discussing sites for a telescope such as the 65-meter dish. It will be part of the National Radio Astronomy Observatory, and will be operated for the benefit of visiting and staff scientists following the policies and practices already well-established by national observatories. This operation would be much easier if the telescope were sited to be near, or even a part of, an existing or planned national observatory site. This is not an over-riding consideration, but if, in judging a list of sites, several can be found which are about equal in other respects, it would then become the decisive factor in choosing the site. With this in mind, therefore, we shall include the Green Bank site in our list of sites and discuss it first.

(b) Green Bank, West Virginia.

Latitude +38°26'      Longitude 79°50' W  
 Altitude 2700 feet - 823 meters  
 Clear days per year - 80

The atmosphere above Green Bank is definitely cloudy. This causes difficulties with single-dish observations at frequencies as low as 2 GHz (15-cm wavelength) and cloud effects can be very troublesome for observations at 10 GHz (3-cm wavelength). There are times, on some winter nights, when  $W_v$  at Green Bank falls to values as low as about 1 mm. However, summer days and nights can be quite humid ( $W_v = 20$  mm) and the Green Bank interferometer does not show good phase stability at 3.7-cm wavelength (8.1 GHz) during the summer.

The radio environment is controlled around Green Bank by the radio quiet zone and by a West Virginia Zoning Act. The mean wind velocity throughout the year is 11.7 miles per hour; the extreme day to night temperature range and the clear night rate of change of temperature are within the limits required by the telescope design; so also are the extreme winds and snow and ice conditions.

Green Bank is a site where the wind speed statistics have been measured (S. von Hoerner Reports Nos. 16 and 23), and it is known that wind at the 100-foot level is above 18 miles per hour for 25 percent of the total time in an average year.

Green Bank meets the secondary criteria very well (though not completely).

The conclusion of the suitability of Green Bank rests heavily on the cloud cover and water vapor effects. As we shall see, other sites in the southwest have up to 260 cloud-free days per year and better  $W_v$  characteristics. The ratio of cloud-free time of 260/80 is so large that the usage of the telescope at millimeter waves at Green Bank would be very low, compared to a southwestern site.

(c) Arizona sites. Four possible sites in Arizona have been considered. This area of the country is obviously good from the point of cloud cover and atmospheric humidity. Tucson is already a major center of astronomical research, so that sites within reach of Tucson deserve study.

(i) Kitt Peak. A possible site on the mountain not far from the NRAO 36-foot telescope, but below the general level of the KPNO optical telescopes, has been considered.

Latitude +31° 57'      Longitude 111° 37' W  
 Altitude 6300 feet - 1920 meters  
 Clear days per year - 260

Precipitable water above this site is low ( $W_v \leq 2$  mm) on many nights during eight months of the year, but the wet season (July, August, September and October) has values of  $W_v$  rising to 20 mm. This season also has the cloudy months. The millimetric observing quality of the site has been well tested, since it lies only 150 meters from the location of the NRAO 36-foot telescope.

The radio environment on Kitt Peak is not controlled. However, the mountain lies within a Papago Indian Reservation, which extends about 15 km from the site towards Tucson, and this to some extent should provide a block to restrict industrial growth. It is also relevant that the site lies to the west of the mountain top, and hence is rather well shielded from the Tucson area. Mountains far to the north also block the line of sight to Phoenix, about 100 miles north. Automobile traffic up the mountain passes close to the site; this is not a problem for the 36-foot telescope but might as radiometer sensitivity improves become troublesome. The present KPNO policy is to let visitors drive their own cars to the mountain top, and on some weekends this traffic is considerable. The normal KPNO traffic would not be a problem, and even if it proved so in the future, the Observatory vehicles could be fitted with ignition suppressors.

Precipitation would be within the telescope limits, but the general winds could limit observations. The mean wind speed on the mountain is 12.5 miles per hour. Statistics of wind speed (and many other meteorological factors) were studied in the "Final Report on the Site Selection Survey for the National Astronomical Observatory" (Meinel 1963). From that publication the following Table 21 of values for the percentage of time the wind was  $\geq 18$  miles per hour at the 60-foot level above ground was derived. It will be seen from that table that wind will restrict millimeter-wave observations quite significantly, particularly during the months November through June when the atmosphere is clearest and driest.

The survival conditions would be met for a Kitt Peak site. The secondary criteria are all very well met by the proximity to Tucson.

Table 21. Winds Above 18 Miles Per Hour on Kitt Peak

Month and Year	Wind $\geq$ 18 m/h	Month and Year	Wind $\geq$ 18 m/h
Nov. 1956	28.5%	June 1957	30.5%
Dec. 1956	32	July 1957	8.5
Jan. 1957	20	Aug. 1957	8
Feb. 1957	30	Sept. 1957	14
Mar. 1957	26	Oct. 1957	14
Apr. 1957	29	Nov. 1957	20
May 1957	29	Dec. 1957	21

(ii) A site considered for the VLA (Y-23). The site survey for the Very Large Array antenna has dealt in detail with a possible site (indexed as Y-23 in Volume IV of the VLA Report\*) which lies in the Aguirre Valley just north of Kitt Peak. Although this is at a lower elevation than Kitt Peak, it should be included in any list of sites to be considered.

Latitude +32° 05'    Longitude 111° 35' W  
 Altitude 2800 feet - 850 meters  
 Clear days per year - 260

Total precipitable water above this site has been measured over a 30-month period, from July 1966 to November 1968, for the VLA site study (VLA Report Volume III, Chapter 4). The average results for 1968 are shown in Figure 29; they again show the seasonal wet period July through October, but the rest of the year shows reasonably low values. The lower elevation (compared to the mountain top) results in somewhat higher values of  $W_v$ , and these in turn make the site somewhat less attractive from that aspect.

The radio environment is perhaps rather better than that on the mountain top. It is less exposed to interference from noise sources in Tucson, since there is better terrain shielding, and it lies at about the same distance from Route 86.

Precipitation and survival winds would be within the limits of the telescope design. No statistics of wind are available for the site, but the average wind velocity should be about the same as at Tucson (8.1 miles per hour). On the assumption that the distribution of wind

\* "A Proposal for a Very Large Array Radio Telescope", NRAO, Charlottesville, Virginia, 1967-71.



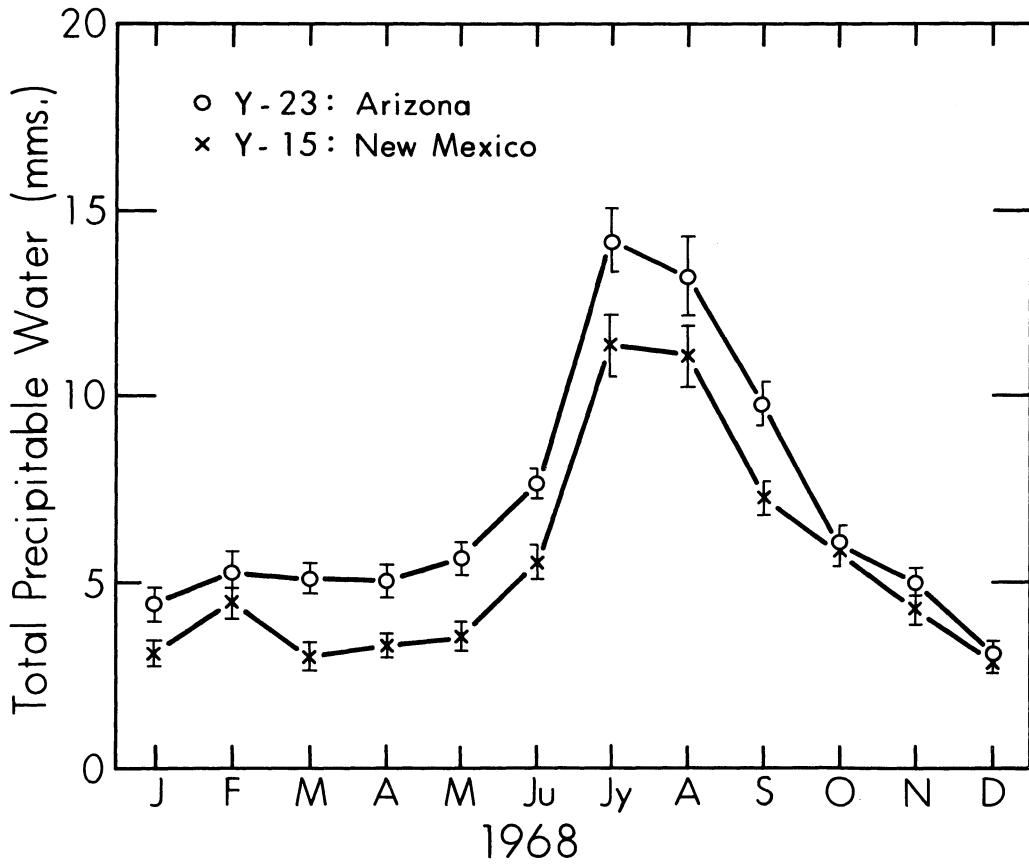


Figure 29. Precipitable water over VLA sites Y15 (New Mexico) and Y23 (Arizona).

of wind speed has a normal shape, this would give about 13 percent of the total time with winds above 18 miles per hour.

The secondary criteria are mainly well-satisfied by this site, but it does lie within the Papago Indian Reservation which could cause difficulty.

(ii) Two more Arizona sites. Two further sites within the low-cloud area of Arizona have been considered. One is near the summit of the Catalina Mountains, and one is near the summit of Mount Hopkins. The Catalina site is Mount Lemmon, well described in Kuiper's paper; the Mount Hopkins site is close to the Smithsonian Astrophysical Observatory. The meteorological conditions on Mount Hopkins are described in "A Meteorological Report for the Mount Hopkins Observatory 1968-1969" (Pearlman et al. 1970).

<u>Mount Lemmon</u>	<u>Mount Hopkins</u>
Latitude: +32° 26'	Latitude: +31° 41'
Longitude: 110° 47' W	Longitude: 110° 53' W
Altitude: 9190 feet - 2800 meters	Altitude: 8375 feet - 2554 meters
Clear days per year - 260	

The precipitable water above Mount Lemmon is known to be low during the dry months of the year. The Lunar and Planetary Laboratory of the University of Arizona has made infrared observations from a site close to Mount Lemmon for several years, and so measures of  $W_v$  are available. Some typical values for 1964 are given below.

Table 22.  $W_v$  Measured on the Catalina Mountains\*

Average During Months Of	No. of Days	$W_v$ mm
February and March	6	1.44 ± 0.25
April	15	1.91 ± 0.15
May	7	2.70 ± 0.36
June	18	3.74 ± 0.19
July, August, September, October	16	7.71 ± 0.71
November	8	1.54 ± 0.21

\* The measurements were reported by Dr. F. J. Low in an NRAO Millimeter Wave Internal Report No. 30, December 1964.

We have no comparable data on  $W_v$  for Mount Hopkins, but the absolute humidity values in the SAO Report suggest that the annual pattern will be very similar to that on Mount Lemmon or on Kitt Peak. The radio environment of Mount Hopkins is compromised by a Channel 11 television transmitter on the mountain. The site is 17 km in a direct line from Route 89 and 60 km in a direct line from Tucson. Mount Lemmon has a definitely poor radio environment. The main television antennas serving Tucson are on the mountain, with other radio installations also. Even though the radio frequencies being transmitted are much below the millimeter wave end of the spectrum, the power levels are very high and the environment would be impossible for longer wavelength work. Tucson itself is within 30 km and the road up the mountain is heavily travelled in both summer and winter. (The mountain top is used for skiing in winter.)

Survival climatic conditions are within limits for both mountains. The average wind at the Observatory on Mount Hopkins is a rather surprisingly low 8.5 miles per hour, and during 1968-69 period the wind was above 18 miles per hour for only 6.5 percent of the total time.

The Mount Lemmon site meets the secondary criteria well. The Mount Hopkins site would require quite extensive work to build a suitable access road. It would be almost impossible to transport the telescope fabricated members over the present 18 mile long, rough mountain road from Amado to the present SAO site, and more road up to the selected site would be needed.

These latter two Arizona sites have been discussed, since both have possibilities, but both appear inferior to the first two described.

(d) Sites in New Mexico. The general distribution of cloud together with the existence of high elevation, fairly level land suggests that suitable sites should exist in the west and southwest areas of New Mexico. The site search for the VLA identified an area in the San Augustin Plains, about 140 km (88 miles) on a line southwest from Albuquerque, as a very desirable site. This and nearby areas have been examined in the present survey with the following results.

(i) San Augustin Plains VLA site (Y-15)

Latitude: +34° 01'      Longitude: 107° 37' W  
 Altitude: 7200 feet - 2200 meters  
 Clear days per year - 220

This site is about four miles south of the suggested center of the VLA (VLA Report Volume 4, Chapter 5). The telescope in this position would not interfere with the VLA and yet would share many facilities. The significant drop in clear days per year from the Arizona area should be noted.

As with two other VLA sites, there has been a 30-month series of observations of precipitable water in the atmosphere above this site, and these are summarized in Figure 29. It can be seen that this site

shows relatively high values for  $W_v$  in the July through October period, but that, in the dry months, the site is preferable to the Aguirre Valley site near Kitt Peak.

The radio environment appears to be good, although there is a microwave tower on the edge of the site. The land area around is mainly used for grazing cattle; the nearby towns are small and the large and growing city of Albuquerque is 140 km (direct line) away. Some useful terrain shielding exists between the site and Albuquerque and parts of the Rio Grande Valley.

Meteorological criteria for survival are met. The operating conditions for temperature changes also are within our limits. The mean wind on the site is 9.6 miles per hour. Wind statistics for the site itself are not known, but making simple assumptions as to the shape of the wind distribution function suggests that the wind speed is above 18 miles per hour for 18 percent of the total time. The quite high thunderstorm activity in the area should be noted--the Langmuir Laboratory for Atmospheric Physics was placed on a mountain east of the site to study thunderstorm activity. There have been, on the average, 45 summer and 33 winter thunderstorms per year in recent years (VLA Report Volume IV, Chapter 5).

The secondary site criteria are satisfactorily met. The site has been well studied as a VLA site and the VLA report gives further details.

(ii) South Baldy Peak. A possible site on a saddle 300 meters northwest of the Langmuir Laboratory has been studied.

Latitude: + 33° 58'      Longitude: 107° 11' W  
 Altitude: 10,400 feet - 3170 meters  
 Clear days per year - 210

Measurements of  $W_v$  are not available for this site. The average values for the mixing-ratio for water vapor show low values (below 4 gm/kgm) for all months except June, July, August, and September. The site could be expected to show the same sort of annual variation of  $W_v$  as the Y-15 site, with the probability that the dry month values would be lower on Baldy as a result of the 1000-meter altitude difference.

The radio environment would be reasonably satisfactory. The site has direct line distances of 30 km from Socorro (population 6000) and 125 km from Albuquerque. The Langmuir Laboratory operates active radar transmitters when thunderstorms are close. These transmissions would prevent observations, but so would the thunderstorms themselves. When no radar is operating, interference from the Langmuir Laboratory would not be troublesome.

The survival meteorological conditions are met. The mean wind over the period 1964-1967 was 8.6 miles per hour. Wind statistics are not available in a reduced form (the observations exist) but a reasonable

estimate suggests that winds of 18 miles per hour would be exceeded 14 percent of the total time.

Secondary criteria are adequately met, except for access, which at present is by a 20-mile length of dirt mountain road from Route 60. This section of road would have to be rebuilt to allow the fabricated parts of the telescope to be carried to the site. If the VLA were to occupy Y-15, many administrative functions would be shared between the two telescopes.

(e) Sites outside the continental United States. Two sites have been considered; one near the summit Mauna Kea in Hawaii and one close to Cerro Tololo in Chile. These were included because both sites are highly regarded by infrared astronomers.

(i) Mauna Kea, Hawaii\*

Latitude: +19° 50'    Longitude: 155° 29.5' W  
 Altitude: 13,500 feet - 4120 meters  
 Clear days per year - 230

This site has been occupied for some years by an Observatory operated by the University of Hawaii; the major instrument is an 88 inch reflector telescope which was dedicated in June 1970. There are possible locations for the 65-meter telescope near the summit and near the optical observatory.

The "clear days per year" figure given above may not be strictly comparable with those quoted earlier for other sites, which are based mainly on Figure 28. The above quoted figure is estimated from the various reports\*.

The total precipitable water above Mauna Kea is always low. A number of measurements and estimates have been made, in addition to the values given in Table 20. As an example, the following measurements of  $W_v$  (mm of precipitable water) were made on Mauna Kea using the 0.935 $\mu$  absorption line instrument already described. Values of  $W_v$  during nine months in 1965 and 1966 ranged from 0.3 mm (low values such as this are hard to measure accurately with this instrument) up to one value of 5.1 mm. Table 23 shows the distribution of these measurements. There is no marked seasonal variability in  $W_v$  above Mauna Kea.

The radio environment at Mauna Kea could be good to very good. Hilo is 40 km away (direct line), the island is unlikely to suffer extensive commercial development and radio noise sources on the surrounding oceans will be in controlled frequency bands.

---

\* Much of the information in this paragraph is derived from reports by Herring, A. K., Lunar and Planetary Laboratory, University of Arizona, November 30, 1965; Jefferies, J. T., and Sinton, W. M., Sky and Telescope, 36, 140-145, September 1968; Jefferies, J. T. and Zirker, J. B. "A Preliminary Report on a Site Survey for an 84" Telescope", U. of Hawaii, February 1966.

Table 23\*. Distribution of Measured Values of  $W_v$  Above Mauna Kea

Range of $W_v$ mm	Number of Observations
0 - 1	21
1 - 2	15
2 - 3	7
3 - 4	1
4 - 5	1
5 - 6	1
Above 6	0

The survival limits of the telescope would be adequate for the environment, although high winds occur more frequently than at other sites. The observational wind limit of 18 miles per hour needs careful study. Present evidence suggests (Jeffries and Zirker, Figure 6) that winds are above this level for about 35 percent of the total time. If this is true, it represents a serious disadvantage for the 65-meter telescope on this site.

The secondary criteria are not well met by a site on Hawaii. Immediate access to the mountaintop will soon be possible by a good road. There are, however, many disadvantages to placing a large radio telescope on such a site. Some support staff would have to live on the mountain, but at a level where hypoxia is not serious. Work on the telescope (changing radiometers, routine maintenance, etc.) would always be dangerous, since even if oxygen-breathing equipment were used, it hampers working efficiency. The isolation of Hawaii from the rest of the United States would make the travel for many visiting scientists arduous and expensive. The University of Hawaii is on Oahu, an airplane flight away.

(ii) Cerro Tololo or Cerro Morado, Chile. There is much interest on the part of some optical astronomers in sites in the Andes. The Cerro Tololo site has been occupied since 1965 by the Kitt Peak National Observatory and a 150-inch telescope is being built there. The general area has been well-surveyed for possible observatory sites, and we have, in what follows, relied on such reports ("Astronomical Observing Conditions in North-Central Chile", J. F. Stock, Chile Site Survey Technical Report No. 2, KPNO, May 1963; "Observatory Site in Chile", J. B. Irwin,

\* Derived from Figure 12 of Jeffries and Zirker, already referenced.

CARSO Report No. 3, Carnegie Institute of Washington, June 30, 1966 are two examples). We will discuss a site near the Cerro Tololo Observatory on Cerro Morado, only a few miles south of Tololo.

Latitude:  $-30^{\circ} 13'$       Longitude:  $70^{\circ} 48' W$   
 Altitude: 7100 feet - 2165 meters  
 Clear nights per year - 260

This is the only site in our list south of the equator, and it should be noted that many astronomers would value highly a site which sees the southern sky. There are at present no millimeter-wave radio telescopes working in the Southern Hemisphere, although one is just starting observations in Brazil. But the southern sky has interesting galactic objects of all kinds. The galactic center is high in the sky; the Southern Coalsack is potentially one of the richest sources of information on molecular lines. A southern radio telescope would find much of great interest in the Gum Nebula, the Carina Spiral Feature, the Magellanic Clouds and NGC 5128.

The estimate of clear nights (as opposed to days for many of our other sites) is derived from 1960-67 statistics given by Sanduleak (1967).

We are not aware of any existing series of measurements of precipitable water vapor in the atmosphere over Cerro Tololo, but the site is included in the Westphal infrared survey, and this information is being collected and soon will be forthcoming. There is much evidence in the reports, both written and verbal, of the high quality of optical seeing on Cerro Tololo, and we will accept this at present as indicating a good, stable and dry atmosphere.

The radio environment should be good. The site is isolated from population centers; the town used as CTIO headquarters, La Serena, is 33 air miles from Cerro Tololo; and there is little activity near the site likely to produce harmful radio interference.

The meteorological conditions at the site for survival are all satisfactory but there are high winds on occasions. Wind observations have been made on Cerro Morado on a 6-meter tower and at Cerro Tololo on a 12-meter and 28-meter tower. From the bi-monthly reports of CTIO we find the following cases between November 1965 (when observations at the 28-meter height started) and September 1971, of a recorded wind speed of greater than 70 miles per hour at the 28-meter height at CTIO.

There are no cases in Table 24 where our survival speed is materially exceeded, but the occurrence of winds of up to 88 miles per hour at the 28-meter (92 foot) level has to be taken into account.

The operating conditions are met by a site on Cerro Morado. The same bi-monthly reports give wind statistics (measured at 6 meters) for all months of 1965. These show that, in that year, winds would have been above our 18 miles per hour limit for approximately 21 percent of the time.

Table 24. Wind Speeds Greater than 70 Miles/Hour Recorded at CTIO (28 meters height above ground)

Month and Year	Wind Speed Recorded Miles/Hour	Month and Year	Wind Speed Recorded Miles/Hour
November 1965	76	October 1969	74
April 1966	78	May 1970	76
June 1966	74	July 1970	80
June 1968	76	October 1970	74
August 1968	77	July 1970	88
April 1969	72	August 1971	72
June 1969	71	September 1971	88

The secondary criteria would be adequately met by the site; the distance from the main centers of radio astronomy in the USA would cause as much (or more) difficulty and cost as for the site on Hawaii.

#### 4. Summary and Conclusions

The requirements for a site for the 65-meter telescope are somewhat more strict than those for a longer wavelength instrument. Nevertheless, there are accessible and administratively practical sites where the telescope would perform well. Within the continental United States the locations near Tucson or the San Augustin Plains are preferred. It seems doubtful whether the possible sites in Hawaii or in Chile should be included. Hawaii has an excellent atmosphere, yet is both distant from most of those who would use and maintain the telescope and would present problems of wind and altitude which would limit the efficiency of the instrument. A southern site must at some time be occupied and used for millimeter-wave radio astronomy. It is, however, questionable whether the present instrument, taking account of all its features, should be the first to be located south of the equator.

It will be clear that this survey of possible sites has not been exhaustive; there are some sites which have not been included (Owens Valley and White Mountain in California and Cerro Diablo in Baja California are examples) but which deserve study before a final choice is made.



References

- Cooney, J. A. 1971. J. of Applied Meteorology, 10, 301-308.
- Fuhrmann, W. P., and Scott, J. B. 1970. "The ECAC Information Utility," 1970 IEEE Electromagnetic Compatibility Symposium Record, Anaheim, California, pp. 127-137.
- Gringarten, I. I., et al. 1966. Air Weather Service (MAC) Tech. Report 191.
- Hinder, R., and Ryle, M. 1971. Mon. Not. Roy. Astr. Soc., 153, 229-253.
- Kuiper, G. P. 1970. "High Altitude Sites and IR Astronomy," Comm. Lunar and Planetary Laboratory, U. of Arizona, Tucson, Arizona.
- McDonald, J. E. 1958, Univ. of Arizona Inst. of Atmospheric Physics Sci. Report No. 7.
- Meinel, A. B. 1963. Kitt Peak National Observatory Contributions No. 43.
- Pearlman, M. R. et al. 1970. Smithsonian Astrophysical Observatory Special Report 327.
- Sanduleak, N. 1967, Contributions from the Cerro Tololo Inter-American Observatory No. 16.

## CHAPTER V

### ESTIMATES OF COST

#### 1. Fabrication and Erection Costs

In making cost estimates for the telescope, the whole project has been subdivided into elements; these have been chosen to reflect the most likely way in which the various parts would in fact be procured. For example, the structural steel which goes into the entire tower and reflector structure is one element of the whole telescope, since it would be procured either by a single contract or by separate fabrication and erection contracts. The main mechanical parts, such as the azimuth trucks, azimuth and elevation bearings and bearing mounts, azimuth motors and gear reducers, elevation drive mount and its associated motors and reducer units, elevation gear rack and similar items have been treated in the estimate as separate procurement items. In this paragraph we will note how the estimates for these various parts of the work have been obtained, and then tabulate the estimated costs in Table 25.

(a) Fabrication of the tower and reflector structure and erection of the telescope. Fabrication estimates have been made separately and independently by the NRAO engineering staff and also by a contractor experienced in antenna construction. The methods of estimating used by both groups have been very similar. The fabrication tasks have been broken down into the various stages, material procurement, cutting to length, preparation of ends, cost of waste material, lengths and complexities of welds required and so on. Unit prices for these various operations have been chosen, based on the best possible information available from companies or individuals with experience. These unit costs were in costs per pound weight (for material) or cost per linear foot of welds. Thus the total fabrication cost of the structure was developed. The estimates prepared within the NRAO and by the firm of LTV Electrosystems agreed well. Although it is not possible to be precise about the location of either the fabricator or of the exact site of the telescope, shipping costs for all fabricated materials from a location near Dallas, Texas to

a point near Tucson, Arizona were included in this fabrication estimate. The figure adopted in the estimate is shown in Table 25.

Before the erection cost was estimated, it was necessary to adopt an erection plan. Accordingly, Mr. A. A. Kester worked as a consultant for the design group and developed the step-by-step procedure for erecting the whole telescope. Mr. Kester has had long experience in erecting antennas; his plan showed the method of erection and the on-site requirements for buildings, cranes, equipment and men through the erection phase. His work was quite detailed and thus the cost of erection was developed by him from his basic estimates of man-hours, rental terms or purchase costs for machinery, expendable materials and similar items. The result of his work again has been compared with estimates made independently within NRAO, and the final figure adopted is in Table 25.

It should be noted that in all the figures adopted in the cost estimates, suitable figures for general and administrative expenses (G&A), fee or profit, burdens on wage or salary rates and insurance have been included as well as they can be estimated.

It will be noted that there is an intermediate structure between the 60 homology points of the dish structure and the surface plates of the reflecting surface. This intermediate structure effects the transition between the widely spaced homology points and the necessarily small surface plates and consists of a space frame structure composed of small diameter tubular members. The cost of this intermediate structure was estimated on a per pound basis by the NRAO engineering staff based on costs secured for space frame structures of small diameter tubes from two antenna manufacturers for the original 300-foot homology design.

Since the elements of this intermediate structure are quite large (approximately 28 feet x 36 feet x 8 feet deep), the final assembly will be made at the erection site in an assembly building whose cost has been included in the erection cost. This assembly building is also required to assemble on site those telescope members whose length preclude shipment in the final length.

(b) The surface plates. The total area to be covered by the surface plates is 38,258 sq. feet, and, as Table 5 shows, there are a total of 2912 plates used. Two designs of surface plate have been shown to be satisfactory; for the cost estimate we have chosen to use the machined-contour surface plate, since the means of manufacture of this plate can be stated with some certainty. The estimate of cost is derived from the Philco-Ford report, and includes all costs up to the mounting of the plates on the telescope. The cost of the final adjustment of the surface has been estimated on the basis of using the Zeiss pentaprism system and the total cost thus arrived at is included in Table 25.

(c) Azimuth trucks and drive motors, pintle bearing, elevation bearings, elevation gear and drive motors. The estimates for these items

have been derived from quotations received from various possible suppliers (SDL Report H-10 contains some details). The estimates cover fabrication and delivery to the site. The cost of erection of these and of other subsidiary components of the telescope is included in the erection cost estimate already described in (a) above.

(d) The foundation and track. This estimate includes all the foundation work needed for the telescope, including that for the azimuth rail track and pintle bearing. The erection plan includes temporary foundations needed for a derrick and false-work towers and the costs of these are included in the erection figure. The estimate is based on work by NRAO engineers and is for the foundation design already described. Final design must await the choice of a specific site, but the present foundation design is likely to be adequate for almost any reasonable choice of site.

(e) Feed support, subreflector and observing cabins. The cost of the steel feed legs, the framework of the observing rooms at the prime and secondary focal points, the cabins themselves with the machinery for rotation and the Cassegrain subreflector and its focussing and adjusting mount are all included in this estimate.

(f) The position reference system. The cost estimate for this system has been derived from costs of the component parts of the system. The first main component is the stable reference platform, which includes the torque motors, precise digital encoders, tachometers and the seven-sided mirror, all in a temperature controlled enclosure. Another main item is the seven 2-axis autocollimators, each of which has an associated tilt sensor. The coarse position encoders and a considerable amount of servo electronics all come into this estimate. The estimates for all the principal items come from possible suppliers, and the cost of engineering and integrating the whole system is included.

(g) The servo drive and control system. The main components here are the azimuth and elevation drive servo motors, servo amplifiers, tachometers and the electronics required for the various functions pictured in Figure 25. The costs have been estimated by the servo designer; again the costs of engineering and integrating the system have been included.

(h) The telescope computer. A typical present-day computer has been used to give the hardware cost, although it is likely that further advances in computer technique will allow of a different choice later. A liberal estimate of the cost of preparing the computer programs is also included in this estimate.

(i) The remaining items. Most of the remaining items in Table 25 are self-explanatory. The costs of preparing the site are included in the table, and are covered in more detail in the following paragraph. Project management and engineering covers the cost which would be expend

by NRAO during the final engineering and construction phase of the work. It should be pointed out that while the present status of the design reflects a considerable amount of design effort in critical areas beyond that normally done in a feasibility study, NRAO plans to perform, by contract, a detailed design of all elements of the antenna prior to entering the fabrication and erection phase of the work. Staff already at NRAO will also be used in this work; their cost is not included.

## 2. Site Development Costs

Although no specific site has yet been chosen for the telescope, it is desirable to show what the development of a site would cost. To do this, we have assumed that the telescope is to be built on the VLA site Y-15 (see Chapter IV, Section 3d). We have also assumed that no site development for the VLA has taken place, so that the 65-meter telescope must carry with itself all site costs.

Table 26 shows the estimated site development costs. The items are largely self-explanatory. The standby generator is larger than is essential, but extra capacity is valuable and not too costly. The telescope service tower (to allow of work and installation at the prime focus) is an integral part of the control building, located on the north side of the telescope.

The erection plan for the telescope includes in its cost the provision on the site of a 160x60 feet building where the large members can be welded together. (They must be shipped in lengths of 40 feet or less.) This building would be retained and adapted to a shop, garage and storage building. The cost for this adaptation is shown in Table 26.

Of course, if it turns out that the VLA and the 65-meter telescope can share the same site (which seems quite possible scientifically), then a number of items in Table 26 would already be provided for the VLA. The site development cost has not been worked out for this situation, but would be significantly less than the \$634,000 in Table 26.

## 3. Operating Manpower and Costs

Table 27 lists the staff who would be needed at the site to operate, maintain and manage the telescope. It also shows the estimated costs of this staff and of the materials, services and supplies needed each year.

We have not included in Table 27 the cost of services which the telescope would need but which would be supplied from the NRAO fiscal, personnel, purchasing and similar divisions. How the telescope would fit into the general Observatory management structure is too detailed for consideration here, but should present no difficulties.

The operation of a new, large millimeter-wave telescope would, of course, also add burdens to the electronics, computer and engineering divisions of the NRAO. These burdens are estimated in the long-term plans for the growth of NRAO insofar as the manpower needs are concerned. There would be a need for increases in the annual amounts spent in electronics, particularly in "other observing equipment" and in "test and repair equipment" which would probably average about \$0.25 million per year. This additional funding would have to start at about the same time as the approval of the telescope construction to give adequate lead-time for equipment development.

#### 4. Final Engineering and Construction

The design work described has brought the project to the stage where it is ready for final engineering, to be followed by construction. The final engineering will result in the complete drawings, design information, fabrication, erection and test specifications needed for construction to start. The amount of work in this phase is large and quite costly; it should only be undertaken when it seems clear that the telescope will be built.

Two ways are possible by which the project could proceed:

(a) Engineering, fabrication and erection under one prime contract. This route implies that a prime contractor is selected on the basis of proposals solicited and received to carry out the complete work, but in two main phases:

Phase 1: Prepare the final engineering design. This phase would only be satisfactorily concluded when NRAO has approved all the engineering work.

Phase 2: After approval of Phase 1, proceed with fabrication and erection on the site.

(b) Separate final engineering from fabrication and erection. This route separates Phases 1 and 2 above. The engineering in Phase 1 is carried out by a contractor selected on the basis of proposals solicited and received. On the satisfactory completion of his work, which includes material needed for solicitation of bids, a prime contractor is selected to fabricate and erect the telescope after a further bidding process.

We need not discuss here the possible advantages and disadvantages of these two possible routes. Whichever is followed, it is possible to show a time and cost schedule of how the work would go. Route (b) would be a few months longer than (a) on account of the second solicitation of proposals, so in Figure 30 we show an approximate time and cost schedule for following (b). There would not be any great difference in overall cost whichever route we followed.

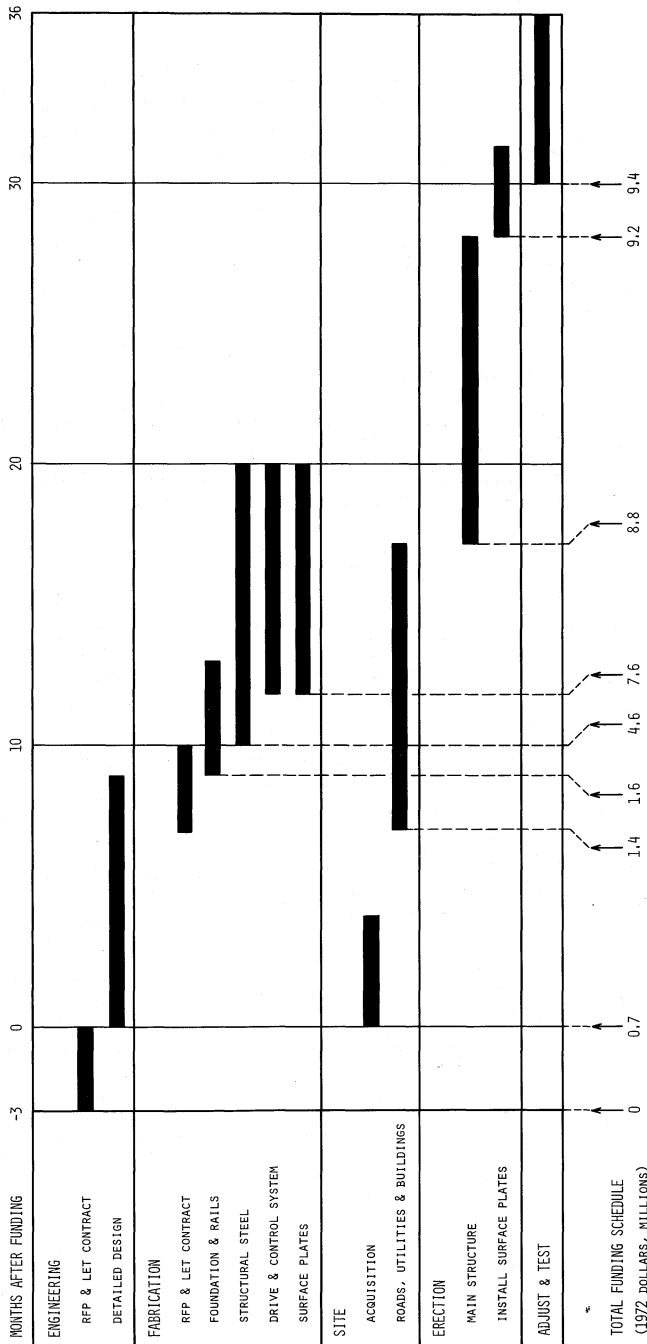


Figure 30. Work and cost schedule.

## 5. Cost Escalation

All the above cost estimates have been prepared on the basis of costs in January 1972. For the first time in many years, wage and price controls are in effect; it is difficult therefore to predict how costs will escalate over the coming years. It seems reasonable to adopt a 6 percent per year escalation of all costs, both for materials and labor.



Table 25. 65-Meter Telescope Cost Estimate (1972 dollars)

	<u>Thousands of \$</u>
Fabrication of reflector and tower structure, including counterweight	1,475
Fabrication of intermediate structure	441
Erection of complete telescope	1,080
Surface plates, installation and adjustment	1,540
Azimuth trucks, gear boxes and motors	340
Pintle bearing	50
Elevation bearings	95
Elevation gear, gear boxes, drive motors	190
Foundation and track	146
Feed and subreflector supports, subreflector instrument cabins	250
Optical position reference system	460
Servo control system	500
Telescope control computer, including software	200
Ladders, walkways, hoists, cable trays	42
Telescope cabling	100
Painting, start-up and test	200
Site preparation	634
Project management and engineering	450
	<u>8,193</u>
Add 15% contingency	Total <u>9,422</u>

Table 26. 65-meter Telescope

---

Site preparation estimates (in 1972 dollars) for placing the 65-meter telescope on the VLA site Y15 (Plains of San Augustin). These estimates assume that no site development for the VLA would have taken place.

---

	<u>Thousands of \$</u>
Site acquisition	5
Grading and draining	40
Roads	10
Water system	52
Sewage system	12
Electric power distribution	35
Stand-by generator (500 kW)	80
Control building (3300 sq. ft.)	140
Dormitory building	115
Shop and garage	35
Telescope service tower (on control building)	110
Total	<u>634</u>

---

Table 27. 65-meter Telescope--Operating Cost Estimate

On-site Personnel	Totals	
Site manager, administrative assistant, clerk, secretary	4	49k
Electronic engineer (3) and electrical/mechanical Technicians, electronic (3) and computer (1)	4	60k
Telescope operators	4	40k
Telescope mechanics	6	60k
Programmer	2	20k
Laborers/handyman/driver	1	15k
Guards (night only)	2	12k
Housekeeper/cook	1	5k
Part-time, temporary, overtime -- 10 percent	-	27k
	<u>Totals</u>	<u>26</u> <u>300k</u>
-----		
Salaries of on-site personnel		300k
Benefits, 15 percent		45k
Travel		15k
Utilities--telephone 5k; power 15k		20k
Materials, services and supplies		100k
One-third cost of painting telescope (paint every three years)		32k
Total Annual Operating		<u>512k</u>

## APPENDICES

[Copies of any of the following appendices may be obtained on request to NRAO.]

### APPENDIX 1. NRAO REPORTS AND MEMORANDA

#### (a) Reports

<u>Report No.</u>	<u>Title</u>	<u>Authors</u>
24	Wind Induced Vibrations of Pipes	S. von Hoerner
31	The Choice of a Cassegrain System	S. von Hoerner
33	Non-homologous Deformations from Joints, Tolerances and Rails	S. von Hoerner
34 & 34A	Structural Design and Revised Structural Design	W-Y. Wong
35	Conditions for Pipe Diameters	S. von Hoerner
36	Thermal and Wind Deformations of the Surface Plates	S. von Hoerner
37	Thermal Deformations of the 65-meter Telescope	S. von Hoerner and V. Herrero
38	Telescope Surface Plates with Internal Adjustment	S. von Hoerner
39	Wind Deformations of the Back-up Structure	S. von Hoerner and V. Herrero
40	The Design of the Panel Structures	S. von Hoerner and Collins Yang

(a) Reports, continued.

<u>Report No.</u>	<u>Title</u>	<u>Authors</u>
41	The Performance of the Panel Structures	Collins Yang and S. von Hoerner
42	The Design of the Feed Legs	W-Y. Wong

(b) Memoranda and Letters

Letter dated July 21, 1970 - The Progress of Tests of the Optical Reference System - by J. Payne

Memorandum dated September 8, 1970 - The Optical Reference System - by J. Payne

Memorandum dated November 20, 1970 - Tests of the Optical Reference System at Green Bank - by J. Payne

Memoranda dated September 14, 1971 and October 25, 1971 on the pointing of the 300-foot transit telescope - by M. M. Davis

## APPENDIX 2. SYSTEMS DEVELOPMENT LABORATORY

Report H-10 - Conceptual Design of a 65-m Diameter Homology Radio Telescope, August 1971 (approximately 400 pages).

Table of Contents

<u>Section</u>	<u>Title</u>	<u>Page No.</u>
A	Table of Contents	1
B	General	2
C	Summary and Conclusion	3
D	Recommendations	6
1.0	Properties and Loads	1.1-1.6
2.0	Reflector Joints	2.1-2.12
3.0	Tower Structure	3.1-3.11
4.0	Azimuth Turntable and Trucks	4.1-4.17
5.0	Pintle Bearing and Foundation	5.1-5.3
6.0	Elevation Bearings	6.1-6.3
7.0	Azimuth and Elevation Gear Trains	7.1-7.13
8.0	Articulating Elevation Drive	8.1-8.7
9.0	Dynamic Analysis	9.1-9.13
10.0	Position Reference System	10.1-10.98
11.0	Drive and Servo System	11.1-11.120
12.0	Cost Estimate	12.1-12.9
13.0	List of Reference Drawings	13.1
14.0	List of Reference Reports	14.1
15.0	List of Specifications	15.1
16.0	Appendix I, Computer Printout - Section 2.4	
17.0	Appendix II, Computer Printout - Section 9	
18.0	Appendix III, Quotations, Specifications, Reports	

## APPENDIX 3. ENGINEERING DRAWINGS

<u>Drawing No.</u>	<u>Description of Title</u>	
111-D-001	Reflector Structure	6
111-D-002	Tower Structure	3
111-D-003	Frame Model-Dynamic Analysis	1
111-D-004	Az-Cabling-Pintle Bearing	1
111-D-005	Elevation Drive	4
111-D-006	Pintle Bearing	1
111-D-007	Elevation Bearing	1
111-D-008	Truck Assembly	3
111-D-009	Az-Torque Motor Drive Concept	1
111-D-010	Azimuth Turntable and Foundation	1
111-D-011	Autocollimator Location	1
111-D-012	Reference Platform	6
56-D-00086	NRAO Surface Plate	1

## APPENDIX 4. REPORTS FROM CONTRACTORS AND OTHERS

## Surface Plate Study:

The Rohr Corporation  
Chula Vista, California

## Surface Plate Design Study: [Approximately 175 pages]

Philco-Ford Corporation  
WDL Division  
Palo Alto, California

Static and Dynamic Analysis of the 65-meter Telescope, Report 9333:  
[20 pages]

Simpson, Gumpertz & Heger, Inc.  
Consulting Engineers  
Cambridge, Massachusetts